REFERENCES

Bertalan, Gy., Marosi, Gy., Anna, P., Ravadits, I., Csontos, I., and Tóth, A. (2001) Role of interface modification in filled and flame-retarded polymer systems. Solid State Ionics, 141-142, 211-215.

Bentley, B.J., and Leal, L.G. (1986) An experimental investigation of drop deformation and breakup in steady, two-dimensional linear flows. J Fluid Mech, 167, 241-283.

Boger, D.V., and Binnington, R.J. (1977) Separation of elastic and shear thinning effects in the capillary rheometer. Trans. Soc Rheol, 21, 515-534.

Cherdhirankorn, T., Lerdwijitjarud, W., Sirivat, A., and Larson, R. G. (2004) Dynamics of vorticity alignment and breakup of isolated viscoelastic droplets in an immiscible viscoelastic matrix Rheol. Acta, 43:246-256.

Elmendorp, J.J. (1986) A study on polymer blending microrheology. Polymer Engineering Science, 26, 418-426.

Elmendorp, J.J., and Maalcke, R.J. (1985) A study on polymer blending microrheology: part1. Polymer Engineering Science, 25, 1041-1047.

Grace, H.P. (1982) Dispersion phenomena in high viscosity immiscible fluid systems and application of static mixers as dispersion devices in such systems. Chemical Engineering Communication, 14, 225-227.

Guido, S., and Villone, M. (1998) Three-dimensional shape of a drop under simple shear flow. J Rheol, 42, 395-415.

Ha and Leal (2001) An experimental study of drop deformation and breakup in extensional flow at high capillary number. Physics of fluids, 13, 1568-1576.

Hayshi, R., Takahashi, M., Kajihara, T., and Yamane, H., (2000) Dynamic interfacial properties of polymer blends under large step strains; shape recovery of a single droplet. Polymer, 42, 757-764.

Lerdwijitjarud, W., Sirivat, A., and Larson, R.G. (2002) Influence of elasticity on dispersed-phase droplet size in immiscible polymer blends in simple shearing flow. Polymer Engineering Science, 42, 798-809.

Lerdwijitjarud, W., Larson, R.G., Sirivat, A., and Solomon, M.J. (2003) Influence of weak elasticity of dispersed phase on droplet behavior in sheared polybutadiene/ Poly(dimethylsiloxane) blends. J Rheol, 47, 37-57.

Lerdwijitjarud, W., Sirivat, A., and Larson, R.G. (2004) Influence of dispersed-phase elasticity on steady state deformation and breakup of droplets in simple shearing flow of immiscible polymer blends. J. Rheol, 48, 843-862.

Mighri, F., Carreau, P.J., and Ajji, A. (1998) Influence of elastic properties on drop deformation and in shear flow. J Rheol, 42, 1477-1490.

Mighri F., and Huneault M.A. (2001) Dispersion visualization of model fluids in a transparent Couette flow cell. J Rheol, 45, 783-797.

Migler, K.B. (2000) Droplet vorticity alignment on model polymer blends. J Rheol, 44, 277-290.

Mo, H., Zhou, C., and Yu, W. (2000) A new method to determine interfacial tension from the retraction of ellipsoidal drops. J. Non Newtoniam Fluid Mech. 91, 221-232.

Palierne, J.F. (1990) Linear rheology of viscous properties of emulsions with interfacial tension. Rheol. Acta, 29, 204-214.

Rumscheidt, F.D., and Mason, S.G. (1961) Particle Motions in Sheared Suspensions. XII. Deformation and burst of fluid drops in shear and hyperbolic flow. J Coll Sci, 16, 238-261.

Taylor G.I. (1932) The viscosity of a fluid containing small drops of another fluid. Proc. R. Soc A, 138, 41-48.

Taylor G.I. (1934) The formation of emulsions in definable fields of flow. Proc R Soc A, 146, 501-523.

Wannaborworn S., Mackley M. R., and Renardy Y. (2002) Experimental observation and matching numerical simulation for the deformation and breakup of immiscible drops in oscillatory shear. J Rheol, 46(5), 1279-1293.

APPENDICES

Appendix A Rheological properties of the samples

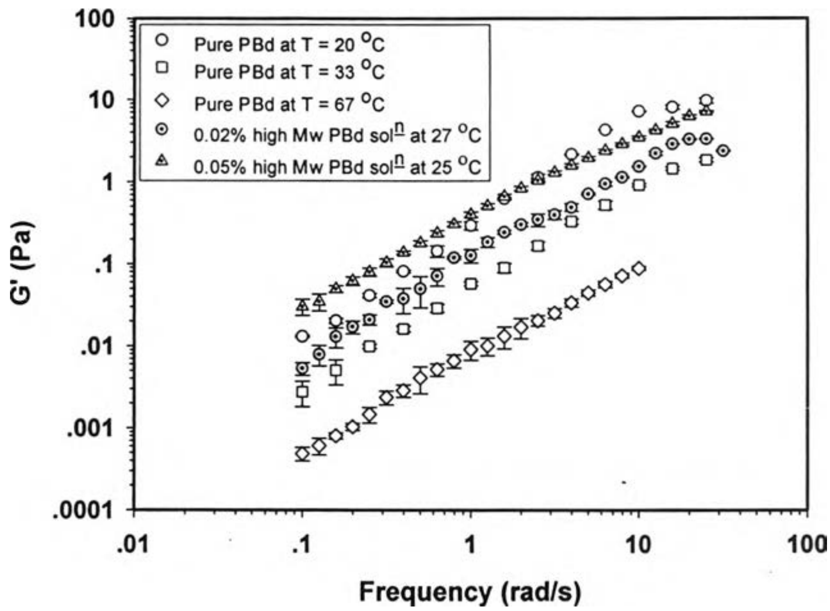

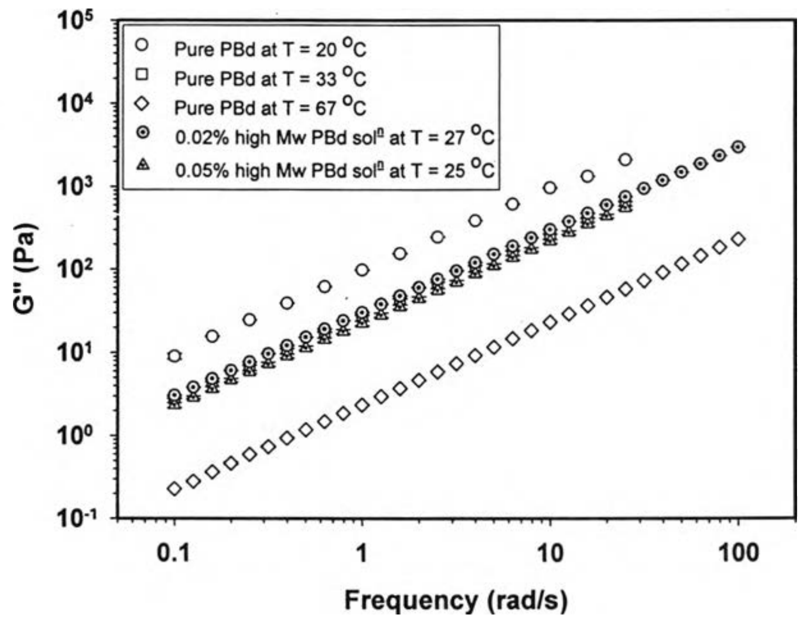

Figure A1 G' and G" vs. frequency of the dispersed phases at different temperatures.

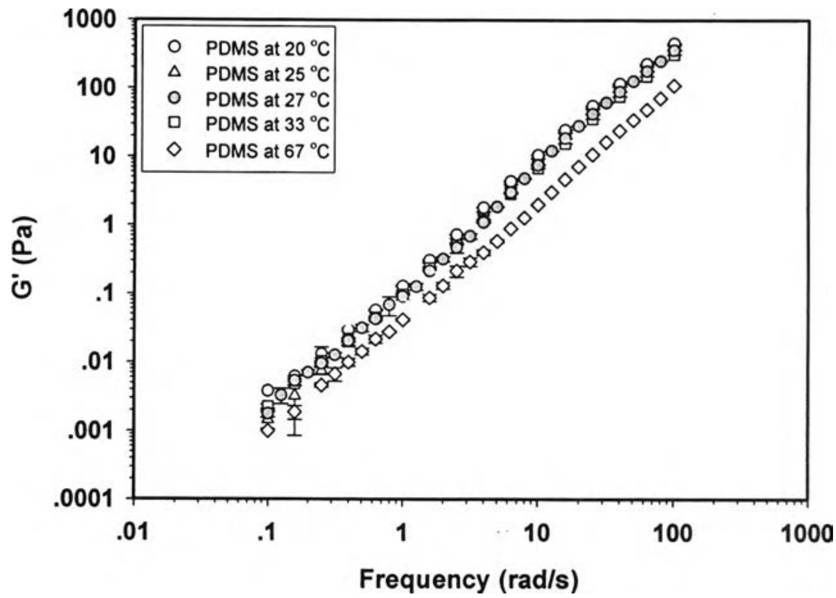

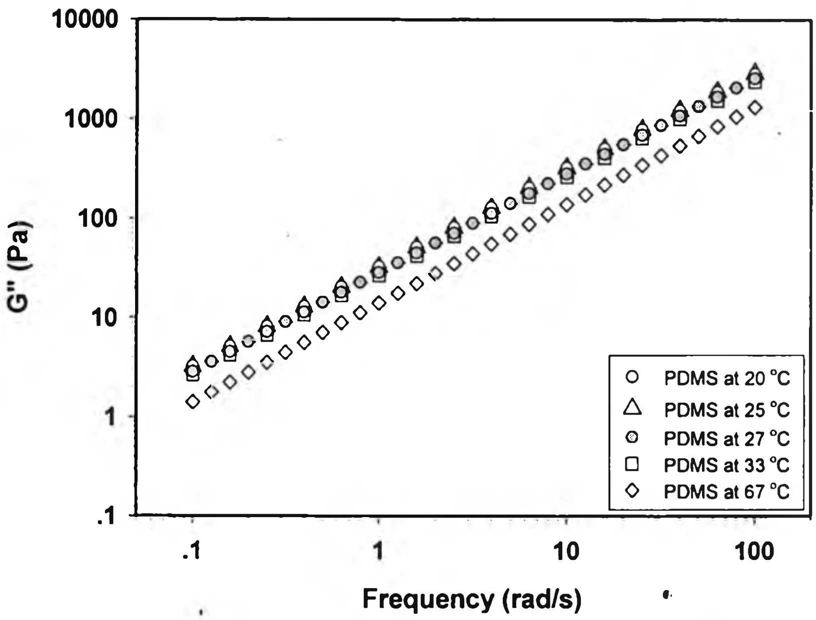

Figure A2 G' and G" vs. frequency of the matrix phase at different temperatures.

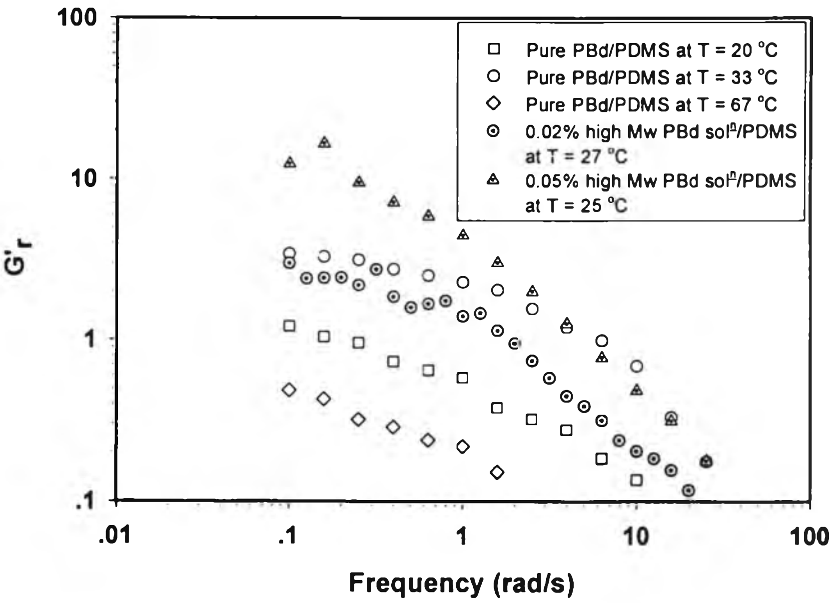

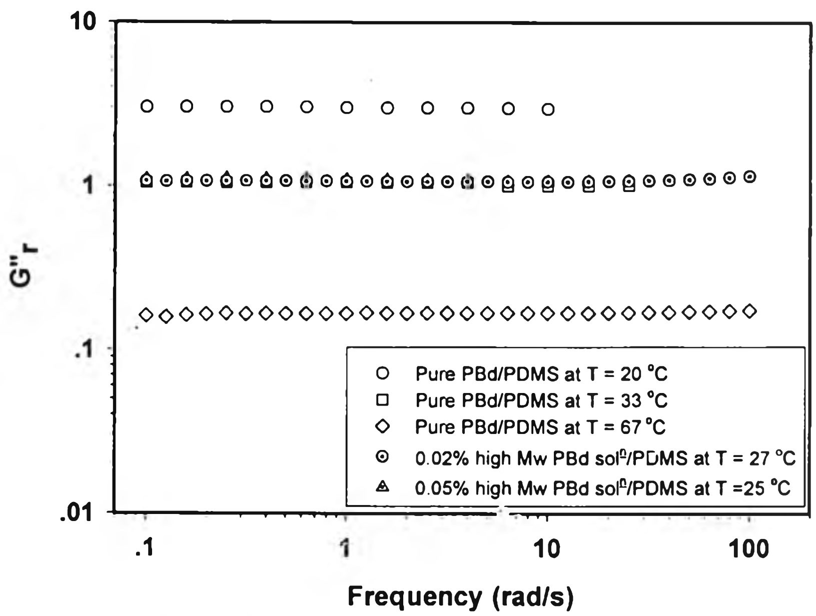

Figure A3 G'_r and G''_r vs. frequency of the blend components at different temperatures.

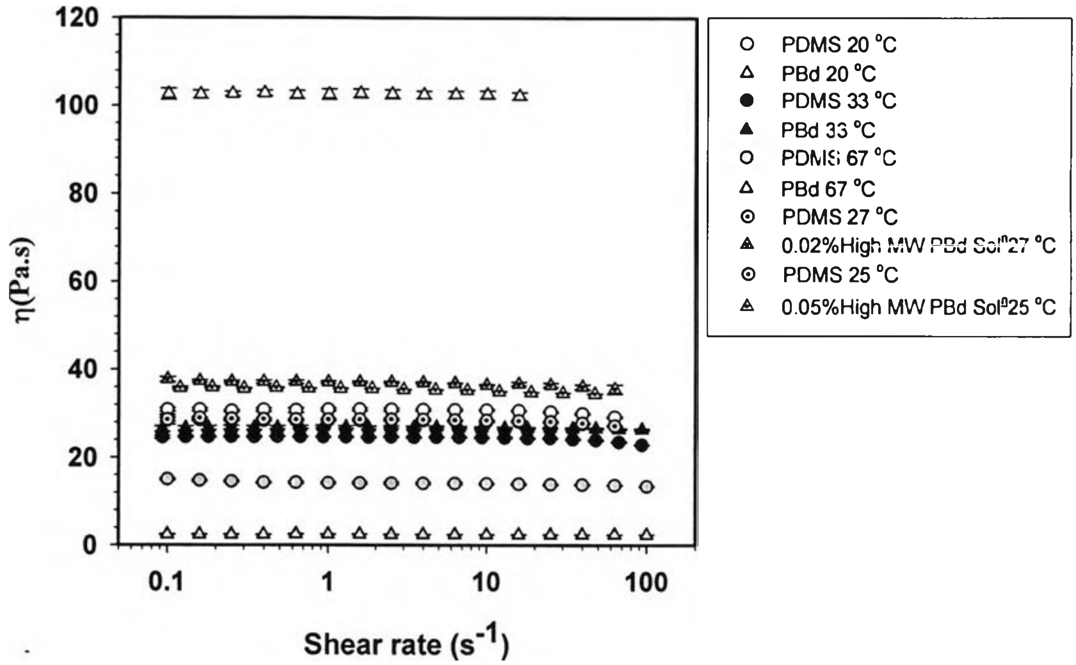

Figure A4 viscosity vs. shear rate of the sample at different temperatures.

Appendix B Relaxation experiment of the blend components

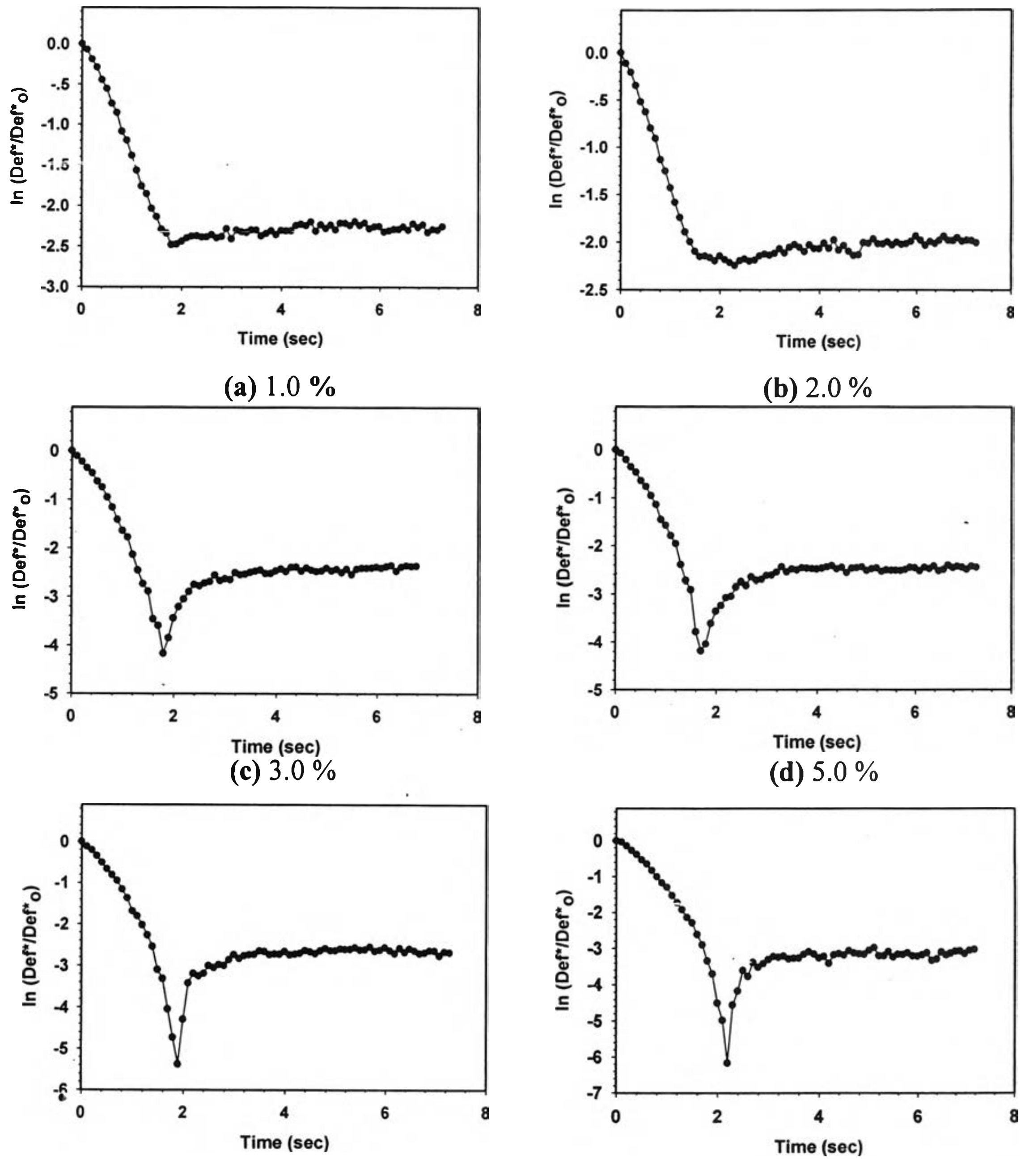

(a) 1.0 %
(b) 2.0 %
(c) 3.0 %
(d) 5.0 %
(e) 10.0 %
(f) 20.0 %

Figure B1 ln (Def*/Def*$_o$) vs. time of pure PBd/PDMS at shear rate = 1 S^{-1}, T = 67 °C, G"$_r$ = 0.16, gap = 2,200 μm, d_o ~ 200 μm at various strain: a) 1.0%; b) 2.0%; c) 3.0%; d) 5.0%; e) 10.0%; and f) 20.0%.

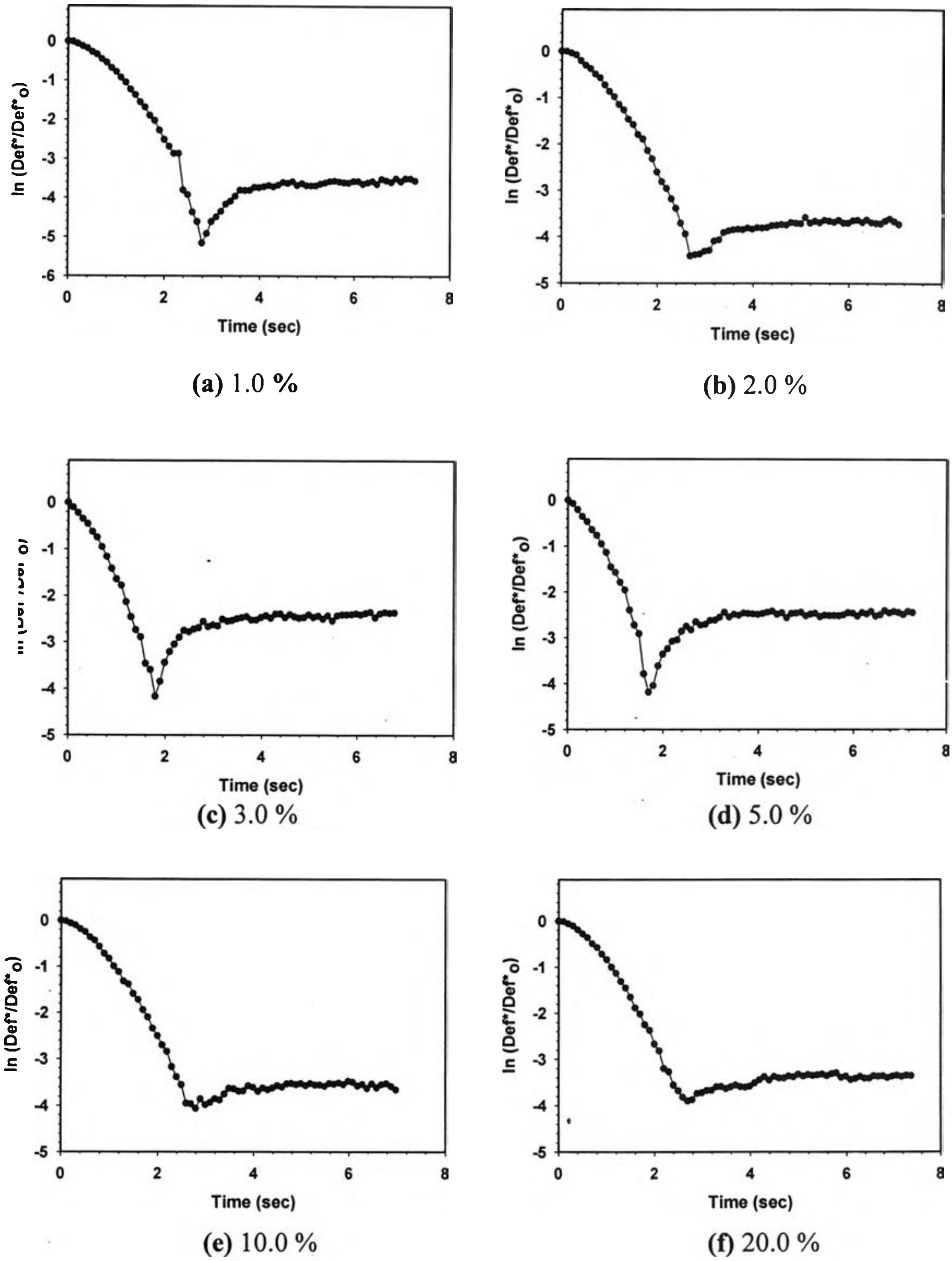

Figure B2 ln (Def*/Def*$_o$) vs. time of pure PBd/PDMS at shear rate = 2 S^{-1}, T = 67 °C, G''_r = 0.16, gap = 2,200 μm, d_o ~ 200 μm at various strain: a) 1.0%; b) 2.0%; c) 3.0%; d) 5.0%; e) 10.0%; and f) 20.0%.

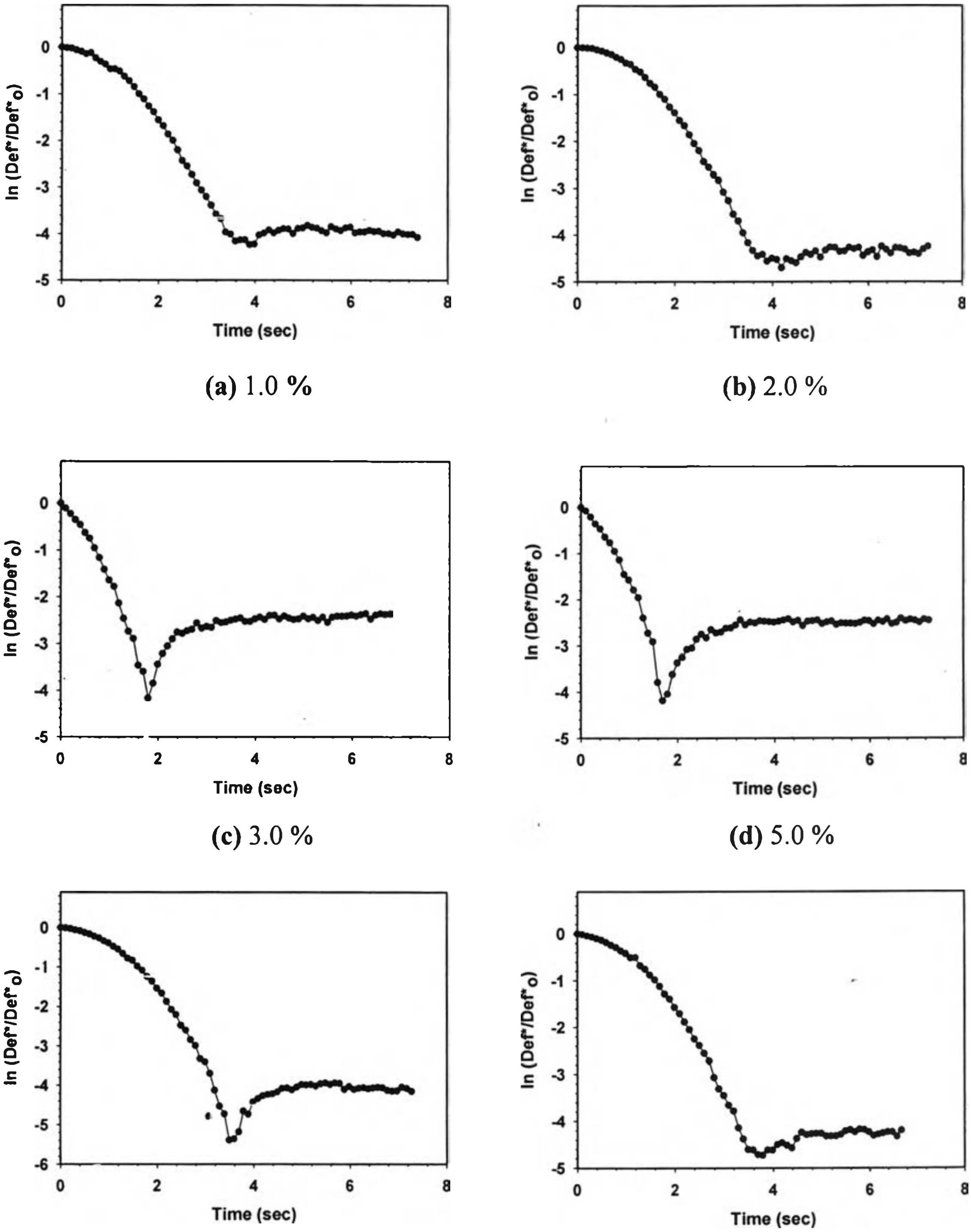

(a) 1.0 %

(b) 2.0 %

(c) 3.0 %

(d) 5.0 %

(e) 10.0 %

(f) 20.0 %

Figure B3 ln (Def*/Def*$_o$) vs. time of pure PBd/PDMS at shear rate = 3 S^{-1}, T = 67 °C, G''_r = 0.16, gap = 2,200 μm, d_o ~ 200 μm at various strain: a) 1.0%; b) 2.0%; c) 3.0%; d) 5.0%; e) 10.0%; and f) 20.0%.

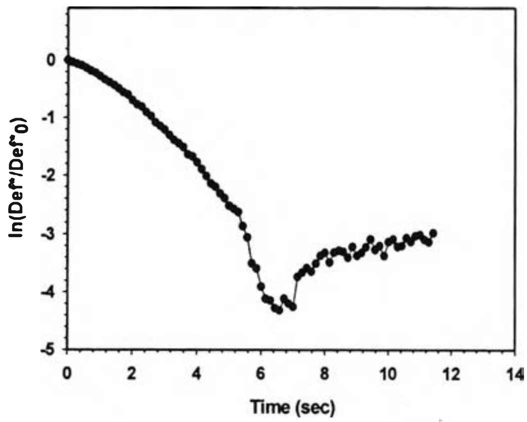

(a) 0.75 %

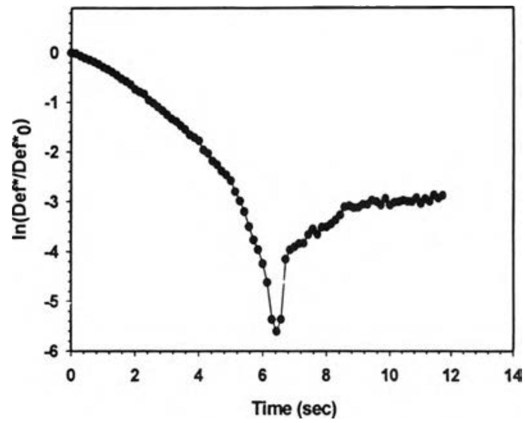

(b) 1.0 %

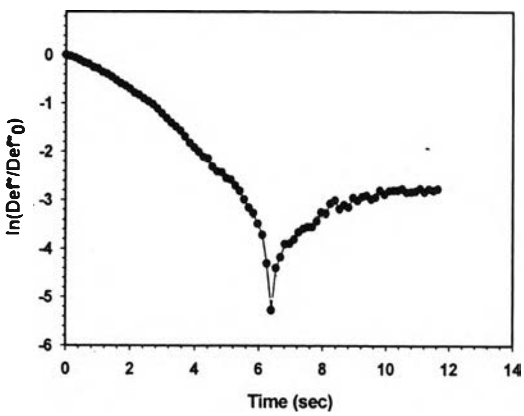

(c) 1.5 %

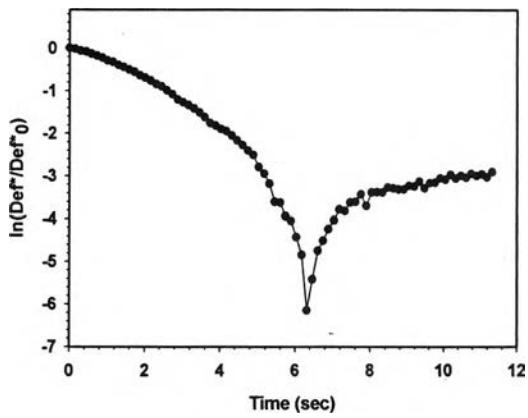

(d) 2.0 %

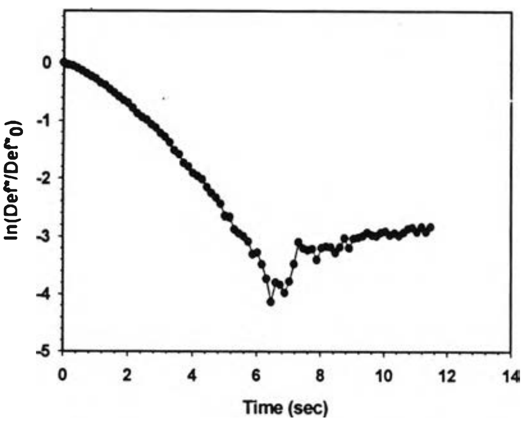

(e) 3.0 %

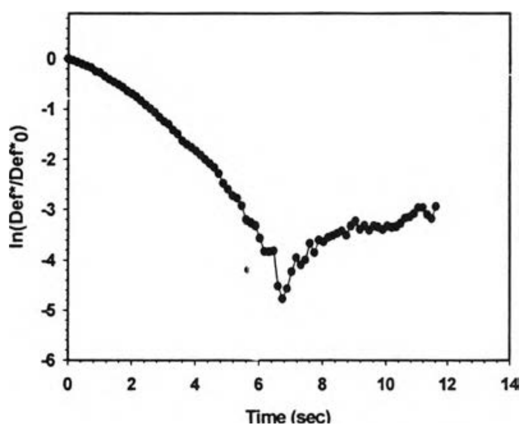

(f) 5.0 %

Figure B4 ln (Def*/Def*$_o$) vs. time of pure PBd/PDMS at shear rate = 1 S^{-1}, T = 33 °C, G''_r = 1, gap = 2,200 μm, d_o ~ 200 μm at various strain: a) 0.75%; b) 1.0%; c) 1.5%; d) 2.0%; e) 3.0%; and f) 5.0%.

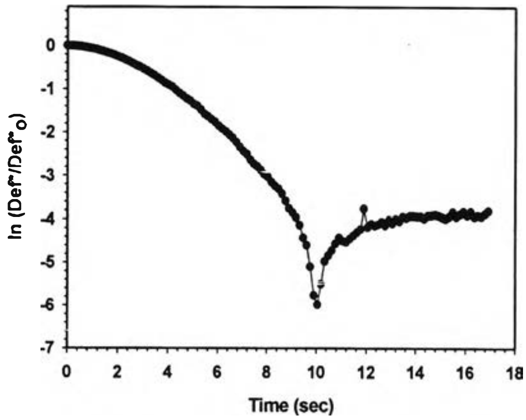

(a) 0.75 %

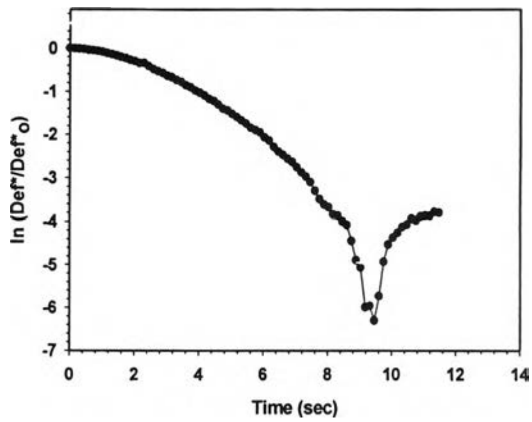

(b) 1.0 %

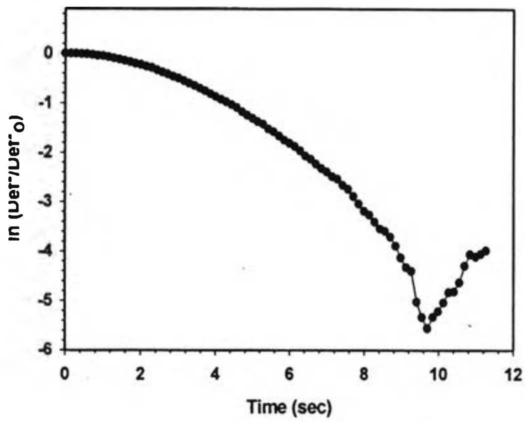

(c) 1.5 %

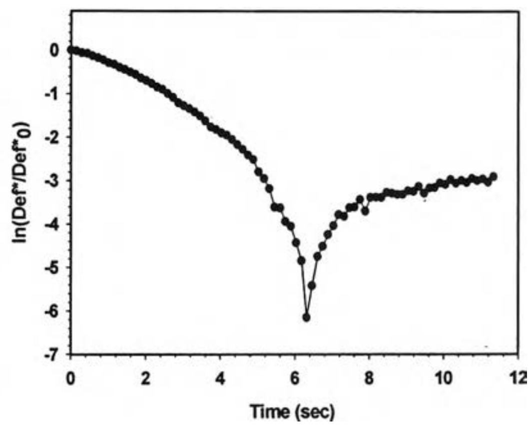

(d) 2.0 %

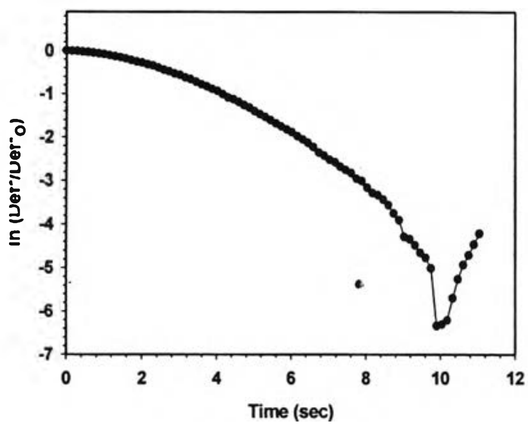

(e) 3.0 %

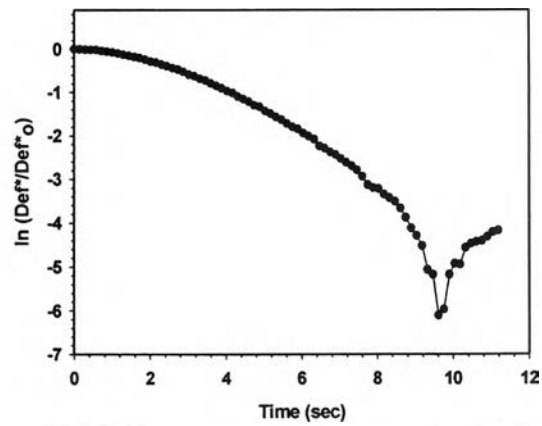

(f) 5.0 %

Figure B5 ln (Def*/Def*$_o$) vs. time of pure PBd/PDMS at shear rate = 2 S^{-1}, T = 33 °C, G''_r = 1, gap = 2,200 μm, d_o ~ 200 μm at various strain: a) 0.75%; b) 1.0%; c) 1.5%; d) 2.0% e) 3.0%; and f) 5.0%.

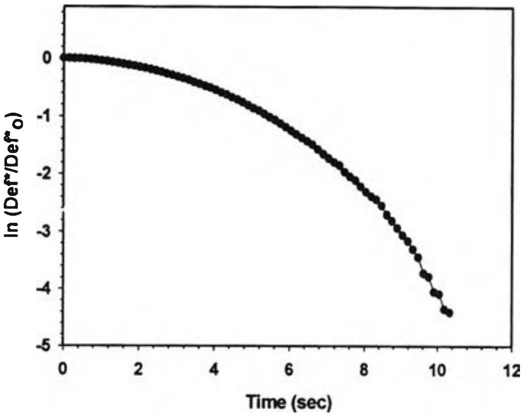

(a) 0.75 %

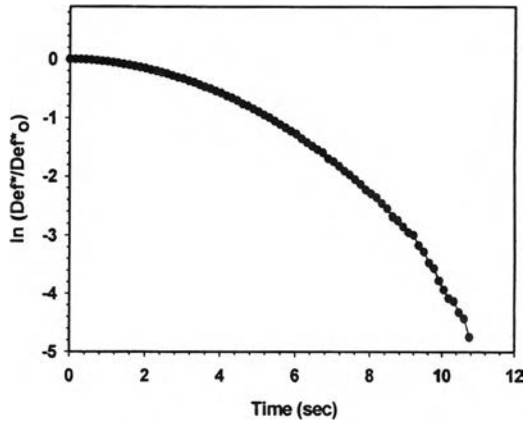

(b) 1.0 %

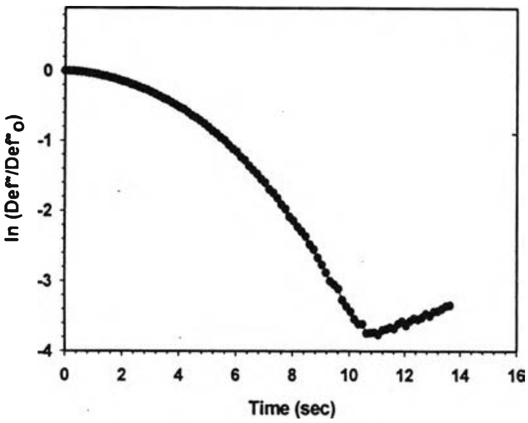

(c) 1.5 %

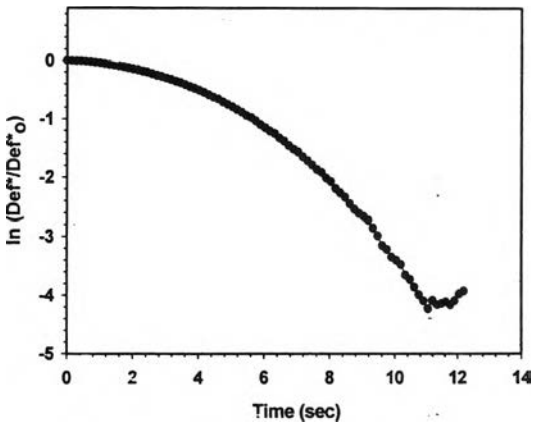

(d) 2.0 %

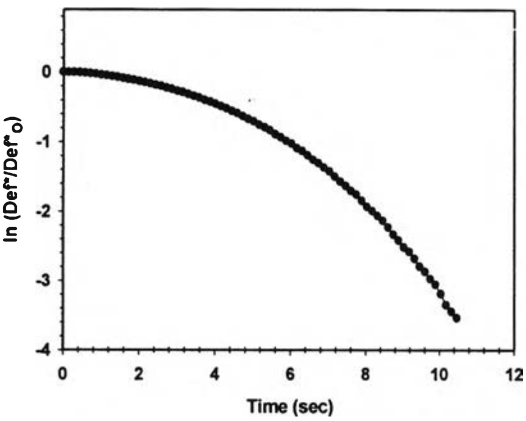

(e) 3.0 %

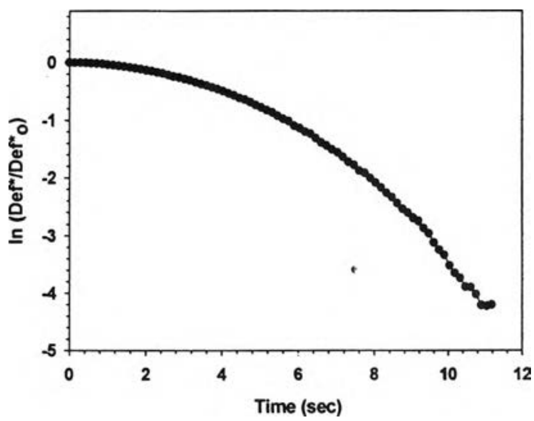

(f) 4.0 %

Figure B6 ln (Def*/Def*$_o$) vs. time of pure PBd/PDMS at shear rate = 3 S^{-1}, T = 33 °C, G''_r = 1, gap = 2,200 μm, d_o ~ 200 μm at various strain: a) 0.75%; b) 1.0%; c) 1.5%; d) 2.0%; e) 3.0%; and f) 4.0%.

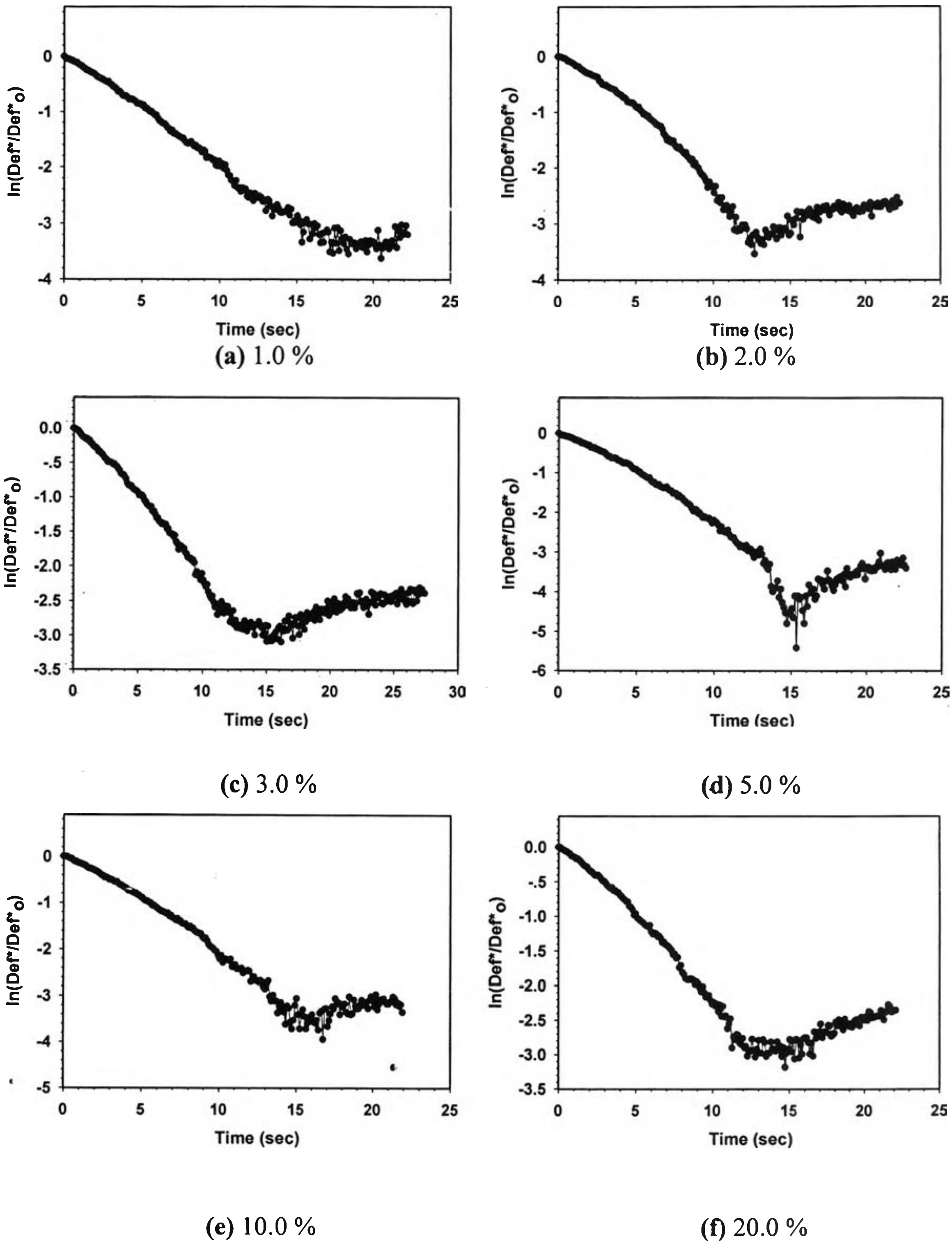

Figure B7 ln (Def*/Def*$_o$) vs. time of pure PBd/PDMS at shear rate = 1 S^{-1}, T = 20 °C, G''_r = 3.0, gap = 2,200 μm, d_o ~ 200 μm at various strains: a) 1.0%; b) 2.0%; c) 3.0%; d) 5.0%; e) 10.0%; and f) 20.0%.

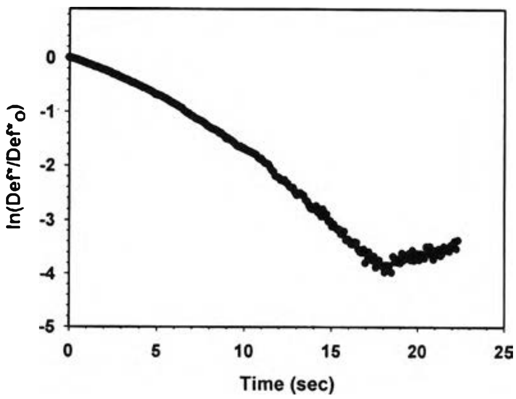

(a) 1.0 %

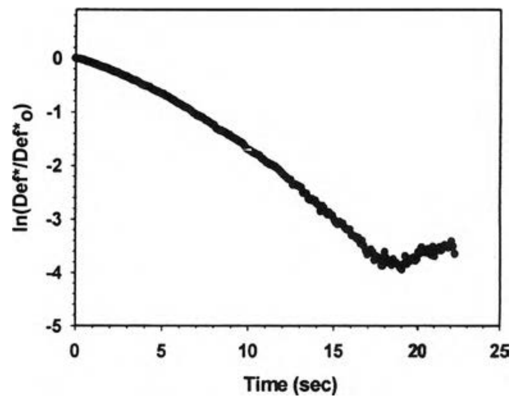

(b) 2.0 %

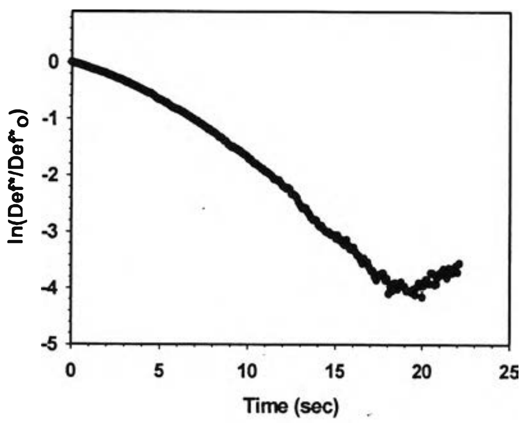

(c) 3.0 %

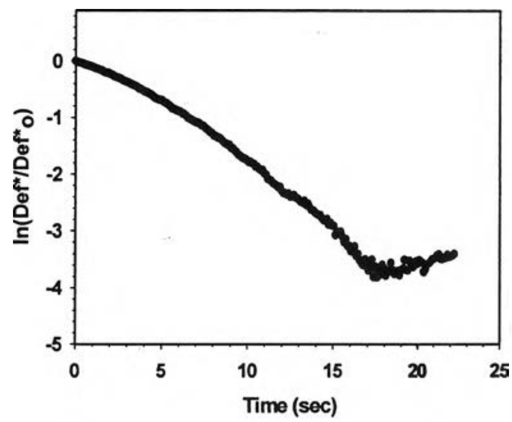

(d) 5.0 %

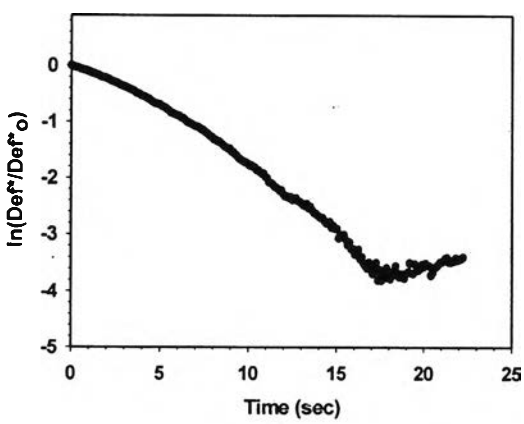

(e) 10.0 %

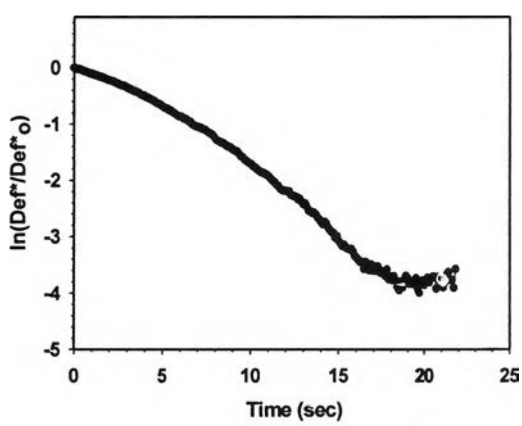

(f) 20.0 %

Figure B8 ln (Def^*/Def^*_o) vs. time of pure PBd/PDMS at shear rate = 2 S^{-1}, T = 20 °C, G''_r = 3.0, gap = 2,200 μm, d_o ~ 200 μm at various strains: a) 1.0%; b) 2.0%; c) 3.0%; d) 5.0%; e) 10.0%; and f) 20.0%.

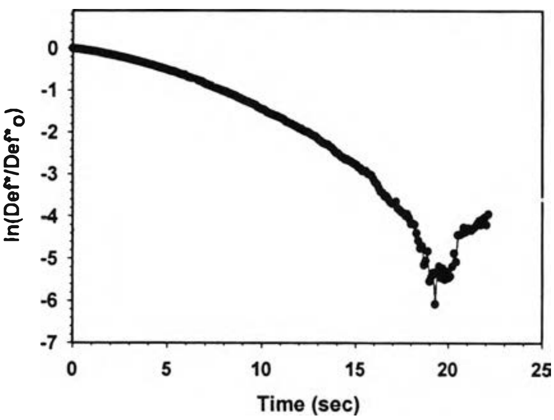

(a) 1.0 %

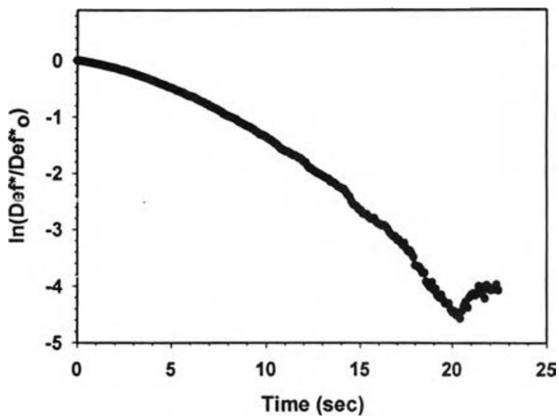

(b) 2.0 %

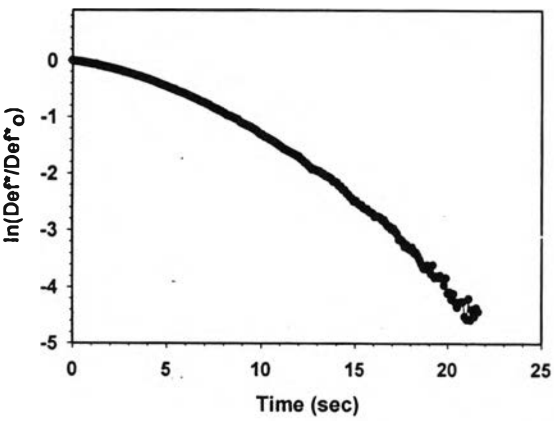

(c) 3.0 %

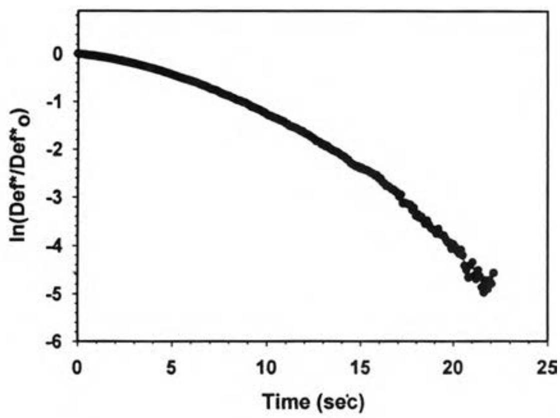

(d) 5.0 %

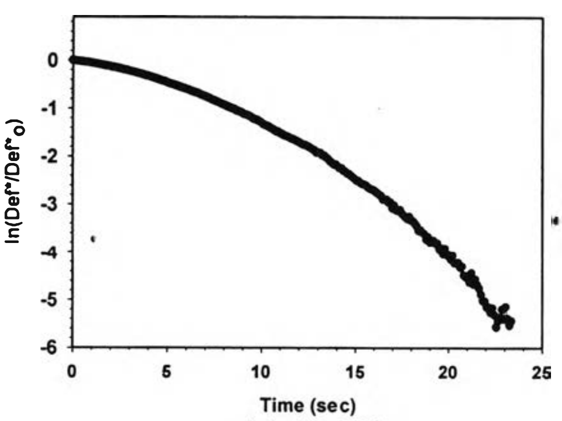

(e) 10.0 %

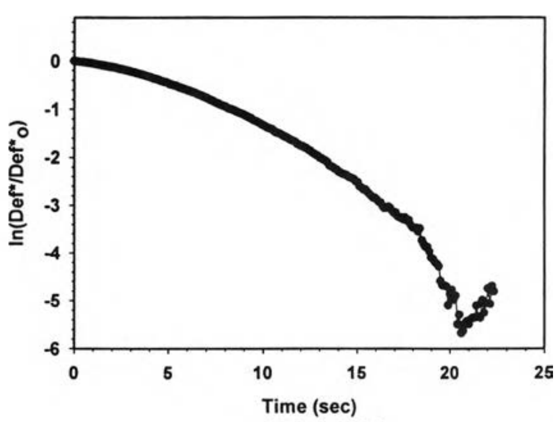

(f) 20.0 %

Figure B9 ln (Def*/Def*$_o$) vs. time of pure PBd/PDMS at shear rate = 3 S^{-1}, T = 20 °C, G''_r = 3.0, gap = 2,200 μm, d_o ~ 200 μm at various strains: a) 1.0%; b) 2.0%; c) 3.0%; d) 5.0%; e) 10.0%; and f) 20.0%.

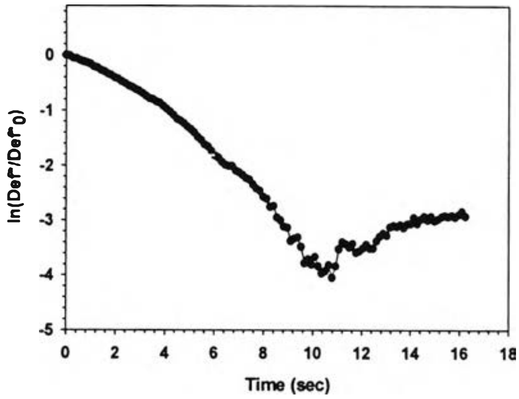

(a) 1.0 %

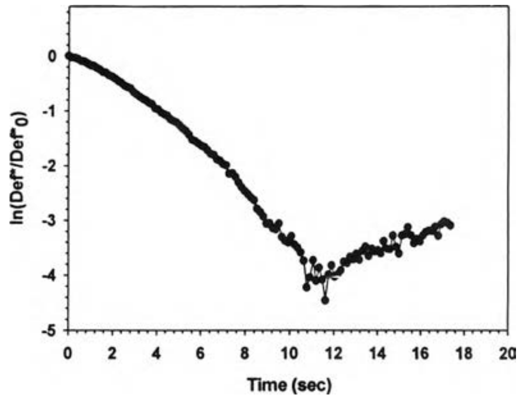

(b) 2.0 %

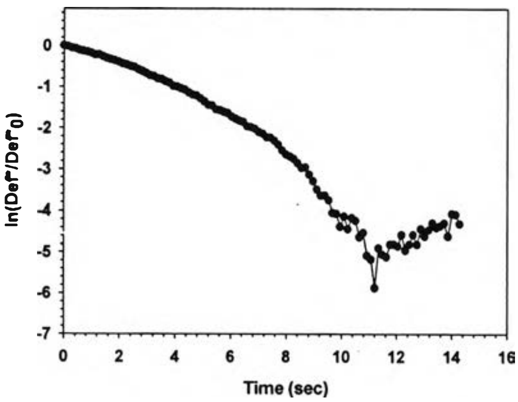

(c) 3.0 %

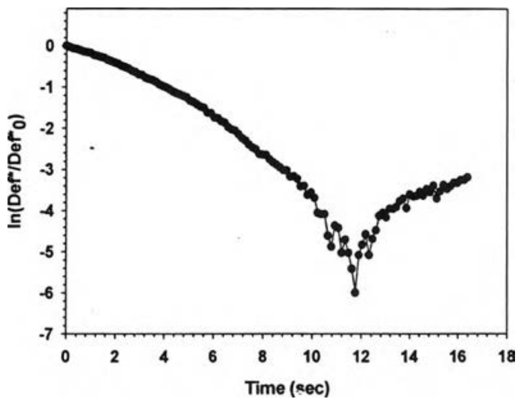

(d) 5.0 %

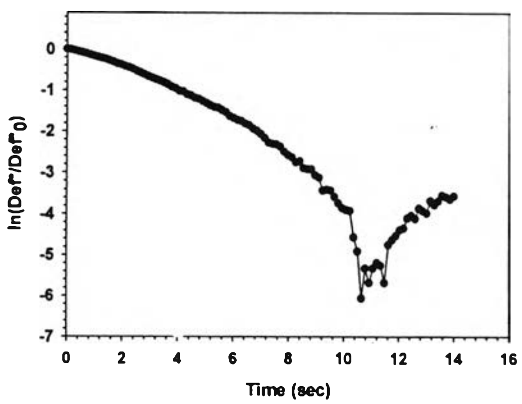

(e) 10.0 %

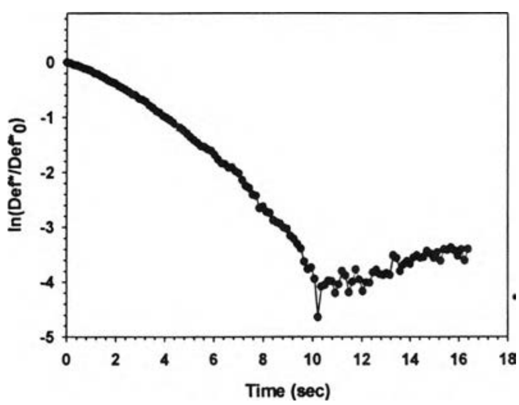

(f) 20.0 %

Figure B10 ln (Def^*/Def^*_o) vs. time of 0.02% High Mw PBd Sol$^{\underline{n}}$/PDMS at shear rate = 1 S^{-1}, T = 27 °C, gap = 2,200 μm, d_o ~ 200 μm at various strains: a) 1.0%; b) 2.0%; c) 3.0%; d) 5.0%; e) 10.0%; and f) 20.0%.

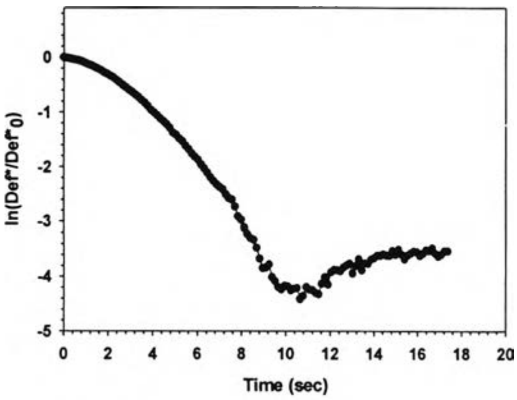

(a) 1.0 %

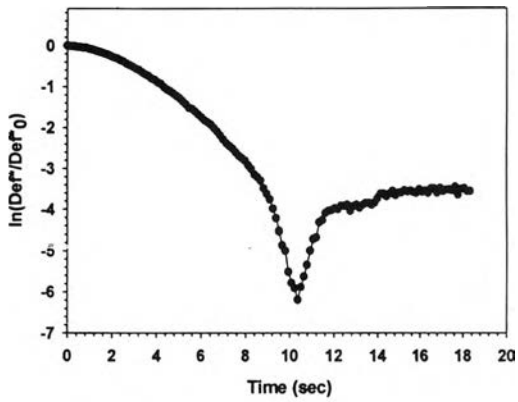

(b) 2.0 %

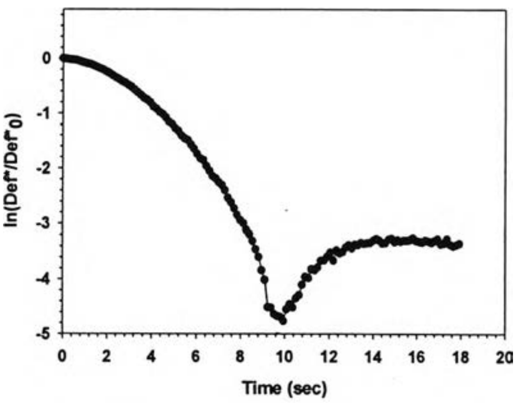

(c) 3.0 %

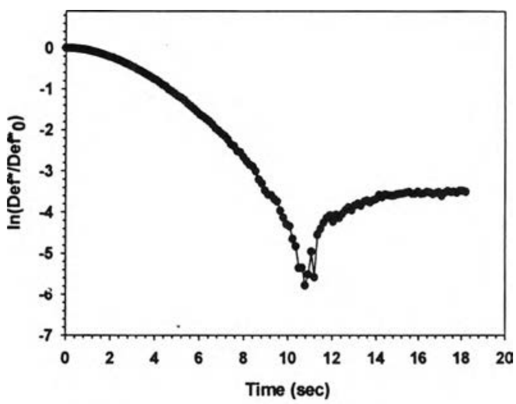

(d) 5.0 %

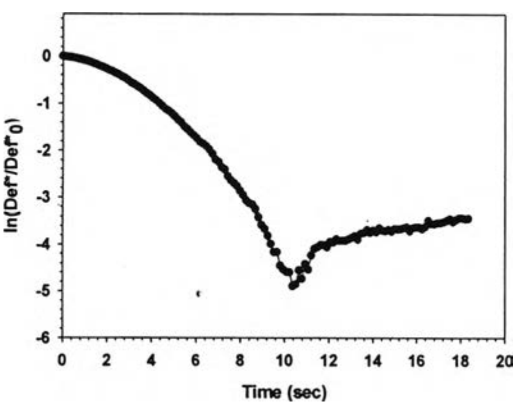

(e) 10.0 %

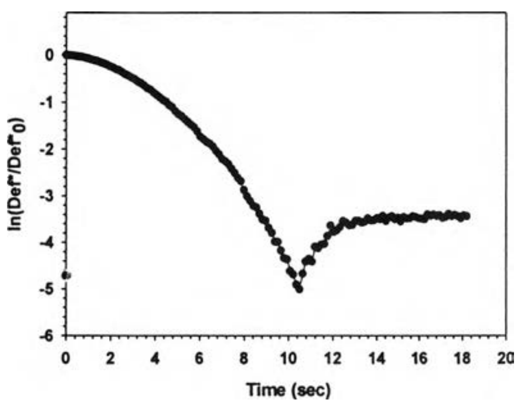

(f) 20.0 %

Figure B11 ln (Def*/Def*$_o$) vs. time of 0.02% High Mw PBd Sol$^{\underline{n}}$/PDMS at shear rate = 2 S^{-1}, T = 27 °C, gap = 2,200 μm, d_o ~ 200 μm at various strains: a) 1.0%; b) 2.0%; c) 3.0%; d) 5.0%; e) 10.0%; and f) 20.0%.

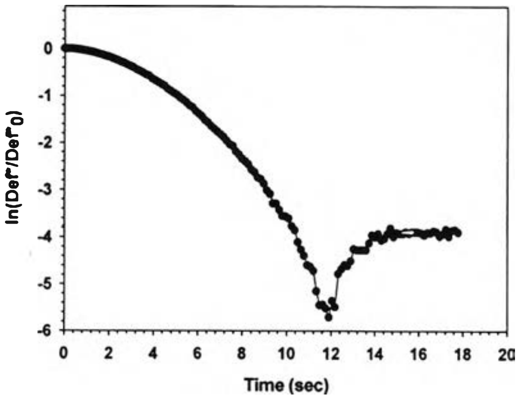

(a) 1.0 %

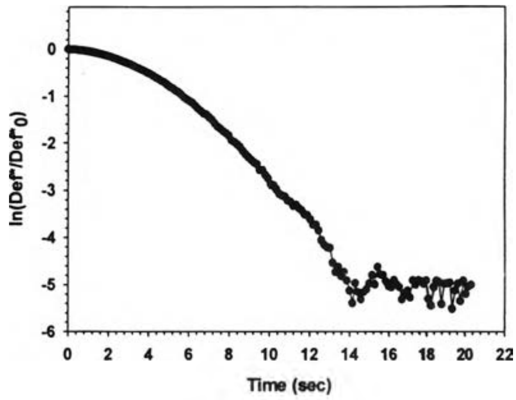

(b) 2.0 %

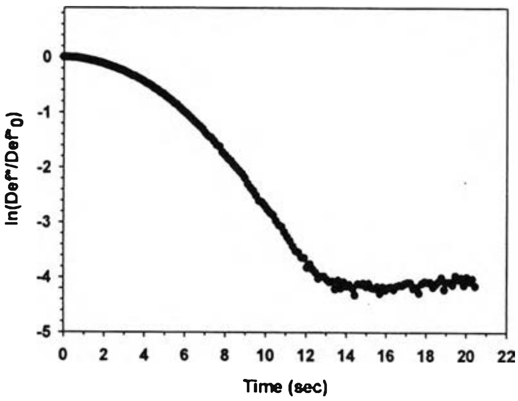

(c) 3.0 %

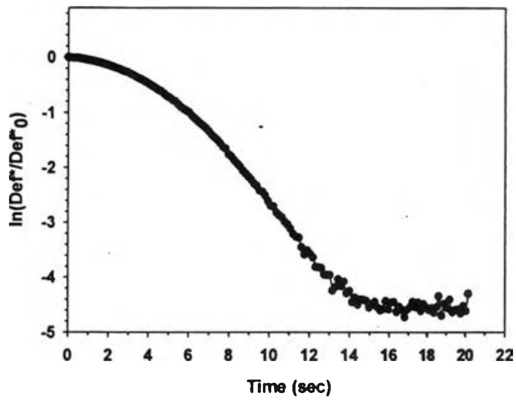

(d) 5.0 %

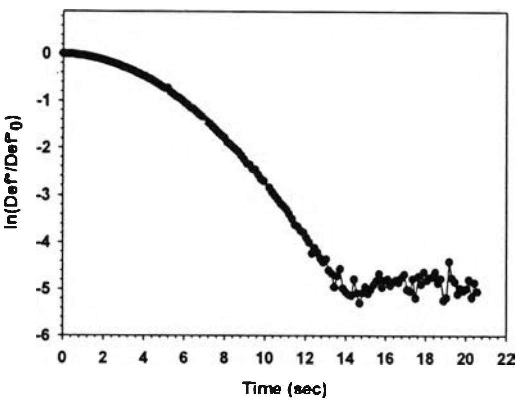

(e) 10.0 %

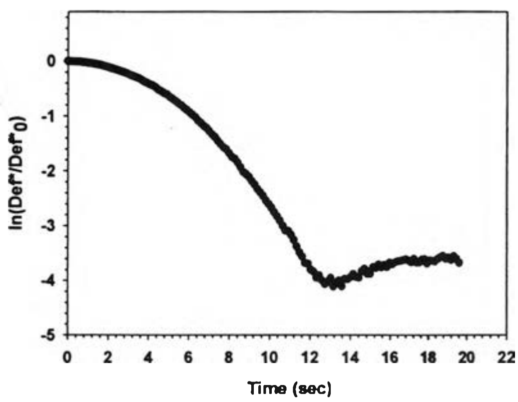

(f) 20.0 %

Figure B12 ln (Def*/Def*$_o$) vs. time of 0.02% High Mw PBd Sol^{n}/PDMS at shear rate = 3 S^{-1}, T = 27 °C, gap = 2,200 μm, d_o ~ 200 μm at various strains: a) 1.0%; b) 2.0%; c) 3.0%; d) 5.0%; e) 10.0%; and f) 20.0%.

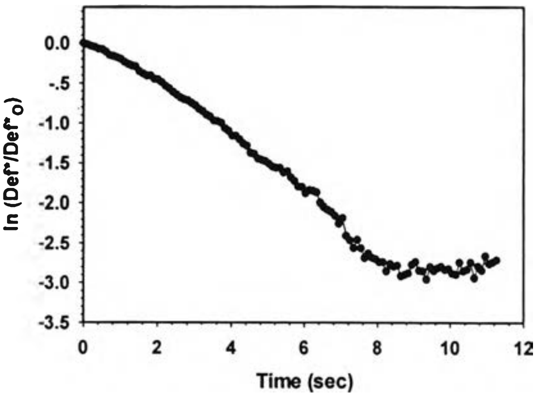

(a) 1.0 %

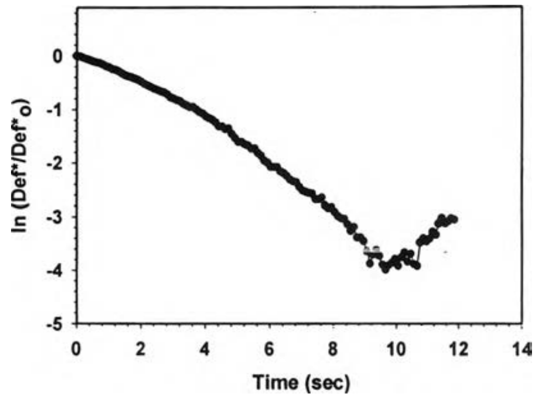

(b) 2.0 %

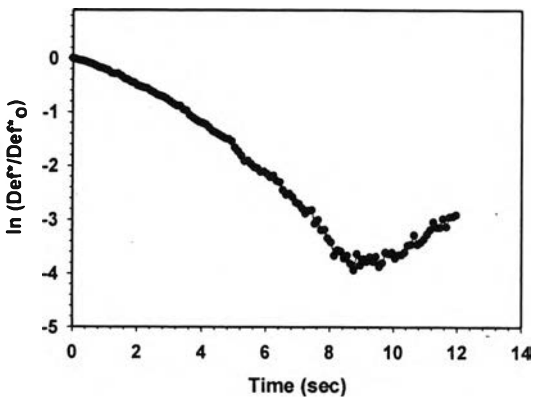

(c) 3.0 %

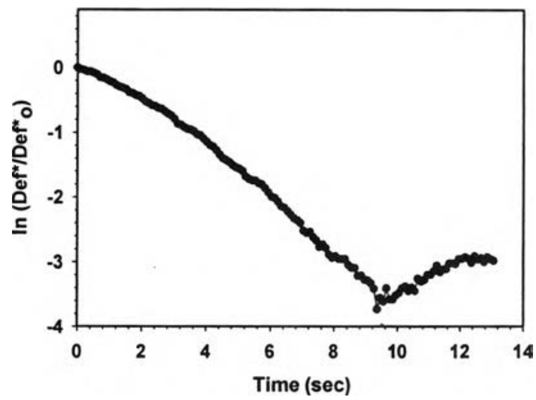

(d) 5.0 %

2D Graph 5

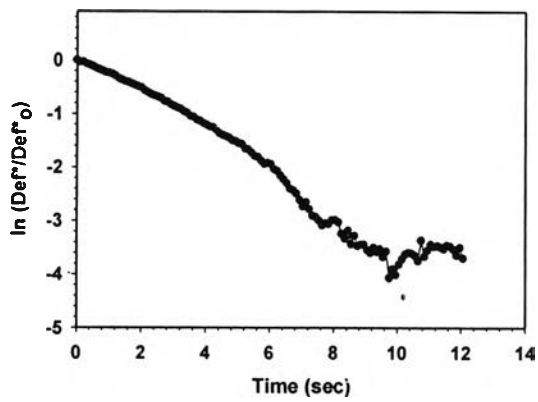

(e) 10.0 %

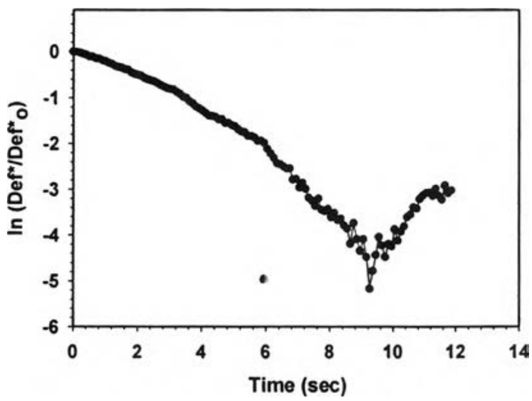

(f) 20.0 %

Figure B13 ln (Def*/Def*$_o$) vs. time of 0.05% High Mw PBd Sol$^{\underline{n}}$/PDMS at shear rate = 1 S^{-1}, T = 25 °C, gap = 2,200 μm, d_o ~ 200 μm at various strains: a) 1.0%; b) 2.0%; c) 3.0%; d) 5.0%; e) 10.0%; and f) 20.0%.

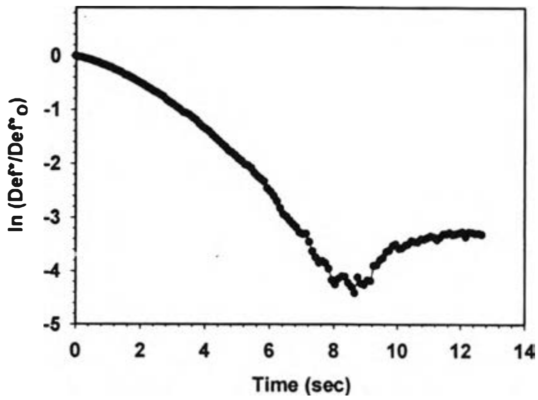

(a) 1.0 %

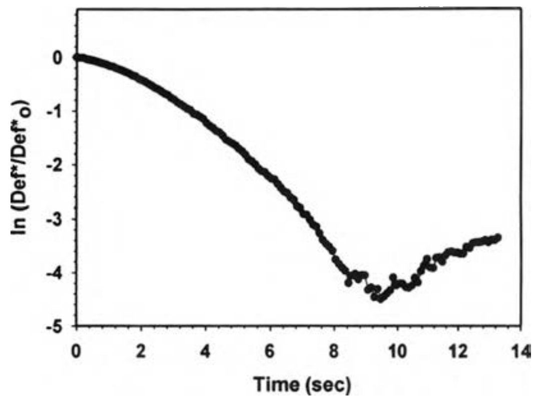

(b) 2.0 %

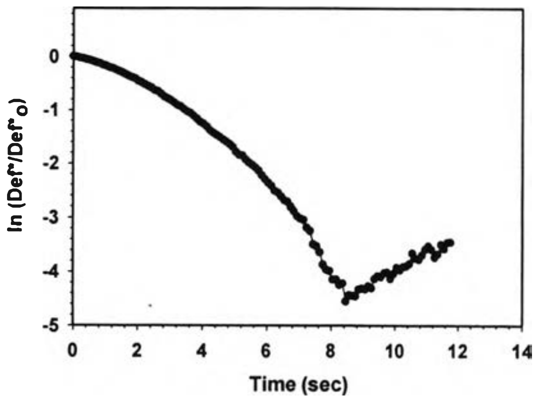

(c) 3.0 %

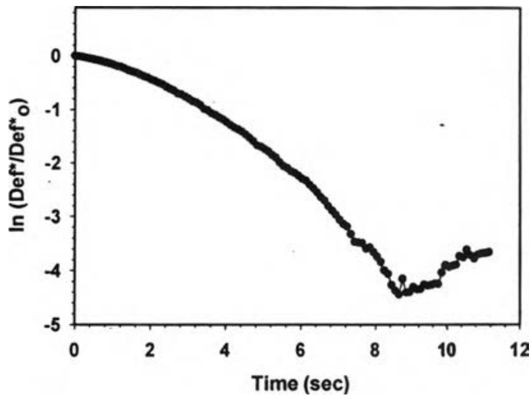

(d) 5.0 %

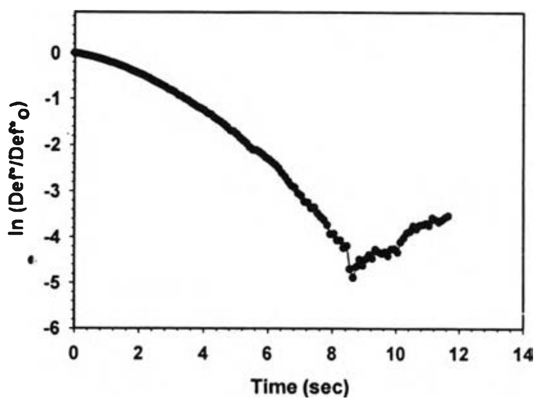

(e) 10.0 %

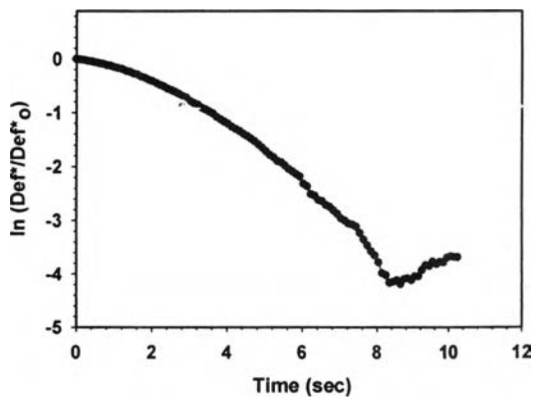

(f) 20.0 %

Figure B14 ln (Def*/Def*$_o$) vs. time of 0.05% High Mw PBd Sol$^{\underline{n}}$/PDMS at shear rate = 2 S^{-1}, T = 25 °C, gap = 2,200 μm, d_o ~ 200 μm at various strains: a) 1.0%; b) 2.0%; c) 3.0%; d) 5.0%; e) 10.0%; and f) 20.0%.

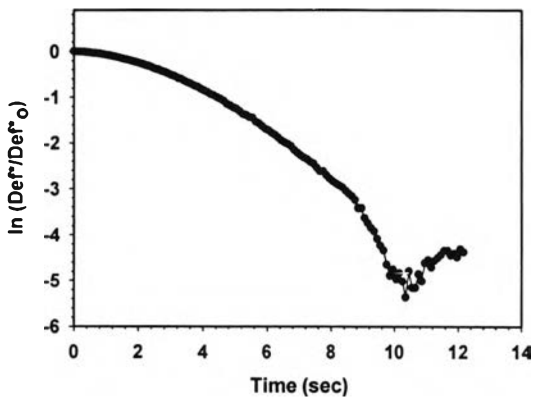

(a) 1.0 %

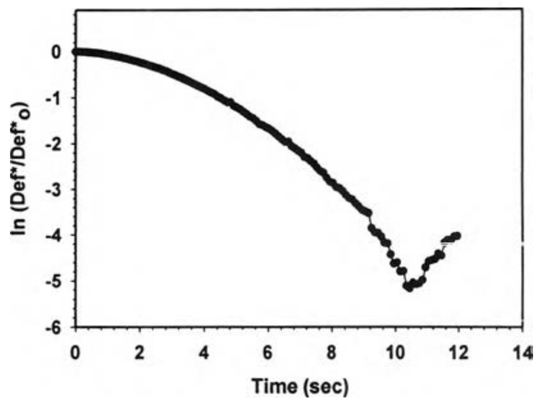

(b) 2.0 %

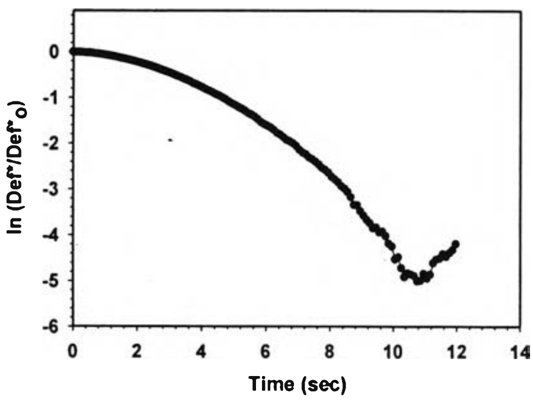

(c) 3.0 %

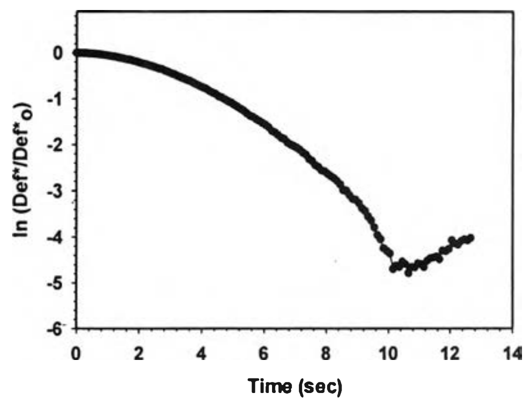

(d) 5.0 %

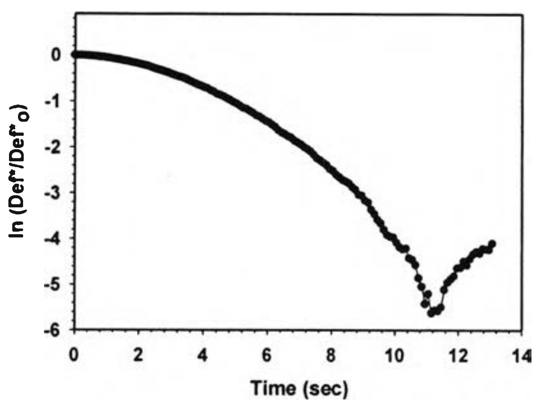

(e) 10.0 %

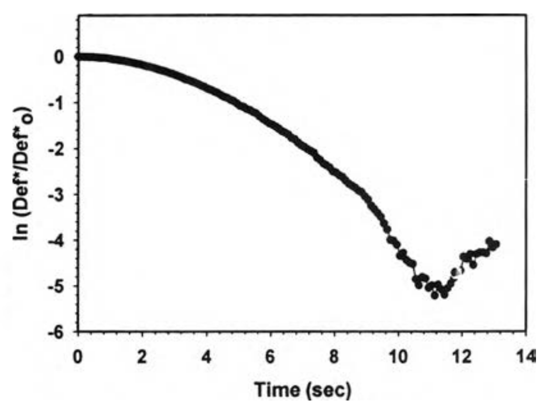

(f) 20.0 %

Figure B15 ln (Def*/Def*$_o$) vs. time of 0.05% High Mw PBd Sol$^{\underline{n}}$/PDMS at shear rate = 3 S^{-1}, T = 25 °C, gap = 2,200 μm, d_o ~ 200 μm at various strains: a) 1.0%; b) 2.0%; c) 3.0%; d) 5.0%; e) 10.0%; and f) 20.0%.

Appendix C Characteristic relaxation time of droplet

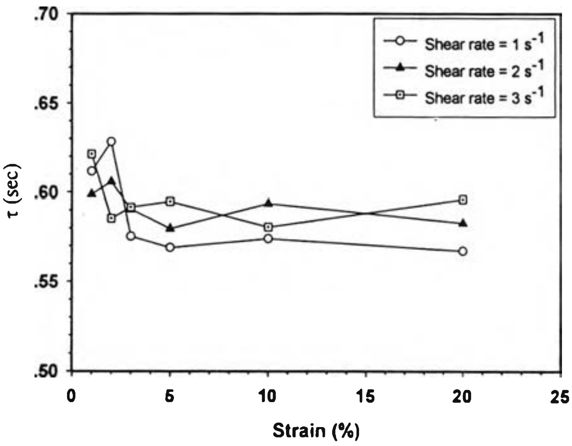

(a)

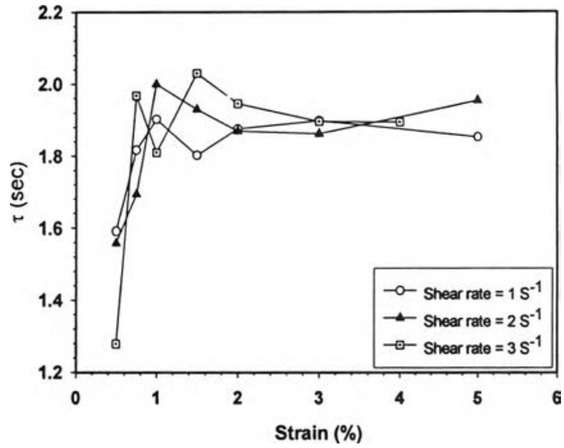

(b)

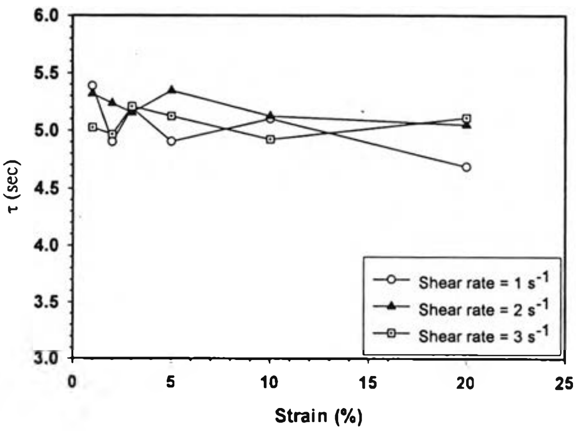

(c)

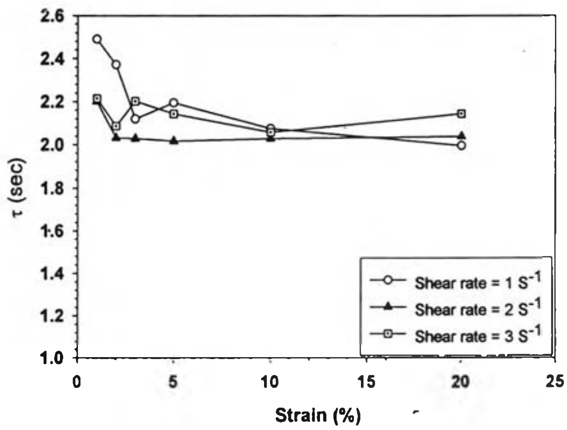

(d)

Figure C1 characteristic relaxation time vs. strain of blend components at different shear rates, strains and temperatures, $d_o \sim 200$ μm, gap = 2,200 μm : a) pure PBd/PDMS at T = 67 °C; b) pure PBd/PDMS at T = 33 °C; c) pure PBd/PDMS at T = 20 °C; d) 0.02% high Mw PBd sol^{n}/PDMS at T = 27 °C ; and e) 0.05% high Mw PBd sol^{n}/PDMS at T = 25 °C.

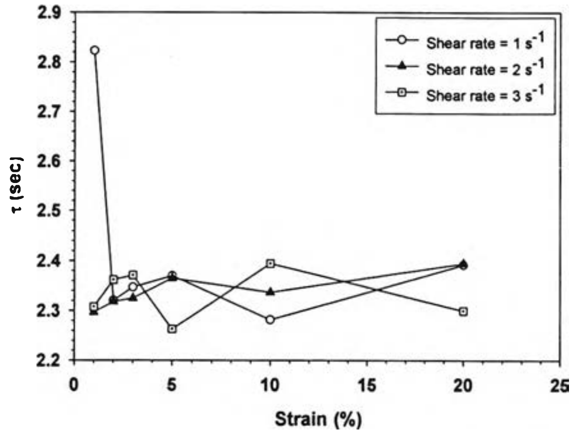

(e)

Figure C1(cont.) characteristic relaxation time vs. strain of blend components at different shear rates, strains and temperatures, $d_o \sim 200$ μm, gap = 2,200 μm : a) pure PBd/PDMS at T = 67 °C; b) pure PBd/PDMS at T = 33 °C; b) pure PBd/PDMS at T = 20 °C; d) 0.02% high Mw PBd sol$^{\underline{n}}$/PDMS at T = 27 °C ; and e) 0.05% high Mw PBd sol$^{\underline{n}}$/PDMS at T = 25 °C.

Appendix D Physical properties of the blend components

Table D1 Physical properties of the blend components

Blend components	T (°C)	G" $_r$	Characteristic relaxation time (sec)	Interfacial tension (N/m)
PBd/PDMS	67	0.16	5.100	3.5×10^{-3}
	33	1.00	1.900	2.9×10^{-3}
	20	3.00	0.585	2.67×10^{-3}
0.02%High Mw PBd sol$^{\underline{n}}$/PDMS	27	1.00	2.02	3.0×10^{-3}
0.05%High Mw PBd sol$^{\underline{n}}$/PDMS	25	1.00	2.30	3.02×10^{-3}

Appendix E Deformation parameters of deformed droplet

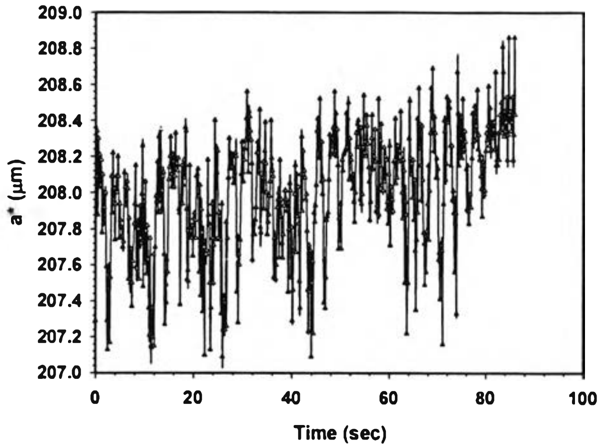

(a)

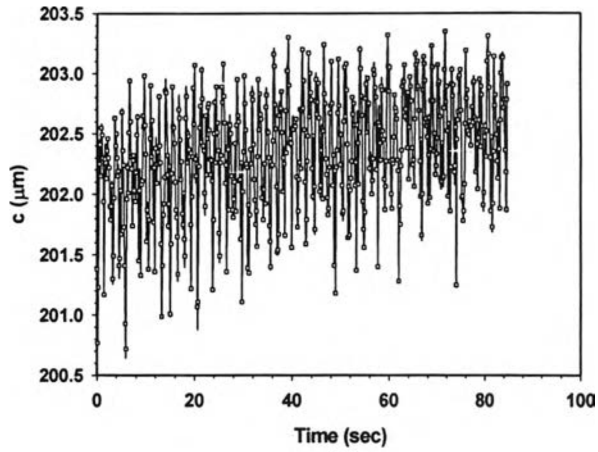

(b)

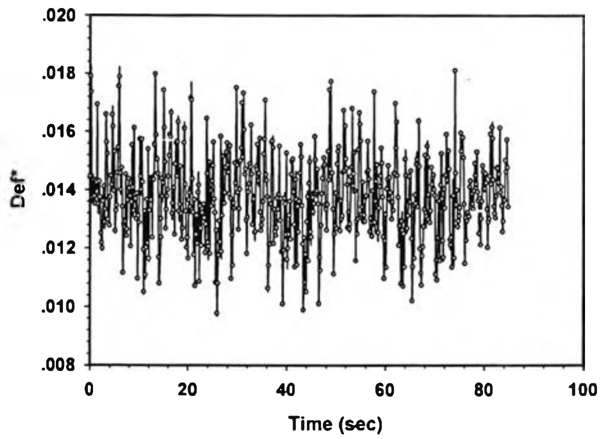

(c)

Figure E1 Deformation parameters vs. time of pure PBd/PDMS at strain 10%, frequency 0.35 Hz, $\tau_r = 0.2$, $G''_r = 0.16$, $d_o \sim 200$ μm, gap = 2,200 μm: a) a* vs. time; b) c vs. time; c) Def* vs. time.

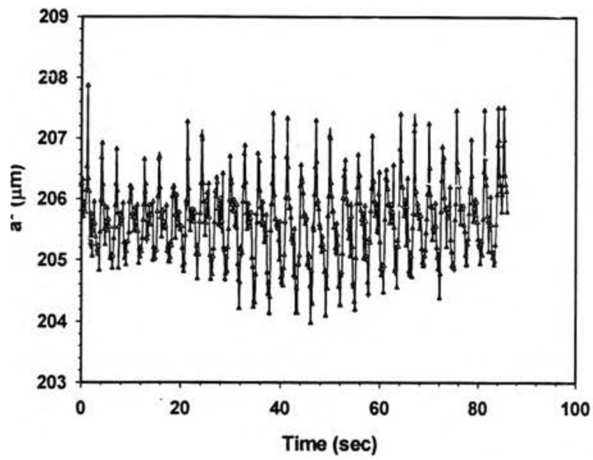

(a)

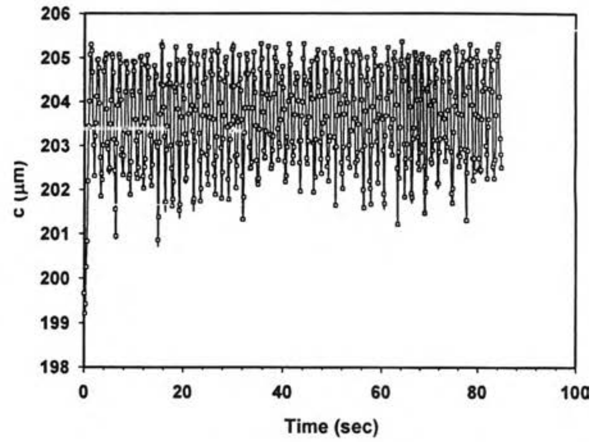

(b)

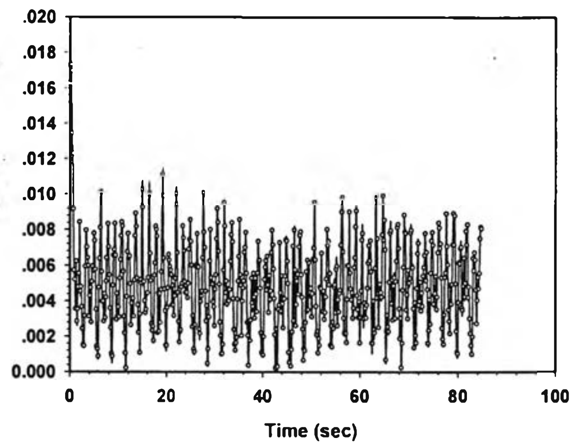

(c)

Figure E2 Deformation parameters vs. time of pure PBd/PDMS at strain 20%, frequency 0.35 Hz, $\tau_r = 0.2$, $G''_r = 0.16$, $d_o \sim 200$ µm, gap = 2,200 µm: a) a* vs. time; b) c vs. time; c) Def* vs. time.

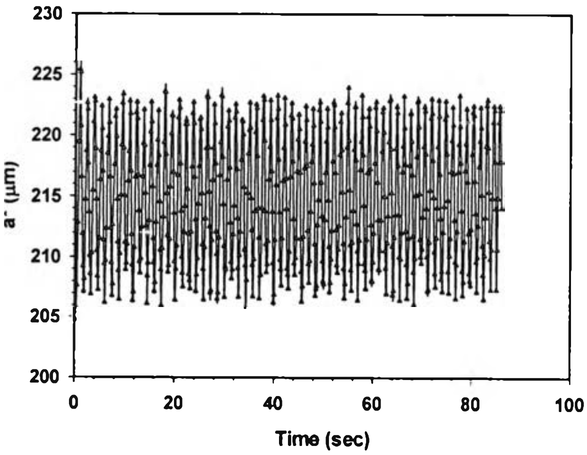

(a)

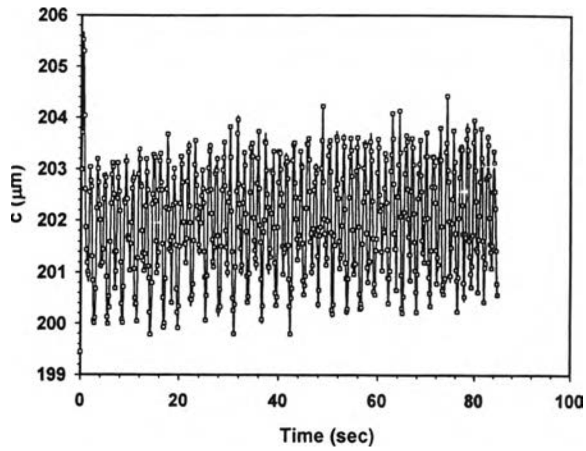

(b)

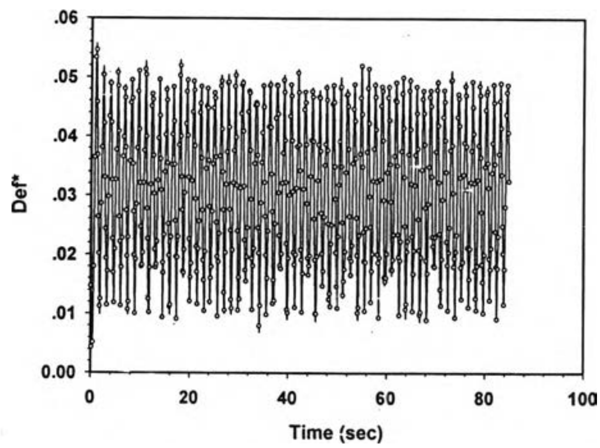

(c)

Figure E3 Deformation parameters vs. time of pure PBd/PDMS at strain 40%, frequency 0.35 Hz, $\tau_r = 0.2$, $G''_r = 0.16$, $d_o \sim 200$ μm, gap = 2,200 μm: a) a* vs. time; b) c vs. time; c) Def* vs. time.

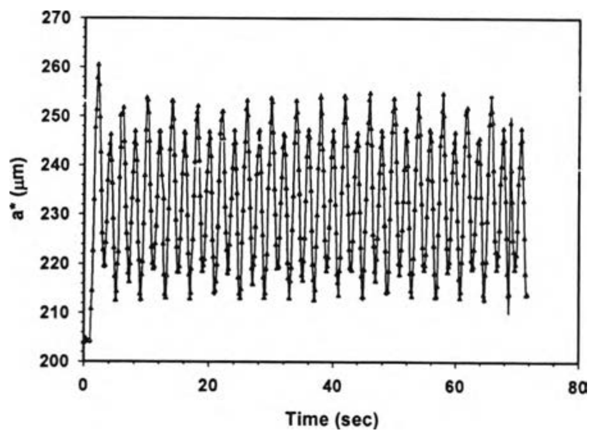

(a)

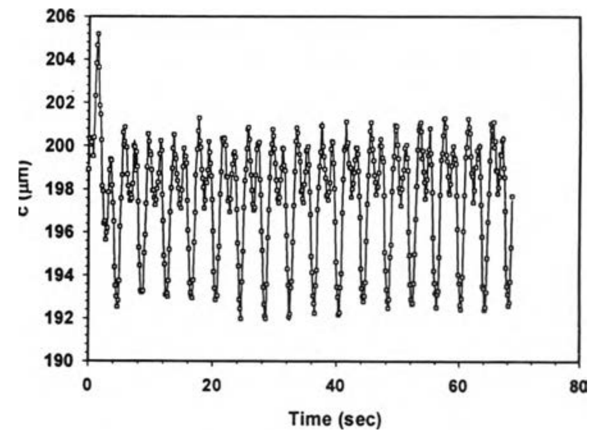

(b)

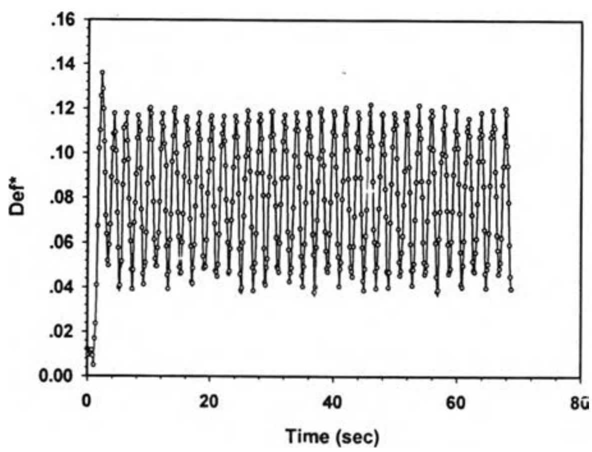

(c)

Figure E4 Deformation parameters vs. time of pure PBd/PDMS at strain 60%, frequency 0.35 Hz, $\tau_r = 0.2$, $G''_r = 0.16$, $d_o \sim 200$ µm, gap = 2,200 µm: a) a* vs. time; b) c vs. time; c) Def* vs. time.

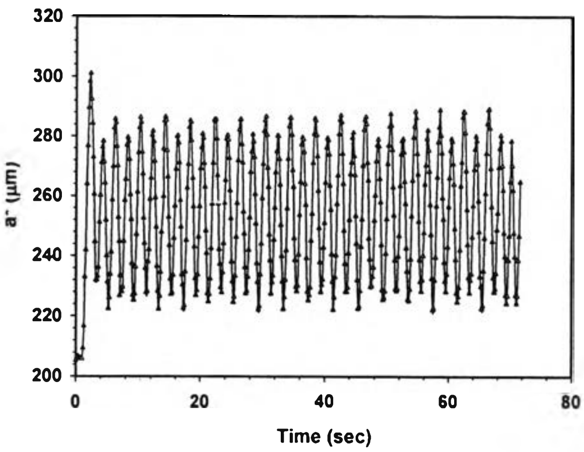

(a)

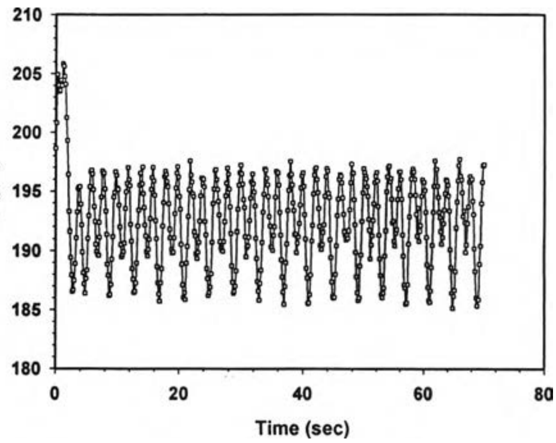

(b)

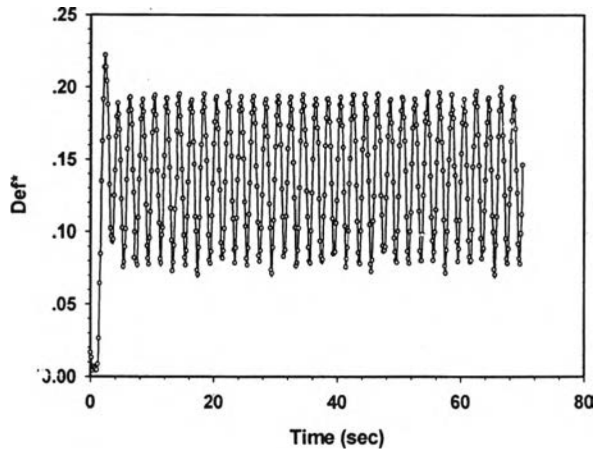

(c)

Figure E5 Deformation parameters vs. time of pure PBd/PDMS at strain 80%, frequency 0.35 Hz, $\tau_r = 0.2$, $G''_r = 0.16$, $d_o \sim 200$ μm, gap = 2,200 μm: a) a* vs. time; b) c vs. time; c) Def* vs. time.

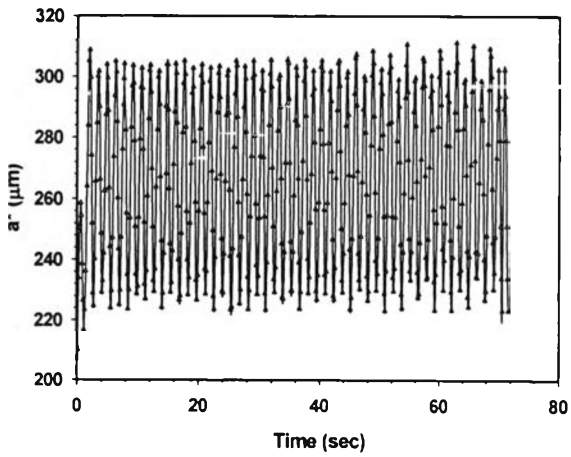

(a)

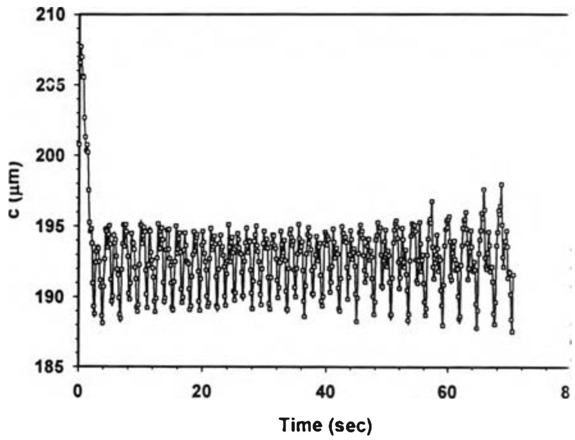

(b)

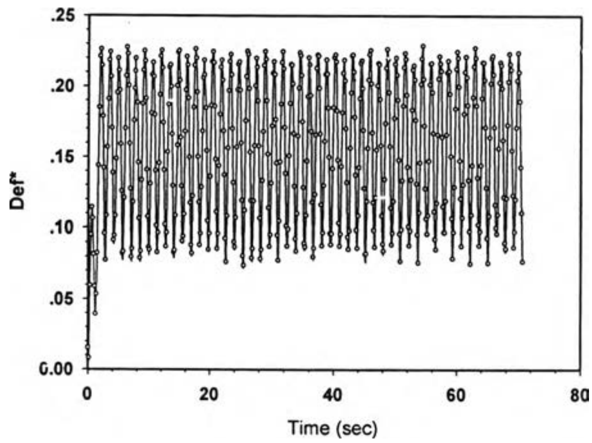

(c)

Figure E6 Deformation parameters vs. time of pure PBd/PDMS at strain 90%, frequency 0.35 Hz, τ_r = 0.2, G"$_r$ = 0.16, $d_o \sim$ 200 µm, gap = 2,200 µm: a) a* vs. time; b) c vs. time; c) Def* vs. time.

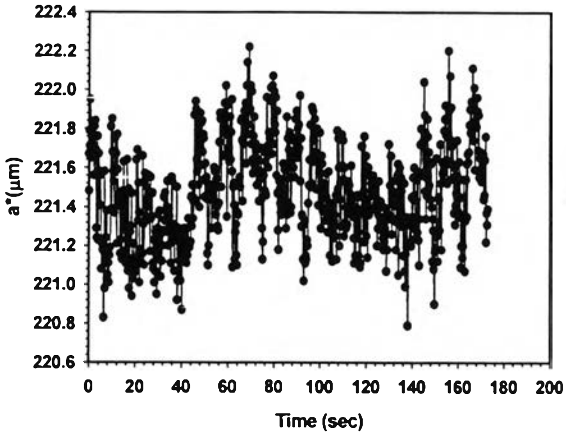

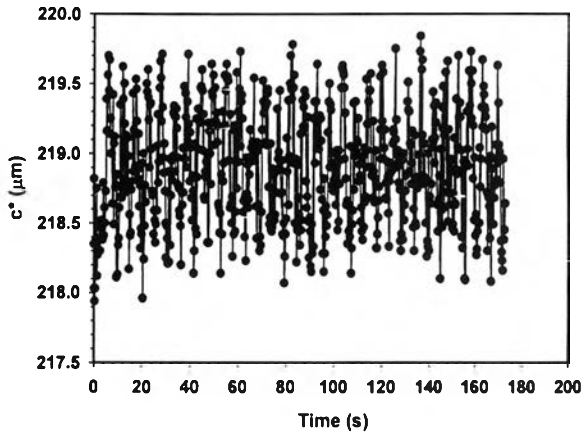

(a)

(b)

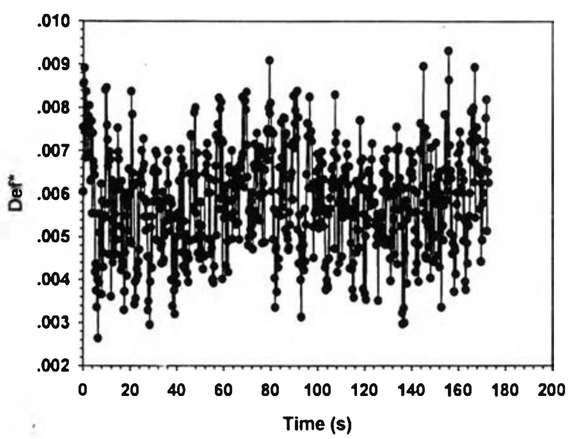

(c)

Figure E7 Deformation parameters vs. time of pure PBd/PDMS at strain 10%, frequency 0.1 Hz, $\tau_r = 0.2$, $G''_r = 1$, $d_o \sim 200$ μm, gap = 2,200 μm: a) a* vs. time; b) c vs. time; c) Def* vs. time.

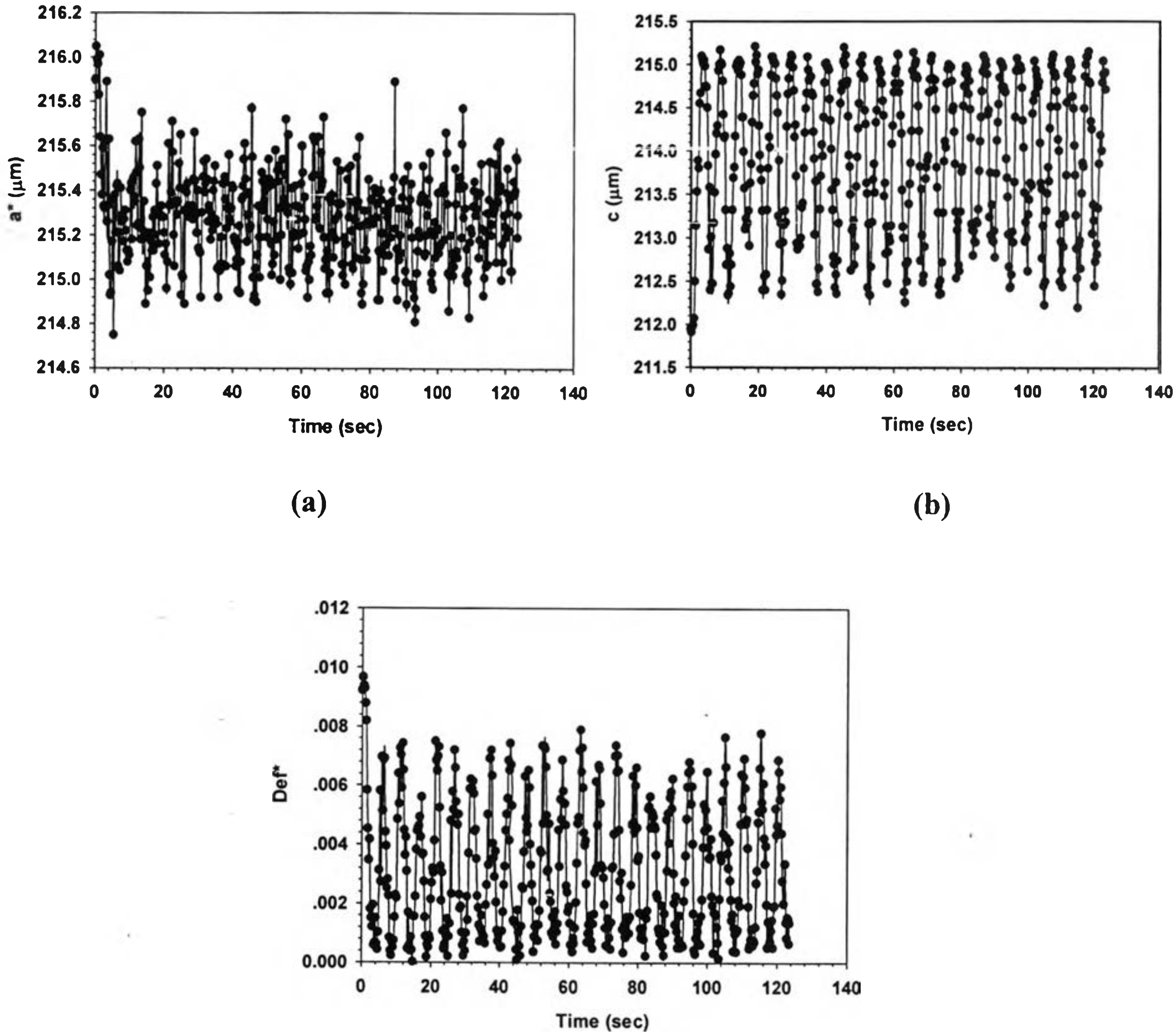

Figure E8 Deformation parameters vs. time of pure PBd/PDMS at strain 20%, frequency 0.1 Hz, $\tau_r = 0.2$, $G''_r = 1$, $d_o \sim 200$ μm, gap = 2,200 μm: a) a* vs. time; b) c vs. time; c) Def* vs. time.

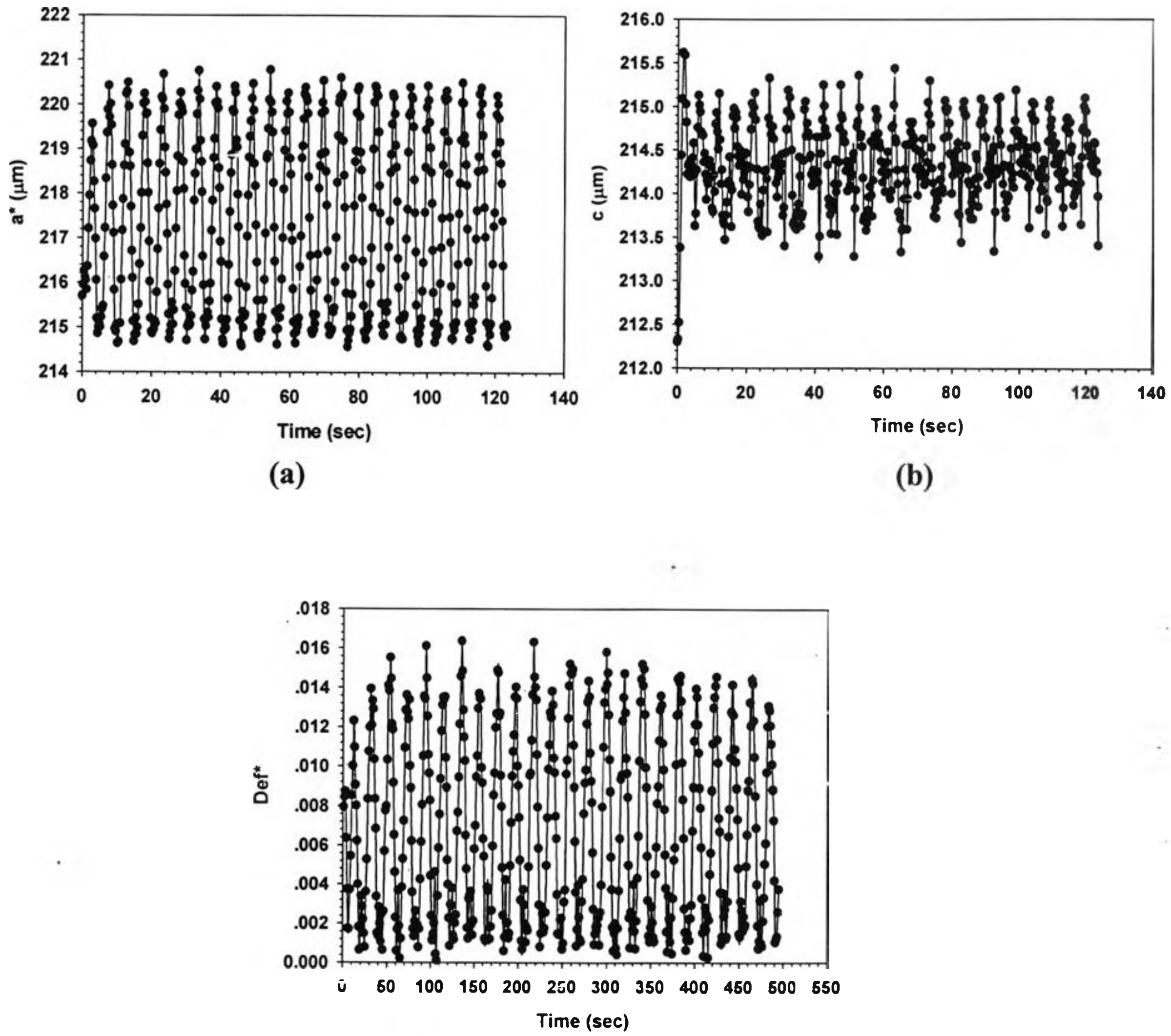

(c)

Figure E9 Deformation parameters vs. time of pure PBd/PDMS at strain 30%, frequency 0.1 Hz, τ_r = 0.2, G"$_r$ =1, d_o ~ 200 μm, gap = 2,200 μm: a) a* vs. time; b) c vs. time; c) Def* vs. time.

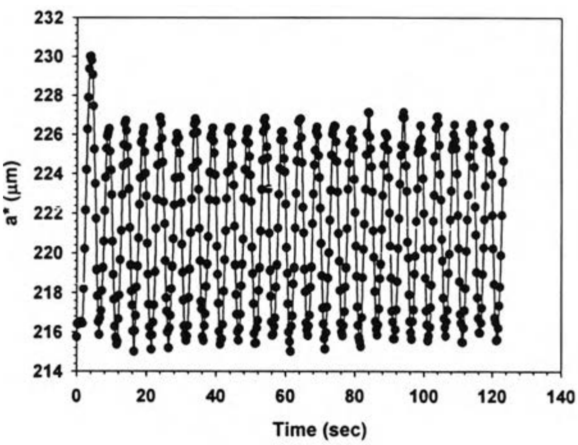

(a)

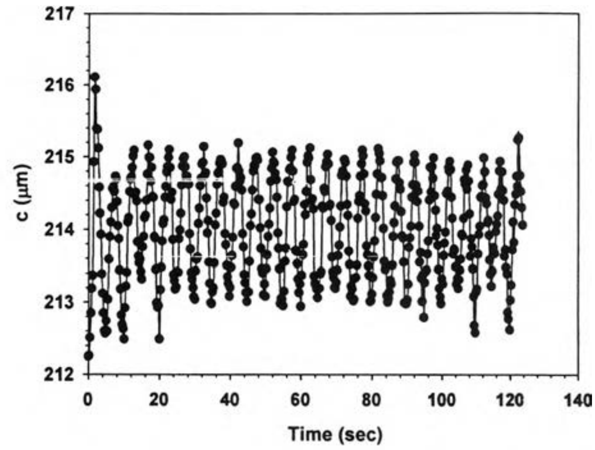

(b)

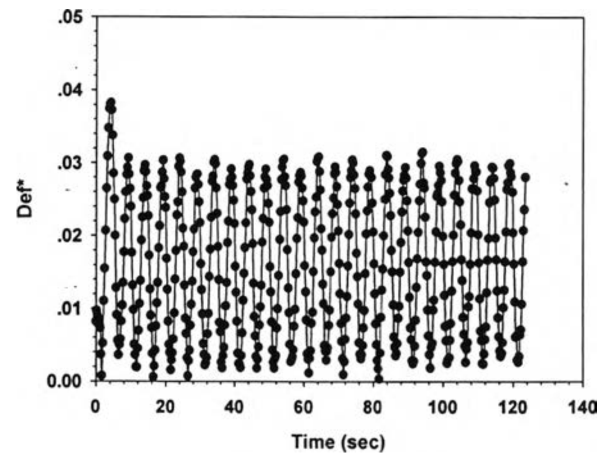

(c)

Figure E10 Deformation parameters vs. time of pure PBd/PDMS at strain 40%, frequency 0.1 Hz, $\tau_r = 0.2$, $G''_r = 1$, $d_o \sim 200$ μm, gap = 2,200 μm: a) a* vs. time; b) c vs. time; c) Def* vs. time.

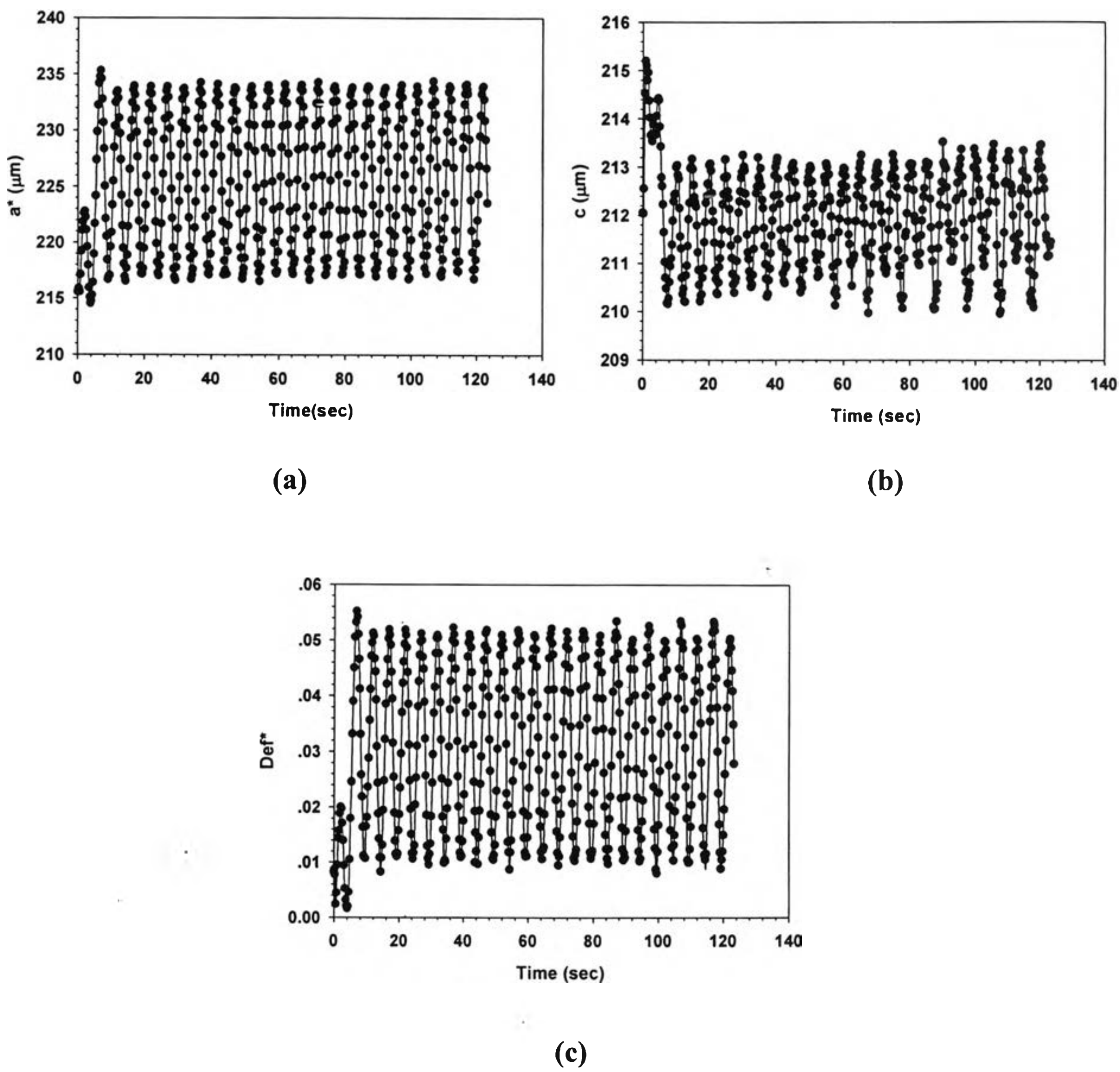

Figure E11 Deformation parameters vs. time of pure PBd/PDMS at strain 50%, frequency 0.1 Hz, τ_r = 0.2, G"$_r$ =1, d_o ~ 200 µm, gap = 2,200 µm: a) a* vs. time; b) c vs. time; c) Def* vs. time.

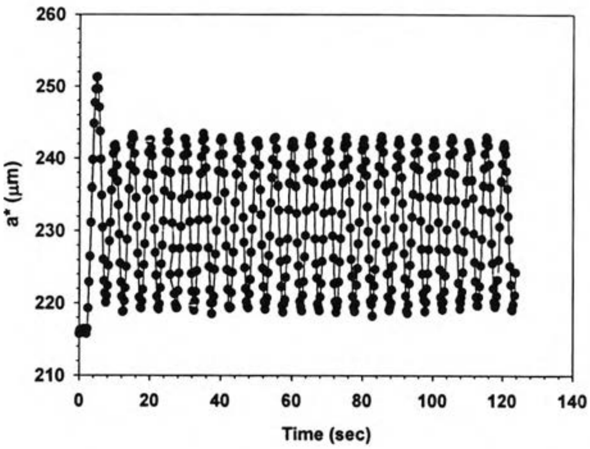

(a)

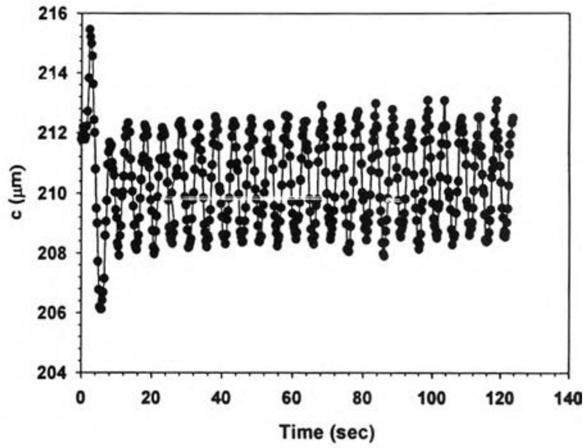

(b)

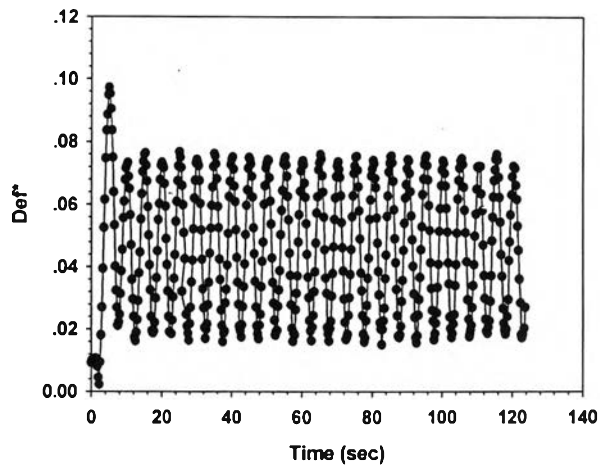

(c)

Figure E12 Deformation parameters vs. time of pure PBd/PDMS at strain 60%, frequency 0.1 Hz, $\tau_r = 0.2$, $G''_r = 1$, $d_o \sim 200$ μm, gap = 2,200 μm: a) a* vs. time; b) c vs. time; c) Def* vs. time.

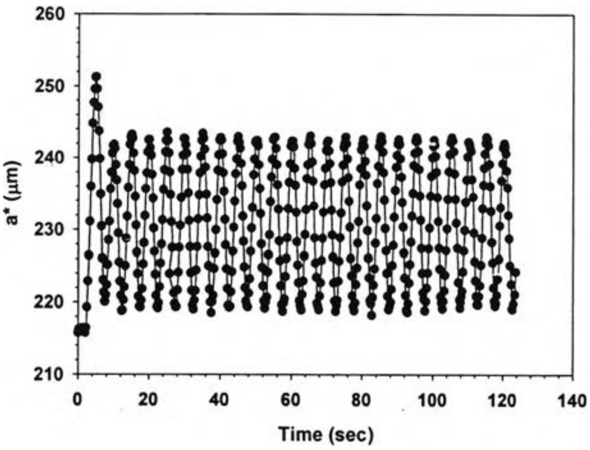

(a)

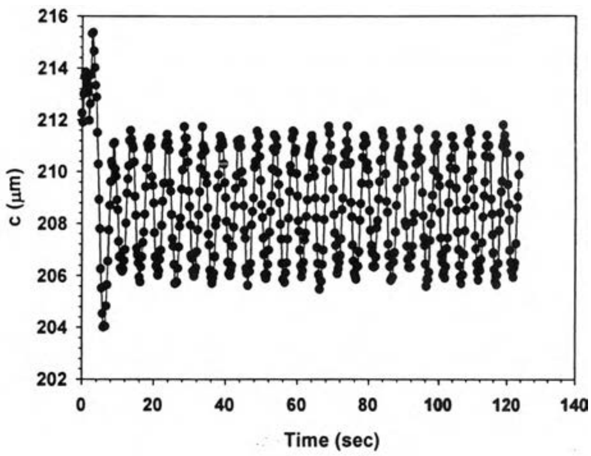

(b)

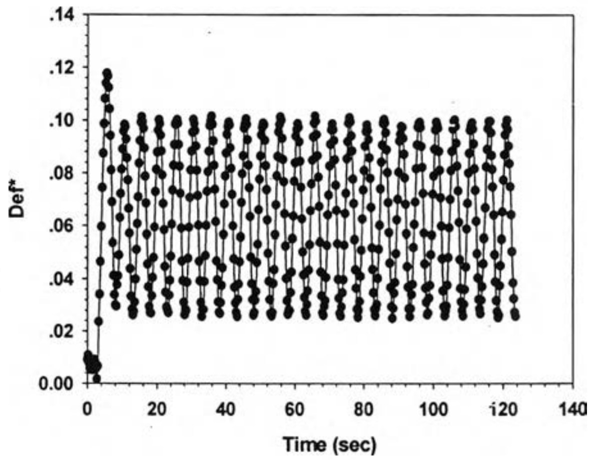

(c)

Figure E13 Deformation parameters vs. time of pure PBd/PDMS at strain 70%, frequency 0.1 Hz, $\tau_r = 0.2$, $G''_r = 1$, $d_o \sim 200$ μm, gap = 2,200 μm: a) a* vs. time; b) c vs. time; c) Def* vs. time.

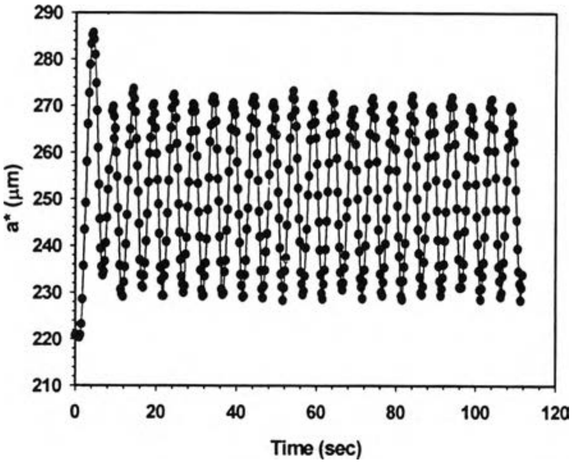

(a)

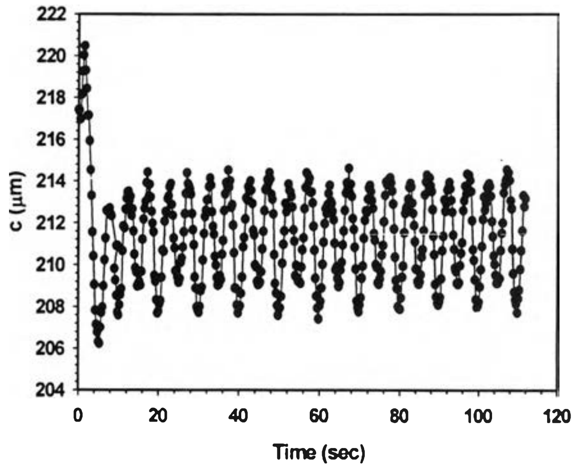

(b)

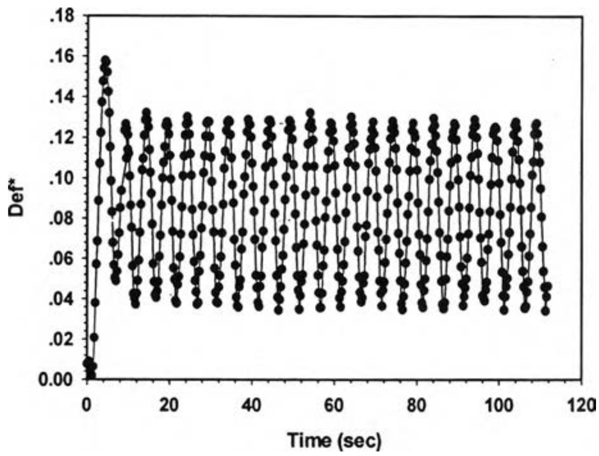

(c)

Figure E14 Deformation parameters vs. time of pure PBd/PDMS at strain 80%, frequency 0.1 Hz, $\tau_r = 0.2$, $G''_r = 1$, $d_o \sim 200$ µm, gap = 2,200 µm: a) a* vs. time; b) c vs. time; c) Def* vs. time.

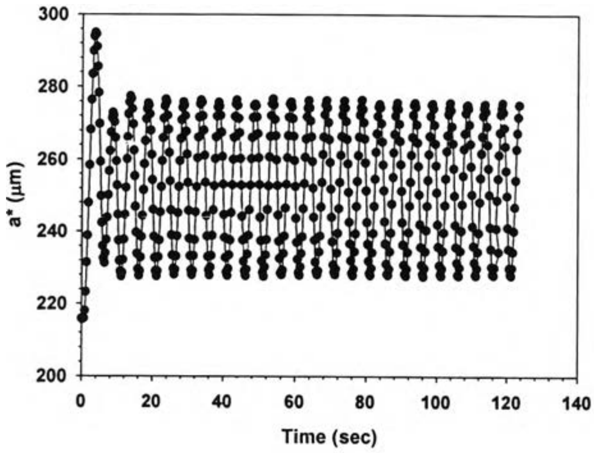

(a)

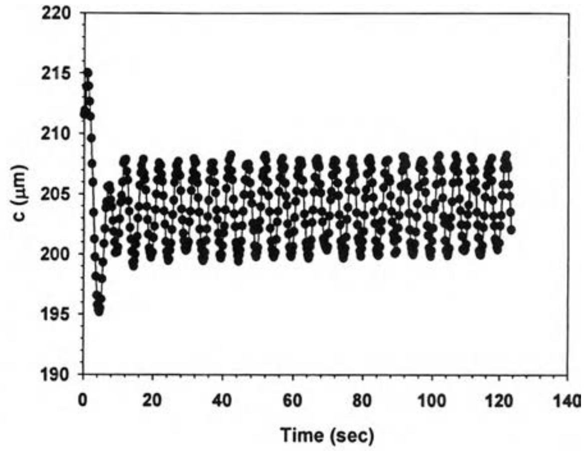

(b)

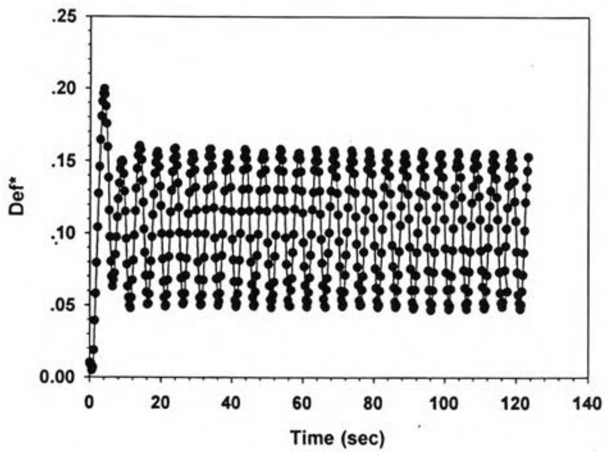

(c)

Figure E15 Deformation parameters vs. time of pure PBd/PDMS at strain 90%, frequency 0.1 Hz, τ_r = 0.2, G''_r =1, d_o ~ 200 μm, gap = 2,200 μm: a) a* vs. time; b) c vs. time; c) Def* vs. time.

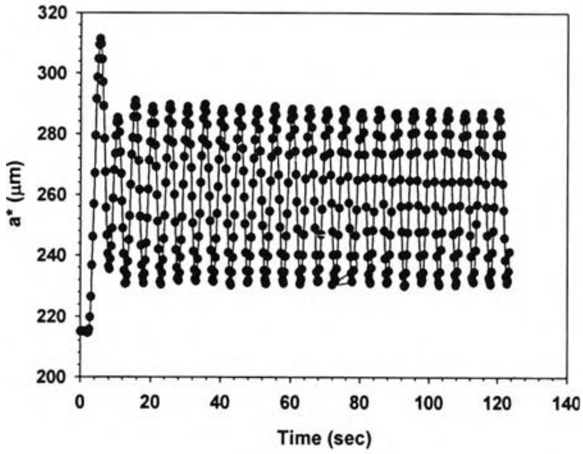

(a)

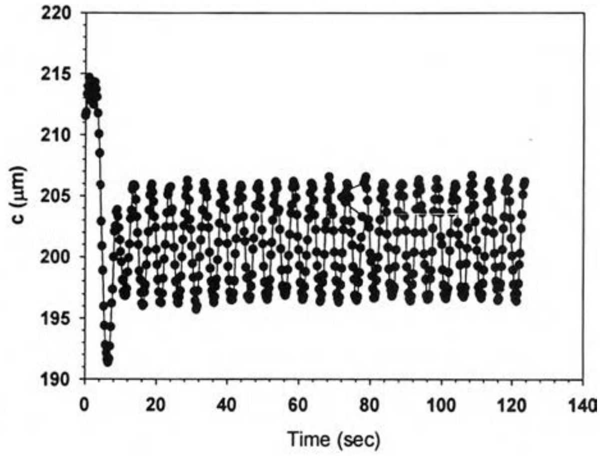

(b)

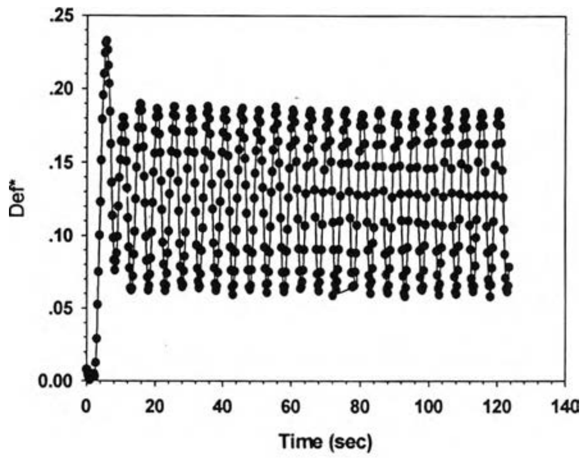

(c)

Figure E16 Deformation parameters vs. time of pure PBd/PDMS at strain 100%, frequency 0.1 Hz, $\tau_r = 0.2$, $G''_r = 1$, $d_o \sim 200$ μm, gap = 2,200 μm: a) a* vs. time; b) c vs. time; c) Def* vs. time.

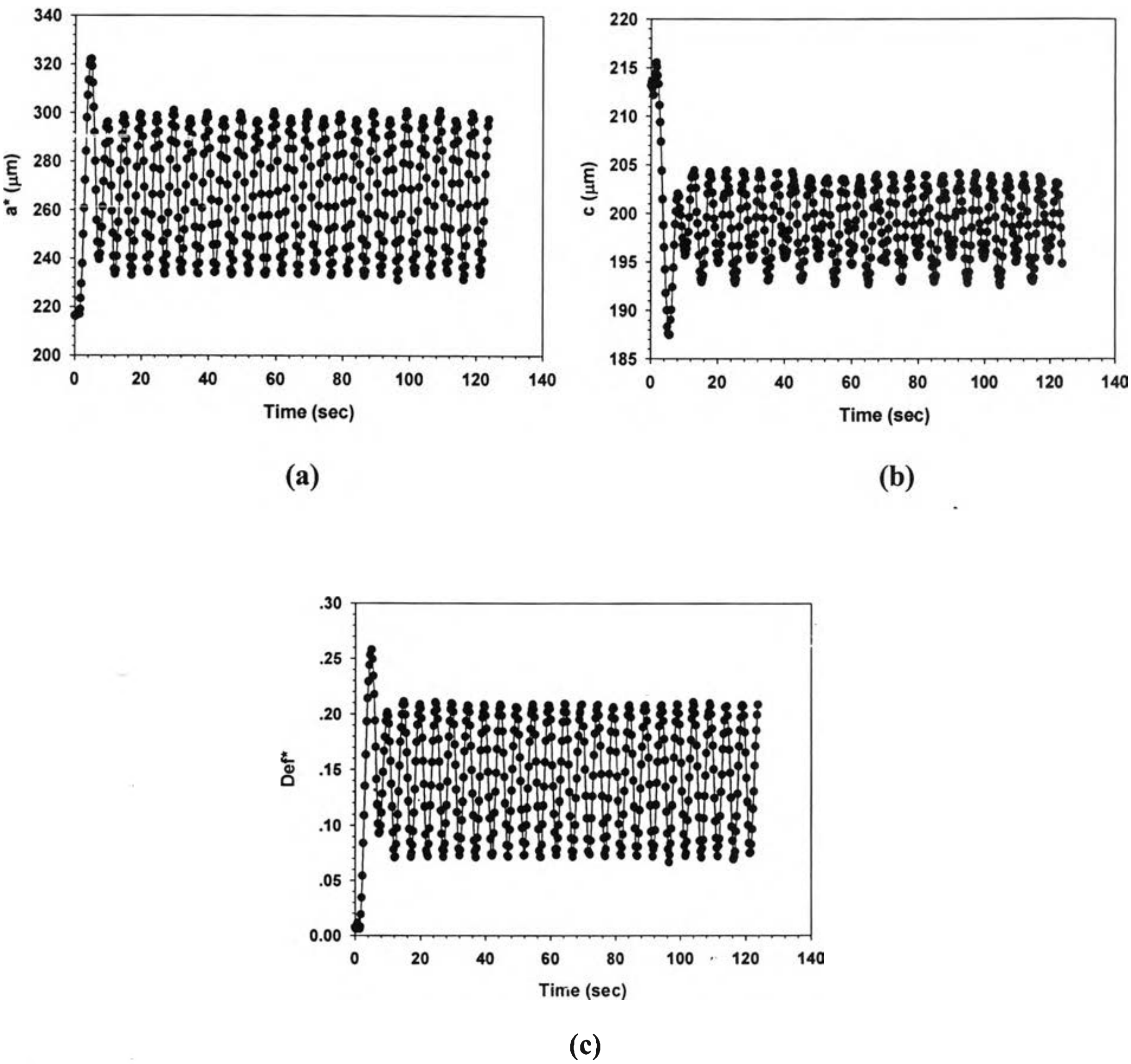

Figure E17 Deformation parameters vs. time of pure PBd/PDMS at strain 110%, frequency 0.1 Hz, $\tau_r = 0.2$, $G''_r = 1$, $d_o \sim 200$ µm, gap = 2,200 µm: a) a* vs. time; b) c vs. time; c) Def* vs. time.

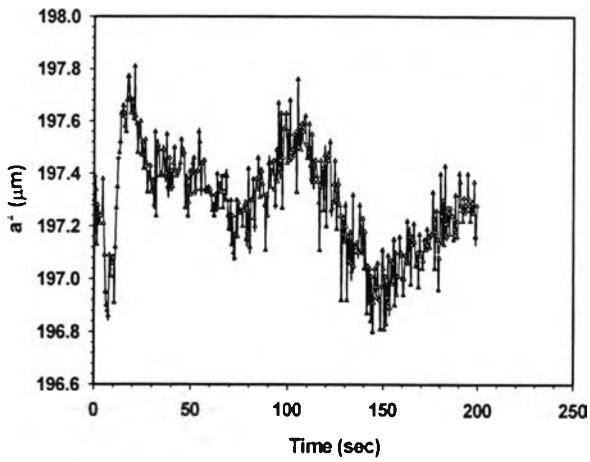

(a)

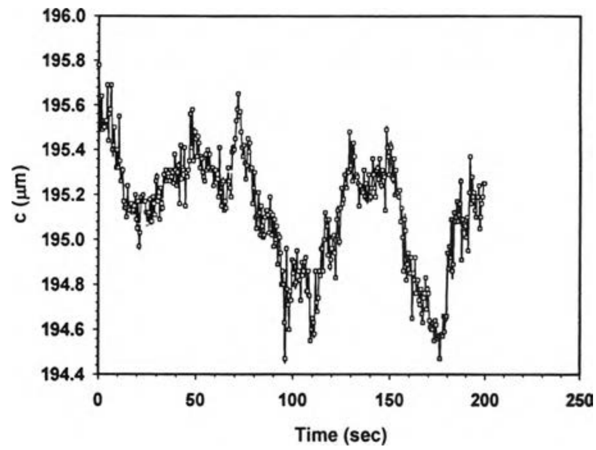

(b)

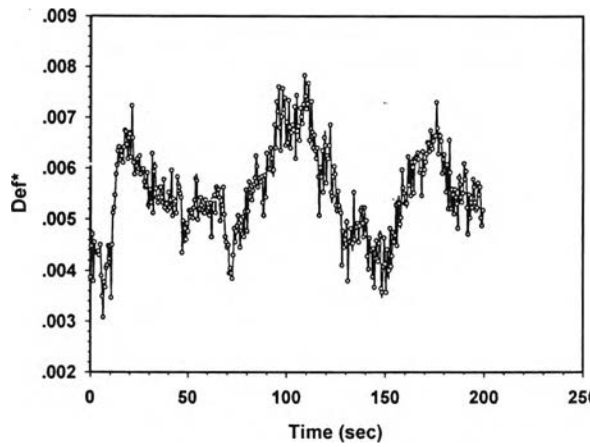

(c)

Figure E18 Deformation parameters vs. time of pure PBd/PDMS at strain 10%, frequency 0.04 Hz, $\tau_r = 0.2$, $G''_r = 3.0$, $d_o \sim 200$ µm, gap = 2,200 µm: a) a* vs. time; b) c vs. time; c) Def* vs. time.

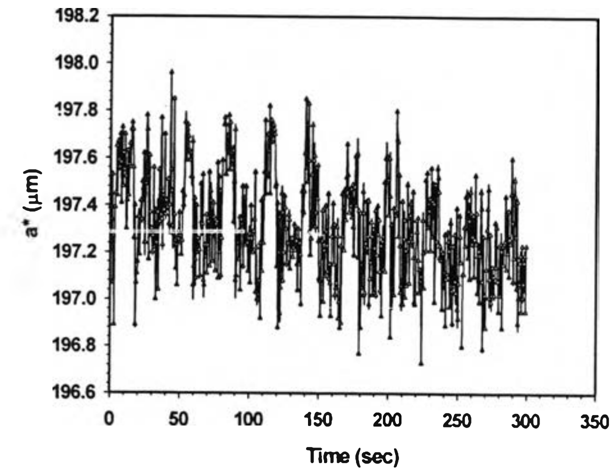

(a)

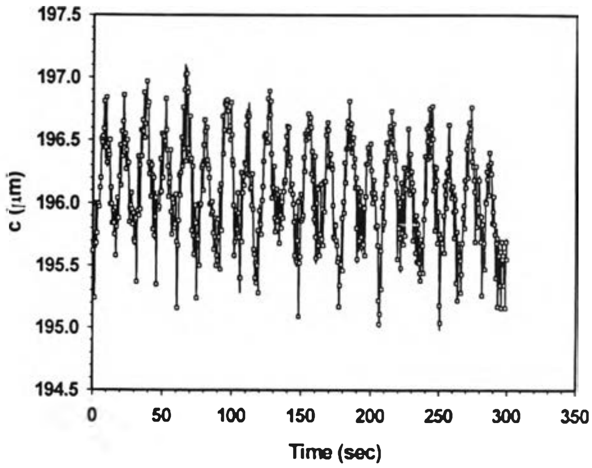

(b)

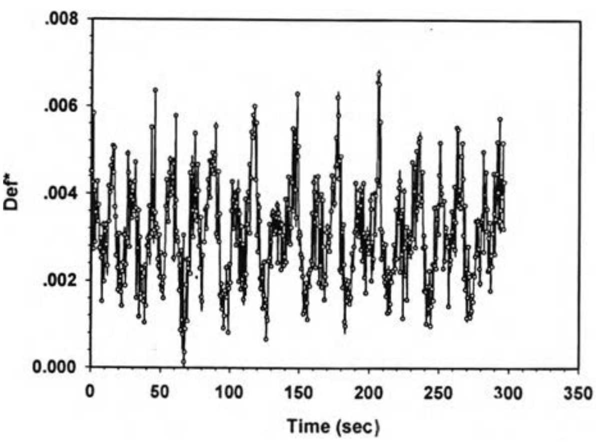

(c)

Figure E19 Deformation parameters vs. time of pure PBd/PDMS at strain 20%, frequency 0.04 Hz, $\tau_r = 0.2$, $G''_r = 3.0$, $d_o \sim 200$ μm, gap = 2,200 μm: a) a* vs. time; b) c vs. time; c) Def* vs. time.

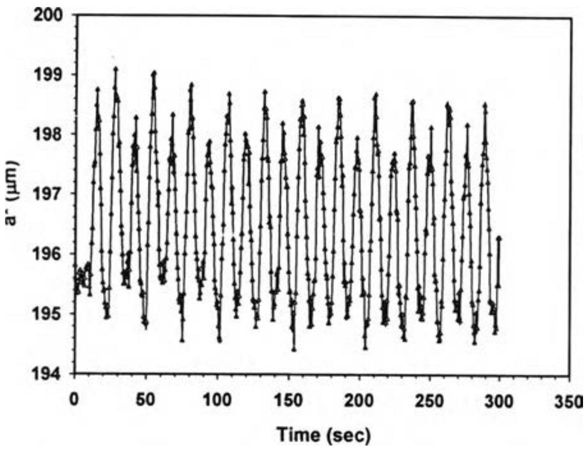

(a)

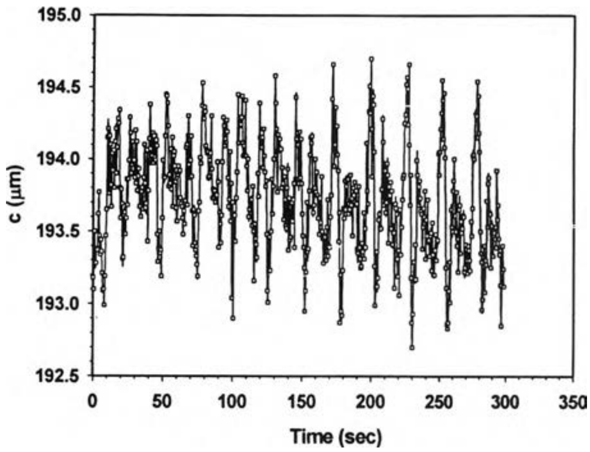

(b)

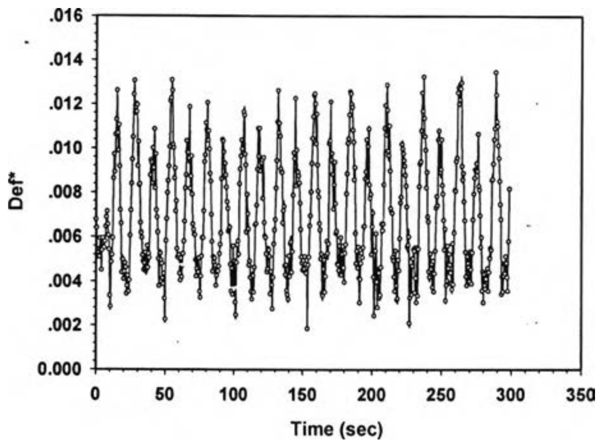

(c)

Figure E20 Deformation parameters vs. time of pure PBd/PDMS at strain 40%, frequency 0.04 Hz, τ_r = 0.2, G''_r = 3.0, $d_o \sim$ 200 µm, gap = 2,200 µm: a) a* vs. time; b) c vs. time; c) Def* vs. time.

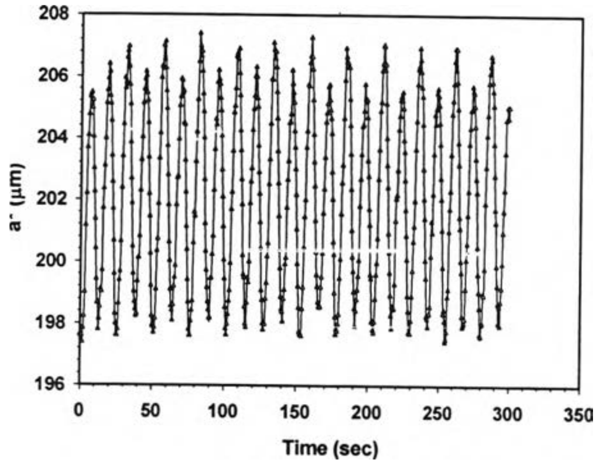

(a)

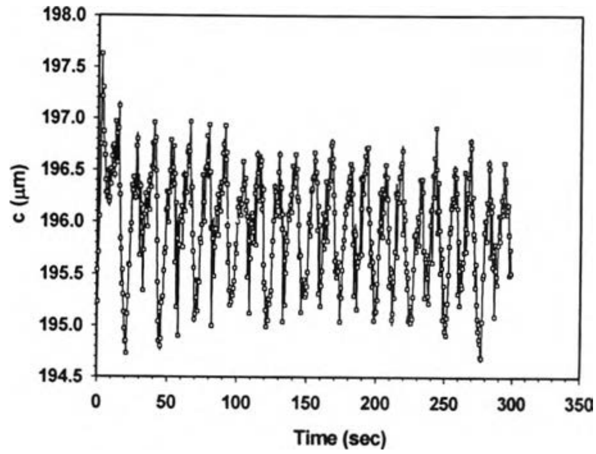

(b)

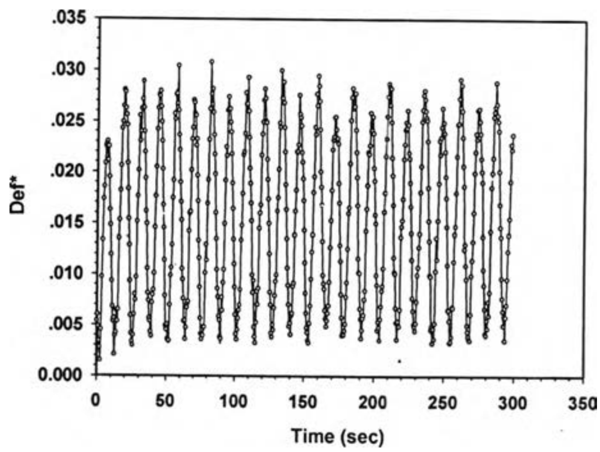

(c)

Figure E21 Deformation parameters vs. time of pure PBd/PDMS at strain 60%, frequency 0.04 Hz, $\tau_r = 0.2$, $G''_r = 3.0$, $d_o \sim 200$ μm, gap = 2,200 μm: a) a* vs. time; b) c vs. time; c) Def* vs. time.

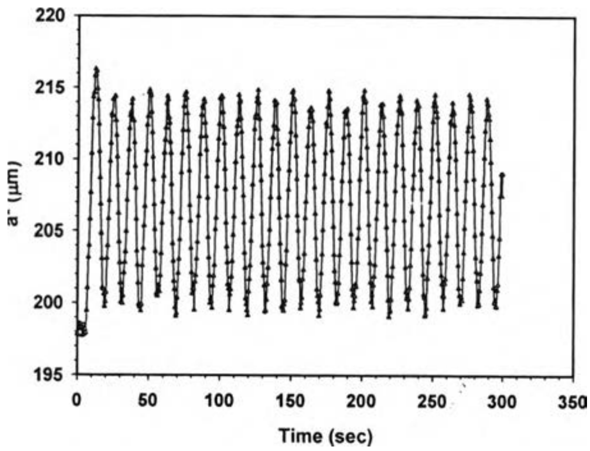

(a)

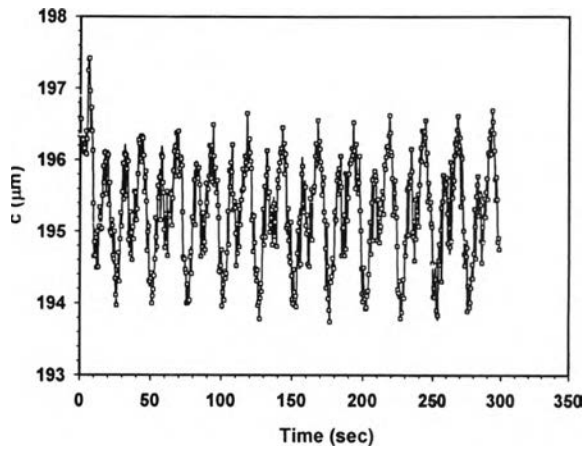

(b)

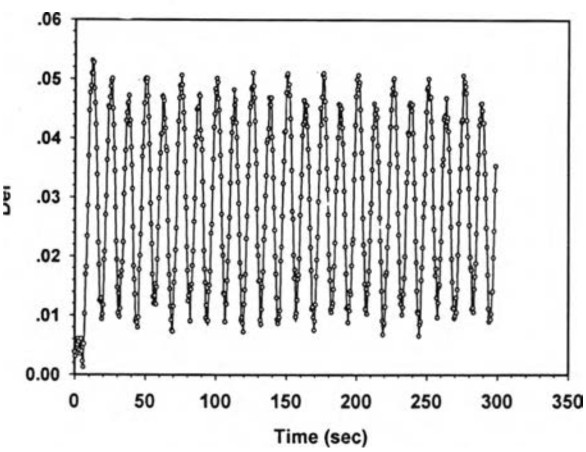

(c)

Figure E22 Deformation parameters vs. time of pure PBd/PDMS at strain 80%, frequency 0.04 Hz, $\tau_r = 0.2$, $G''_r = 3.0$, $d_o \sim 200$ µm, gap = 2,200 µm: a) a* vs. time; b) c vs. time; c) Def* vs. time.

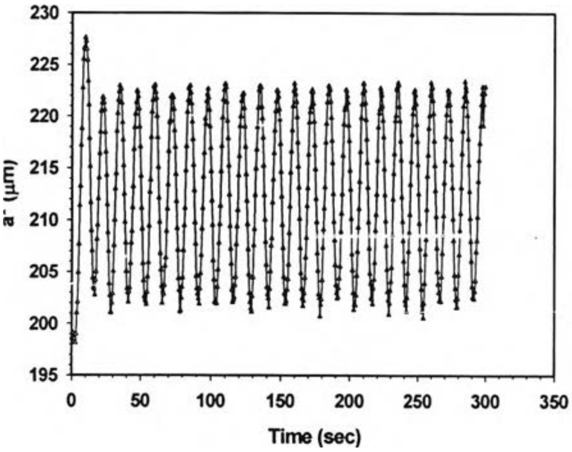

(a)

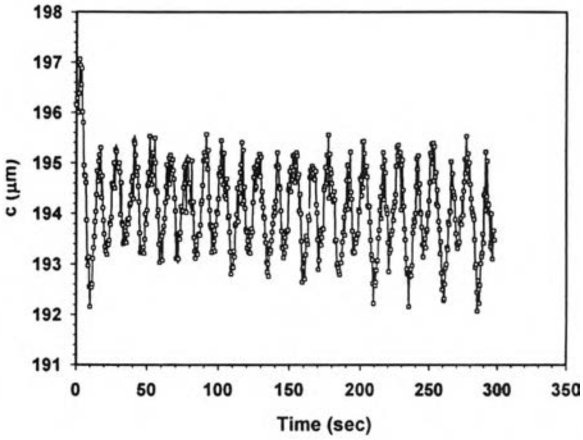

(b)

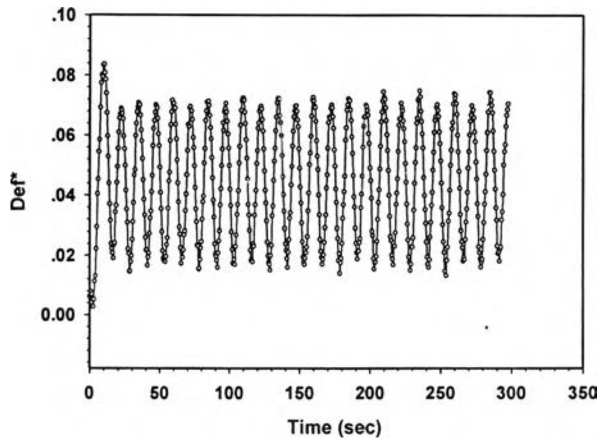

(c)

Figure E23 Deformation parameters vs. time of pure PBd/PDMS at strain 100%, frequency 0.04 Hz, $\tau_r = 0.2$, $G''_r = 3.0$, $d_o \sim 200$ µm, gap = 2,200 µm: a) a* vs. time; b) c vs. time; c) Def* vs. time.

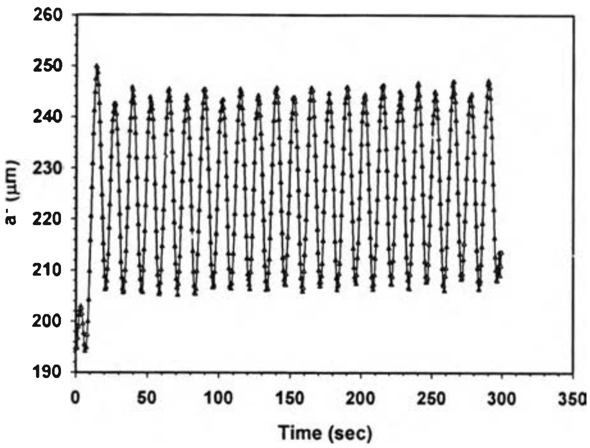

(a)

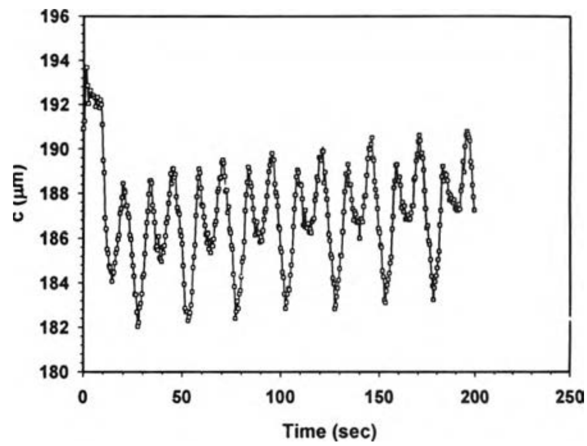

(b)

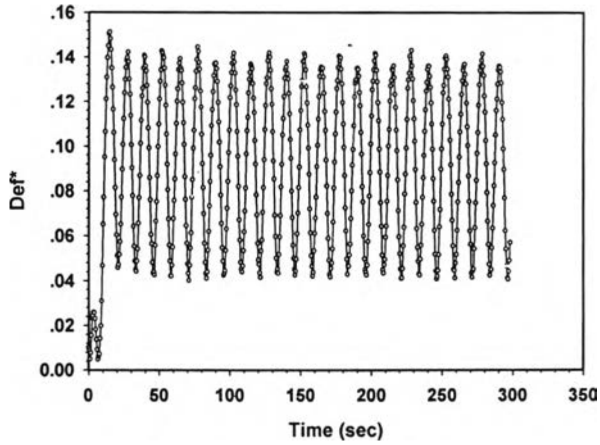

(c)

Figure E24 Deformation parameters vs. time of pure PBd/PDMS at strain 150%, frequency 0.04 Hz, τ_r = 0.2, G"$_r$ = 3.0, d_o ~ 200 μm, gap = 2,200 μm: a) a* vs. time; b) c vs. time; c) Def* vs. time.

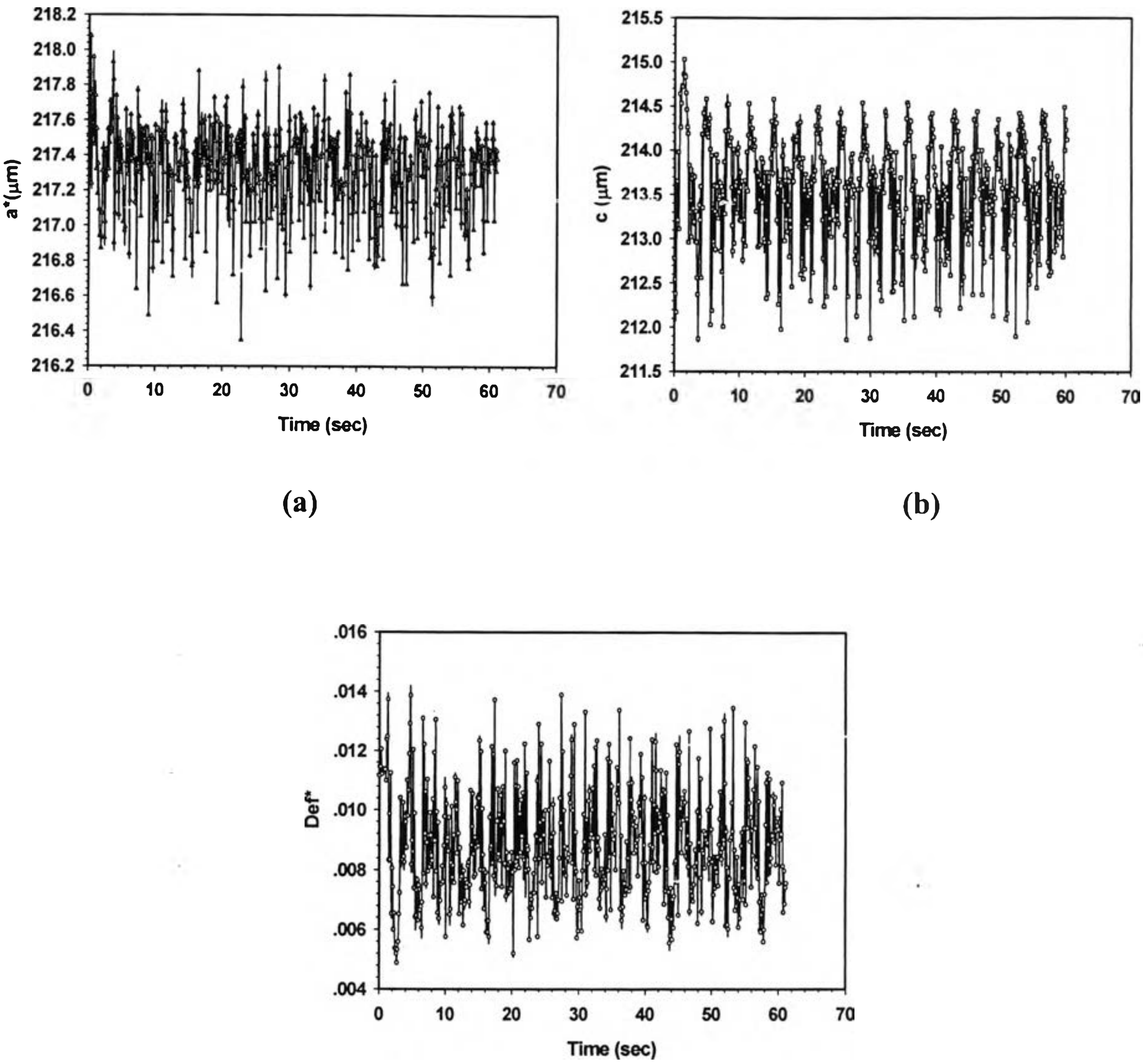

(a) (b)

(c)

Figure E25 Deformation parameters.vs. time of pure PBd/PDMS at strain 10%, frequency 0.3 Hz, τ_r = 0.57, G"$_r$ =1, d_o ~ 200 μm, gap = 2,200 μm: a) a* vs. time; b) c vs. time; c) Def* vs. time.

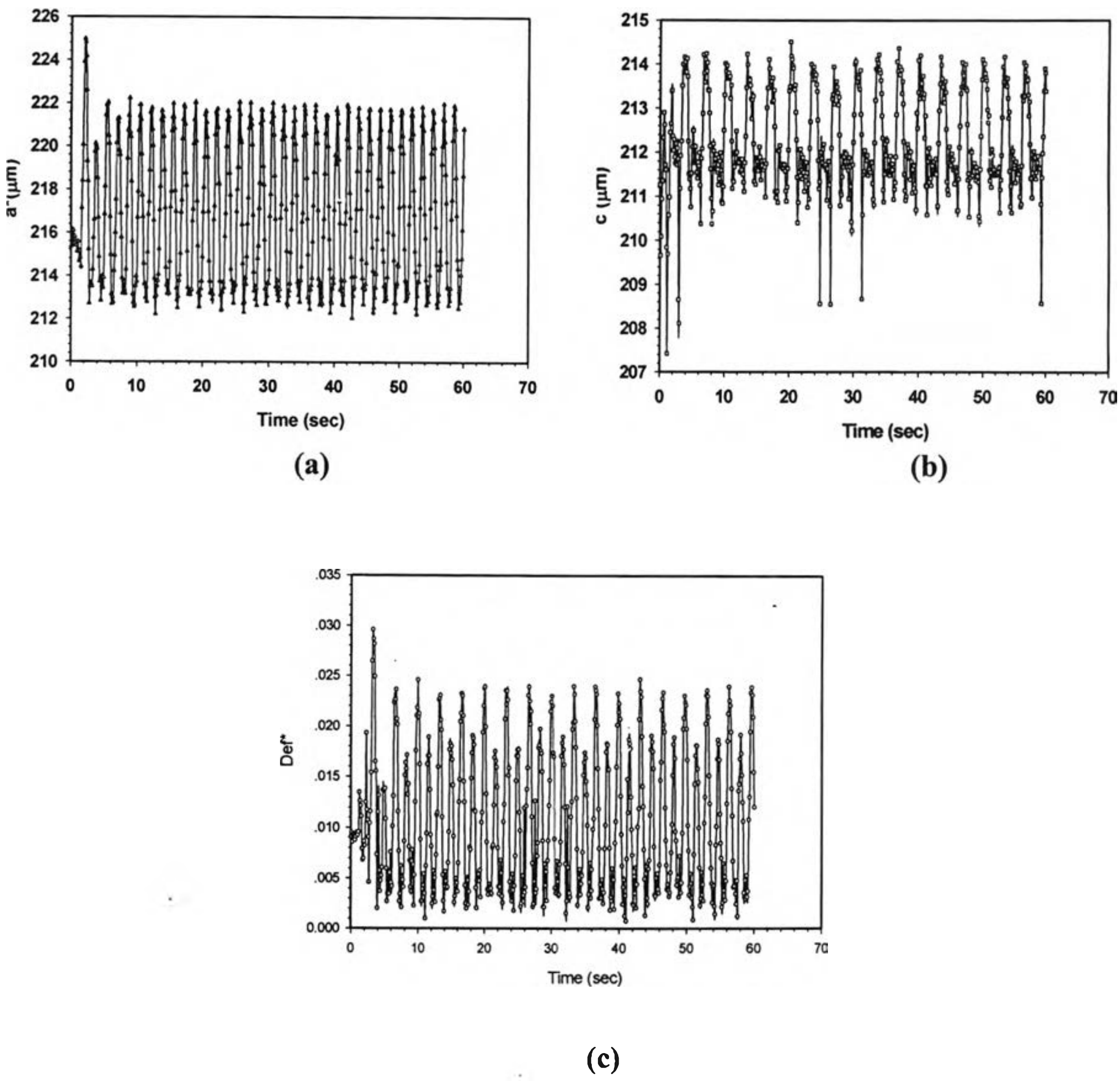

Figure E26 Deformation parameters vs. time of pure PBd/PDMS at strain 30%, frequency 0.3 Hz, $\tau_r = 0.57$, $G''_r = 1$, $d_o \sim 200$ μm, gap = 2,200 μm: a) a* vs. time; b) c vs. time; c) Def* vs. time.

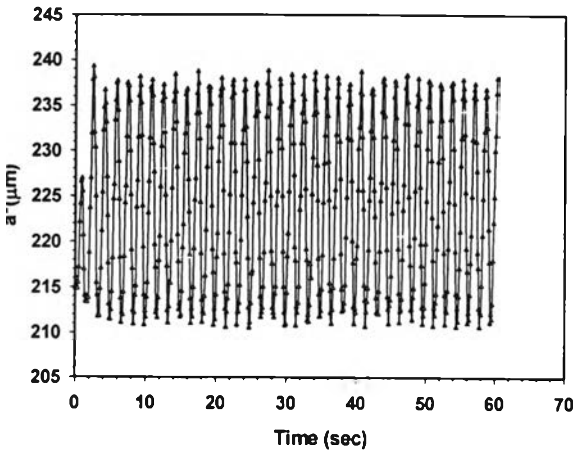

(a)

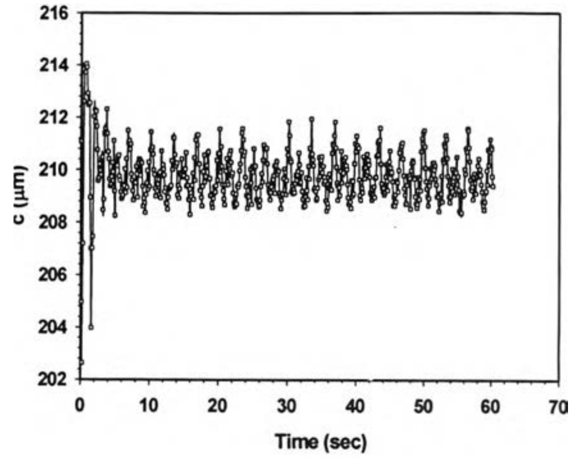

(b)

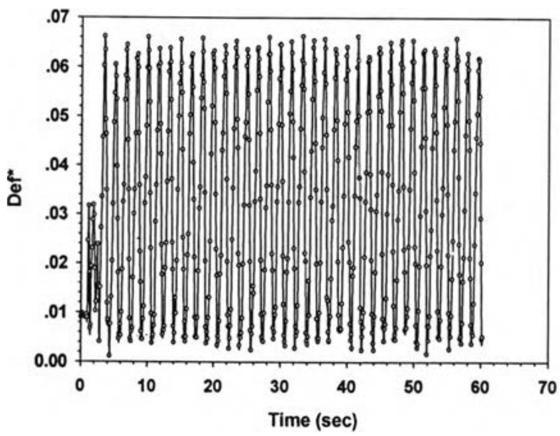

(c)

Figure E27 Deformation parameters vs. time of pure PBd/PDMS at strain 50%, frequency 0.3 Hz, τ_r = 0.57, G''_r =1, d_o ~ 200 µm, gap = 2,200 µm: a) a* vs. time; b) c vs. time; c) Def* vs. time.

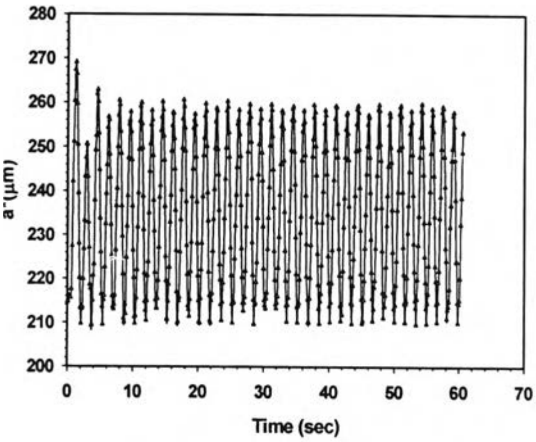

(a)

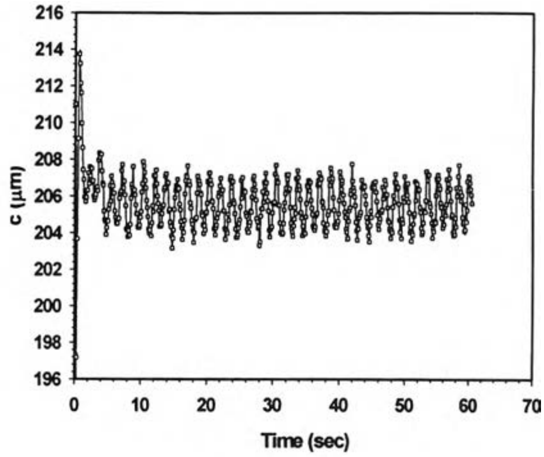

(b)

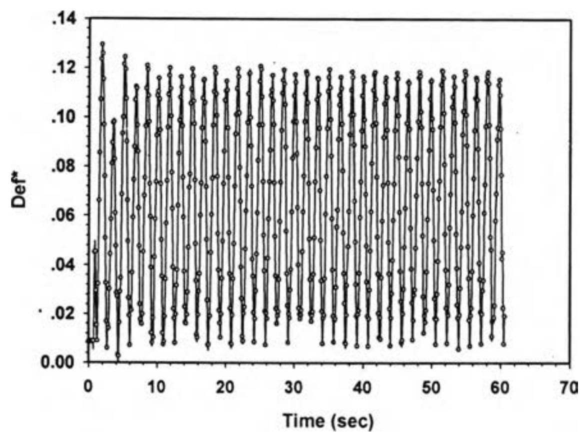

(c)

Figure E28 Deformation parameters vs. time of pure PBd/PDMS at strain 70%, frequency 0.3 Hz, $\tau_r = 0.57$, $G''_r = 1$, $d_o \sim 200$ µm, gap = 2,200 µm: a) a* vs. time; b) c vs. time; c) Def* vs. time.

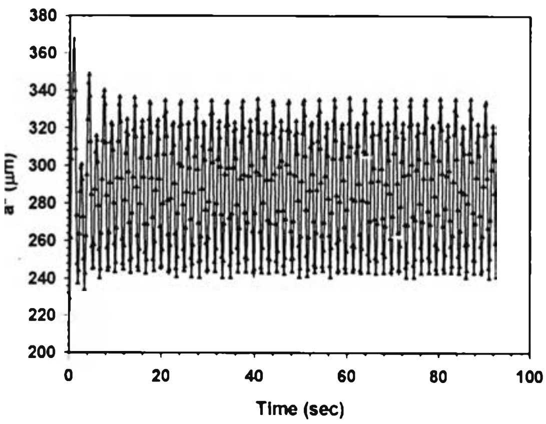

(a)

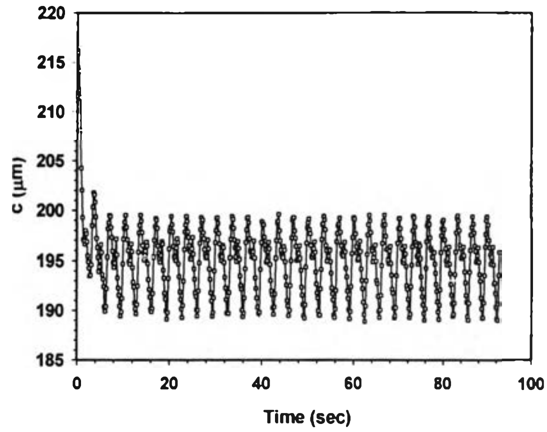

(b)

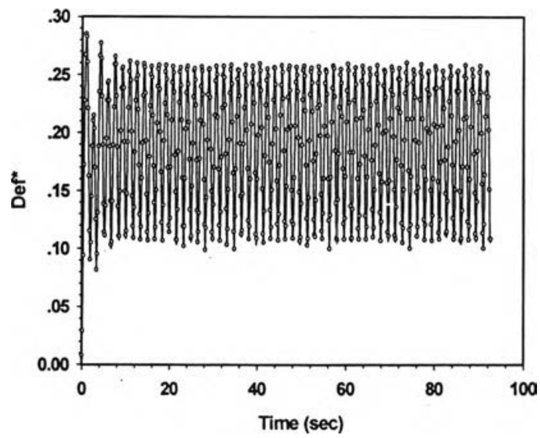

(c)

Figure E29 Deformation parameters vs. time of pure PBd/PDMS at strain 100%, frequency 0.3 Hz, τ_r = 0.57, G''_r =1, d_o ~ 200 µm, gap = 2,200 µm: a) a* vs. time; b) c vs. time; c) Def* vs. time.

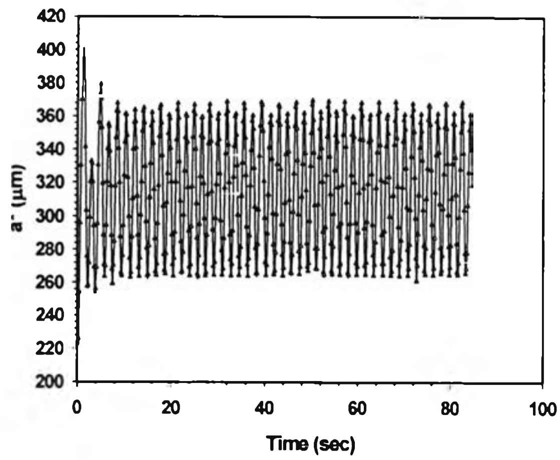

(a)

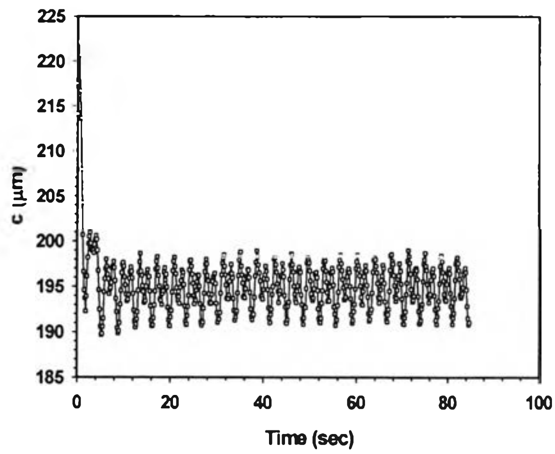

(b)

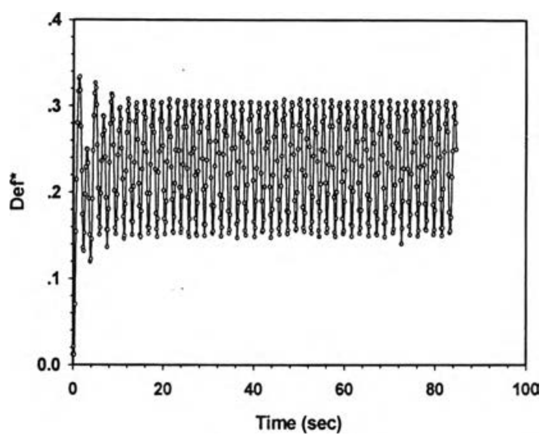

(c)

Figure E30 Deformation parameters vs. time of pure PBd/PDMS at strain 120%, frequency 0.3 Hz, $\tau_r = 0.57$, $G''_r = 1$, $d_o \sim 200$ µm, gap = 2,200 µm: a) a* vs. time; b) c vs. time; c) Def* vs. time.

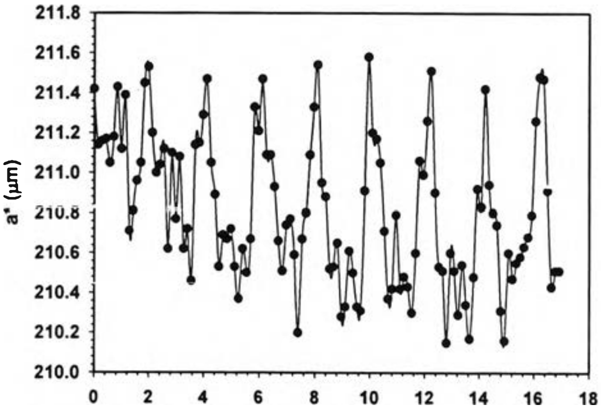

(a)

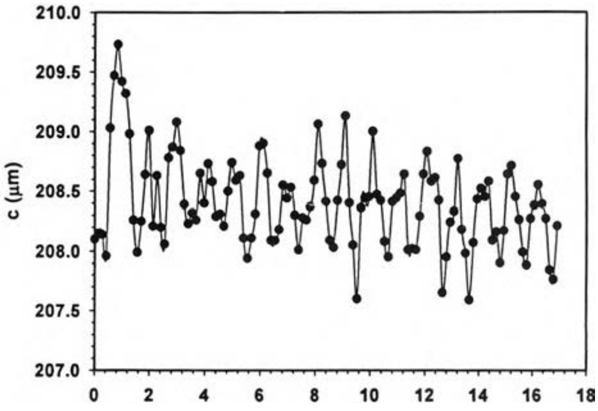

(b)

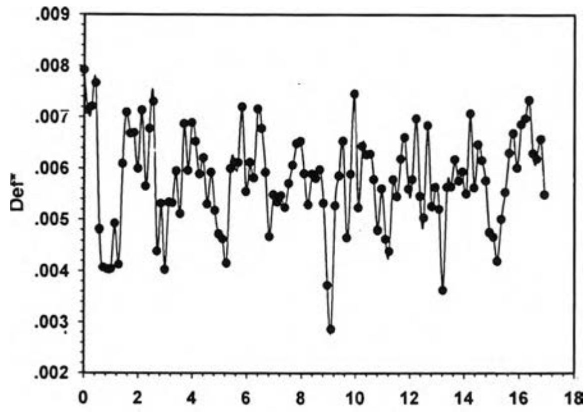

(c)

Figure E31 Deformation parameters vs. time of pure PBd/PDMS at strain 10%, frequency 0.5 Hz, τ_r = 1.0, G''_r =1, $d_o \sim$ 200 μm, gap = 2,200 μm: a) a* vs. time; b) c vs. time; c) Def* vs. time.

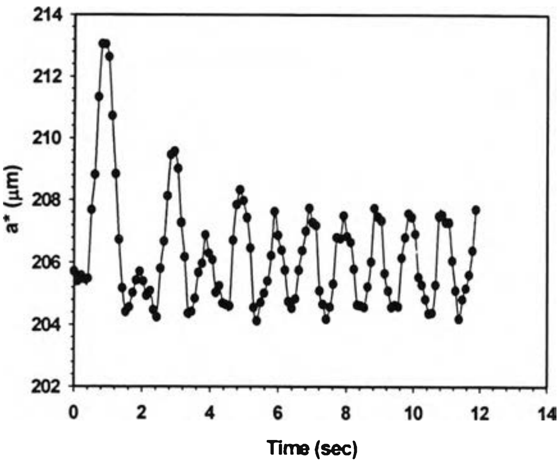

(a)

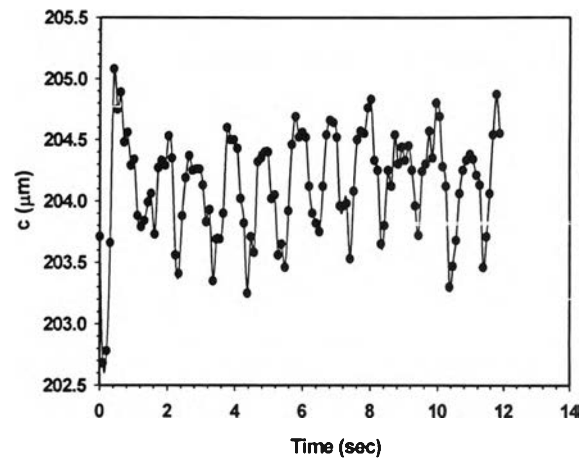

(b)

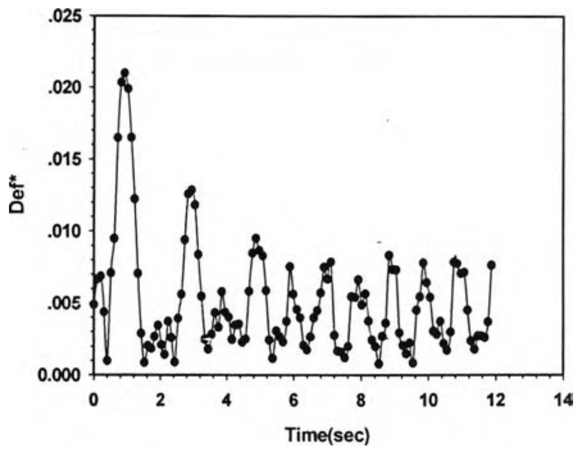

(c)

Figure E32 Deformation parameters vs. time of pure PBd/PDMS at strain 20%, frequency 0.5 Hz, $\tau_r = 1.0$, $G''_r = 1$, $d_o \sim 200$ μm, gap = 2,200 μm: a) a* vs. time; b) c vs. time; c) Def* vs. time.

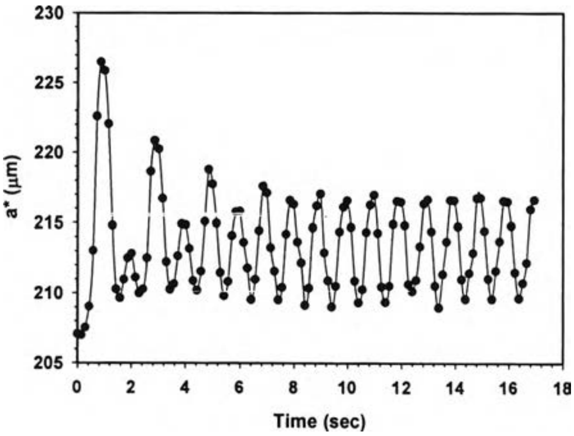

(a)

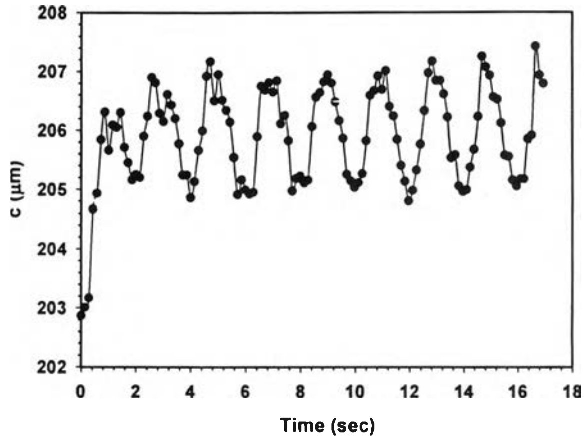

(b)

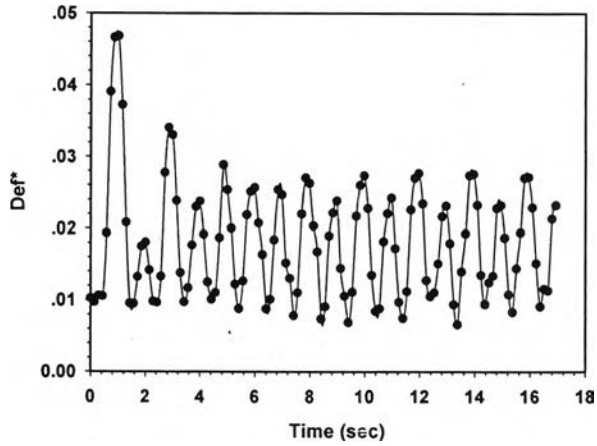

(c)

Figure E33 Deformation parameters vs. time of pure PBd/PDMS at strain 30%, frequency 0.5 Hz, τ_r = 1.0, G"$_r$ =1, d_o ~ 200 μm, gap = 2,200 μm: a) a* vs. time; b) c vs. time; c) Def* vs. time.

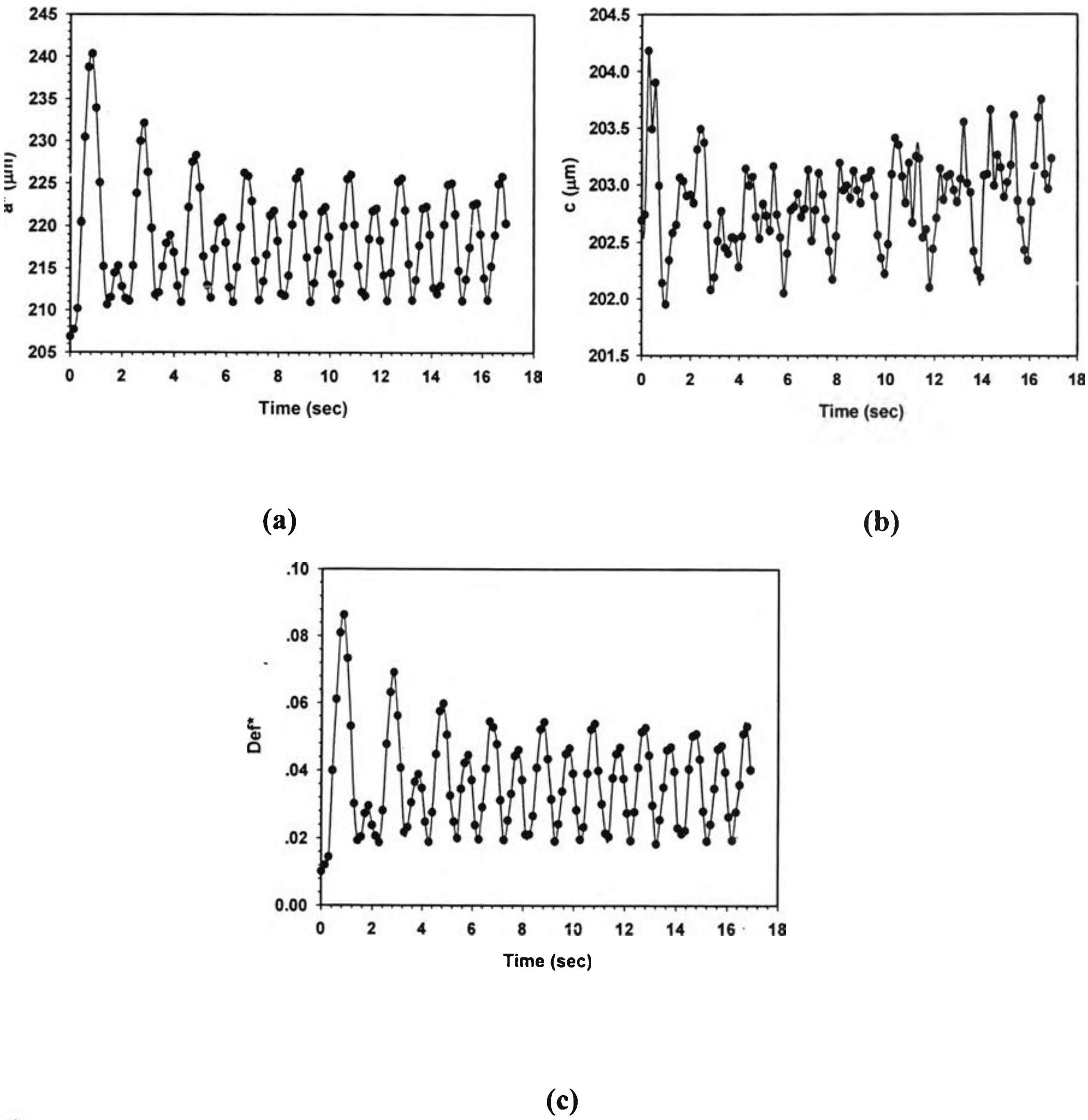

Figure E34 Deformation parameters vs. time of pure PBd/PDMS at strain 40%, frequency 0.5 Hz, τ_r = 1.0, G''_r =1, d_0 ~ 200 μm, gap = 2,200 μm: a) a* vs. time; b) c vs. time; c) Def* vs. time.

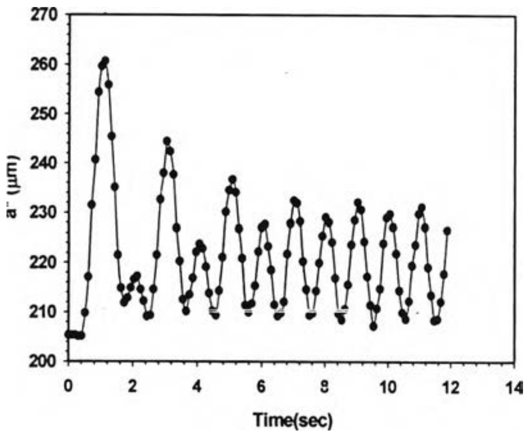

(a)

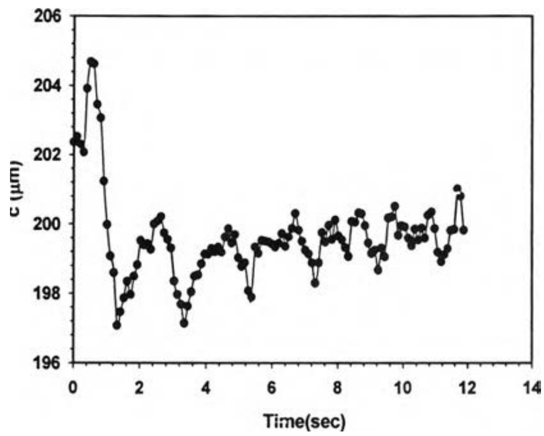

(b)

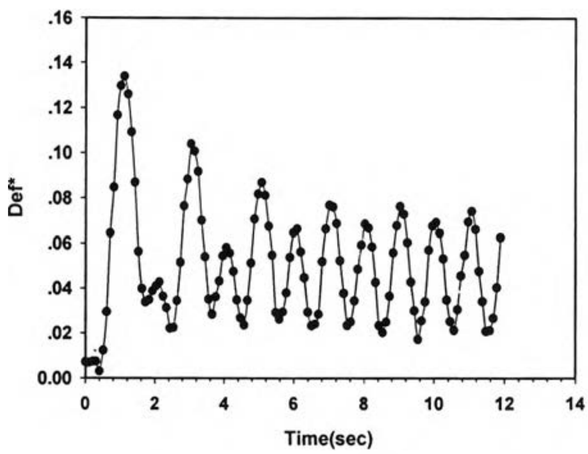

(c)

Figure E35 Deformation parameters vs. time of pure PBd/PDMS at strain 50%, frequency 0.5 Hz, τ_r = 1.0, G"$_r$ =1, d_o ~ 200 µm, gap = 2,200 µm: a) a* vs. time; b) c vs. time; c) Def* vs. time.

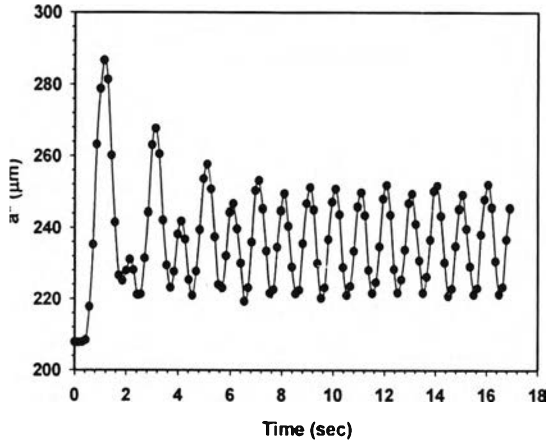

(a)

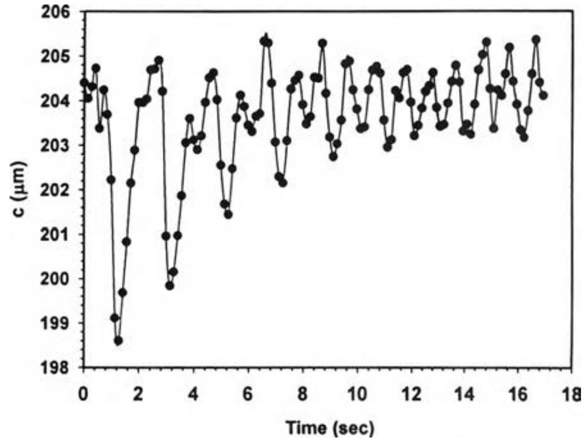

(b)

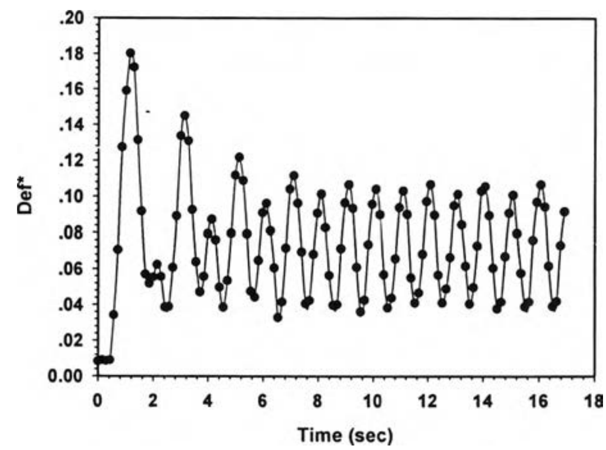

(c)

Figure E36 Deformation parameters vs. time of pure PBd/PDMS at strain 60%, frequency 0.5 Hz, τ_r = 1.0, G"$_r$ =1, d_o ~ 200 μm, gap = 2,200 μm: a) a* vs. time; b) c vs. time; c) Def* vs. time.

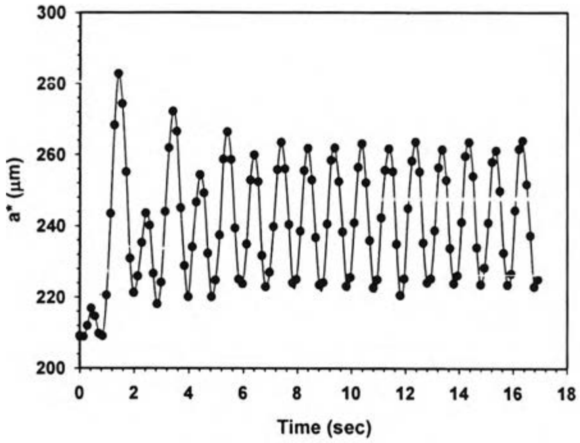

(a)

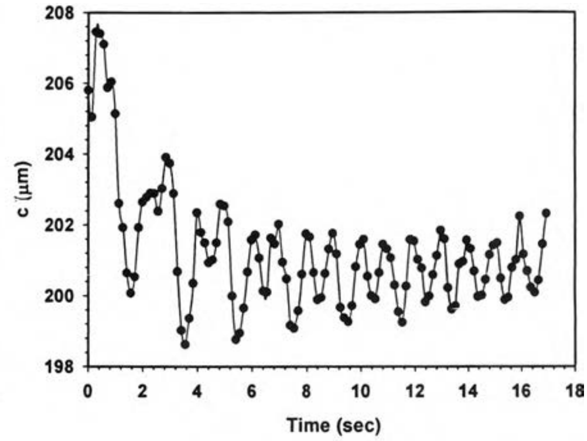

(b)

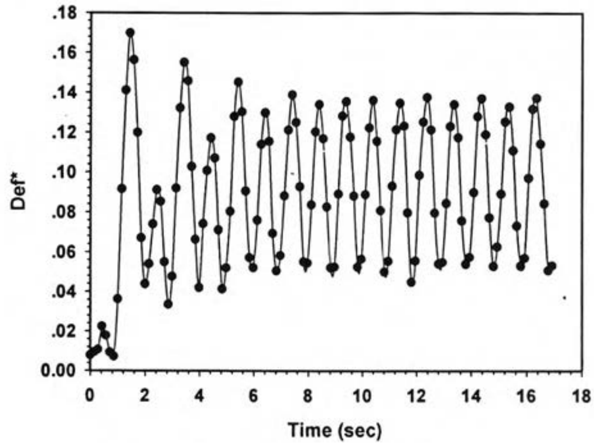

(c)

Figure E37 Deformation parameters vs. time of pure PBd/PDMS at strain 70%, frequency 0.5 Hz, $\tau_r = 1.0$, $G''_r = 1$, $d_o \sim 200$ μm, gap = 2,200 μm: a) a* vs. time; b) c vs. time; c) Def* vs. time.

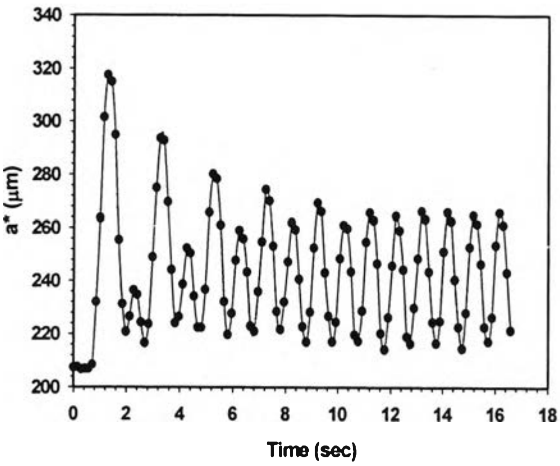

(a)

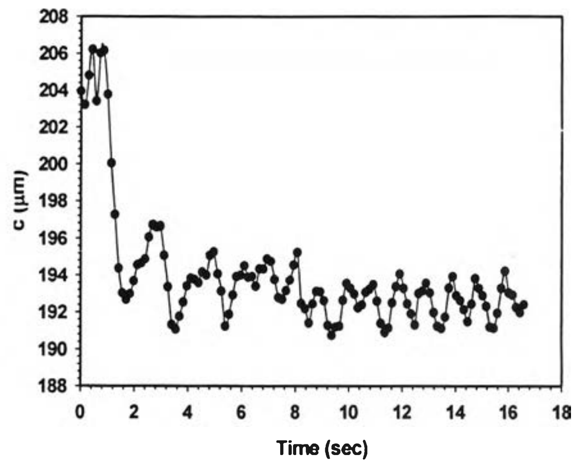

(b)

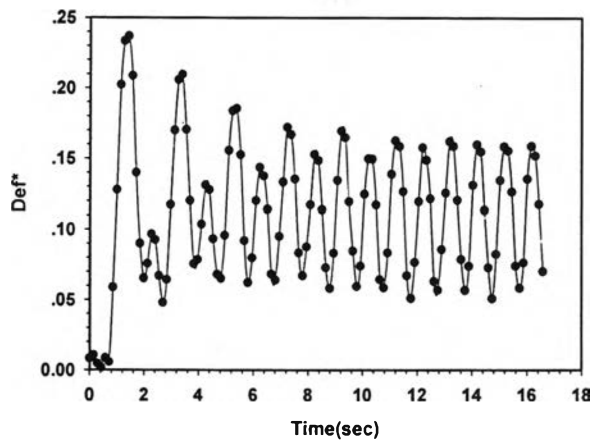

(c)

Figure E38 Deformation parameters vs. time of pure PBd/PDMS at strain 80%, frequency 0.5 Hz, $\tau_r = 1.0$, $G''_r = 1$, $d_o \sim 200$ μm, gap = 2,200 μm: a) a* vs. time; b) c vs. time; c) Def* vs. time.

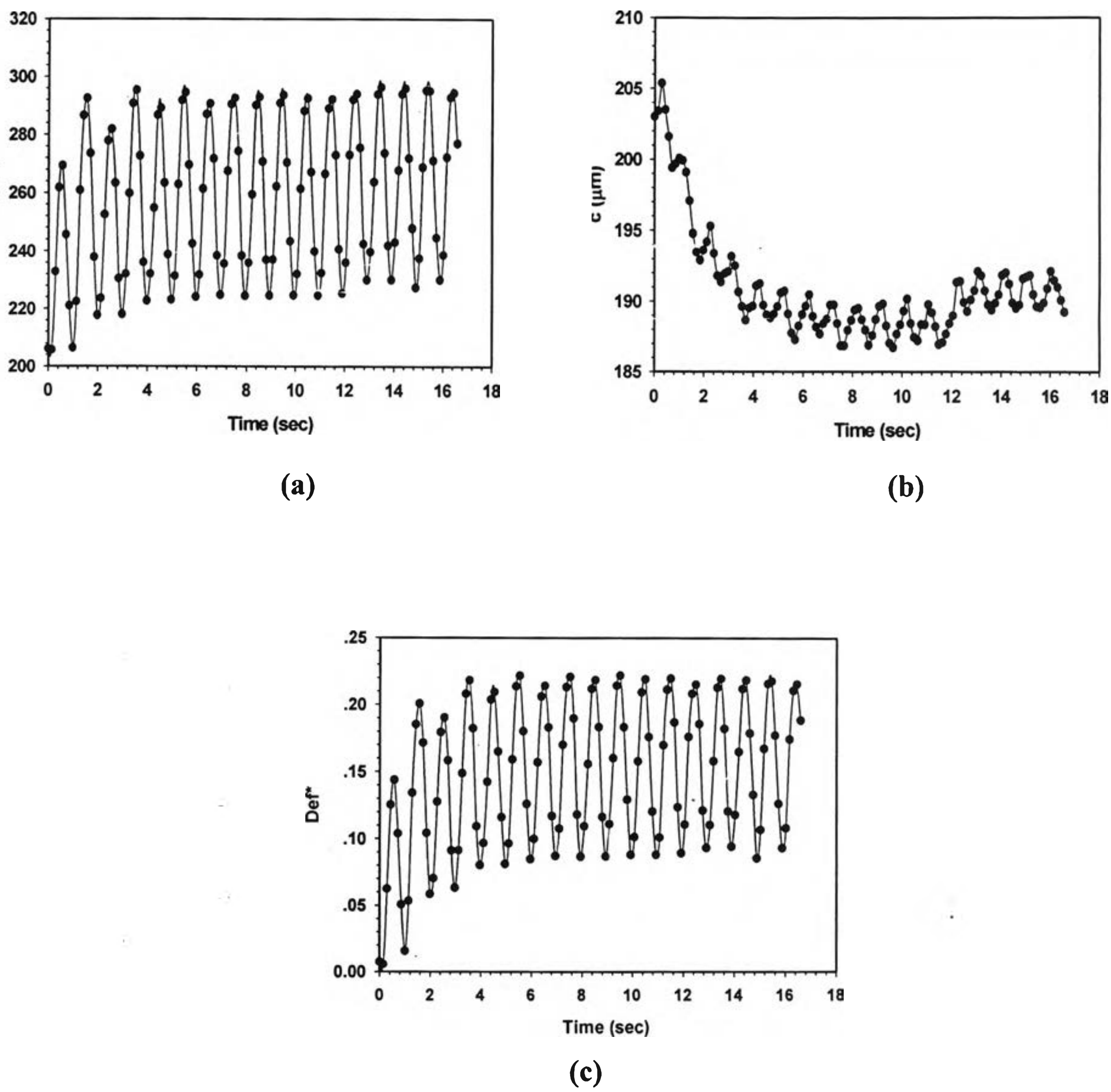

Figure E39 Deformation parameters vs. time of pure PBd/PDMS at strain 100%, frequency 0.5 Hz, τ_r = 1.0, G"$_r$ =1, d_o ~ 200 μm, gap = 2,200 μm: a) a* vs. time; b) c vs. time; c) Def* vs. time.

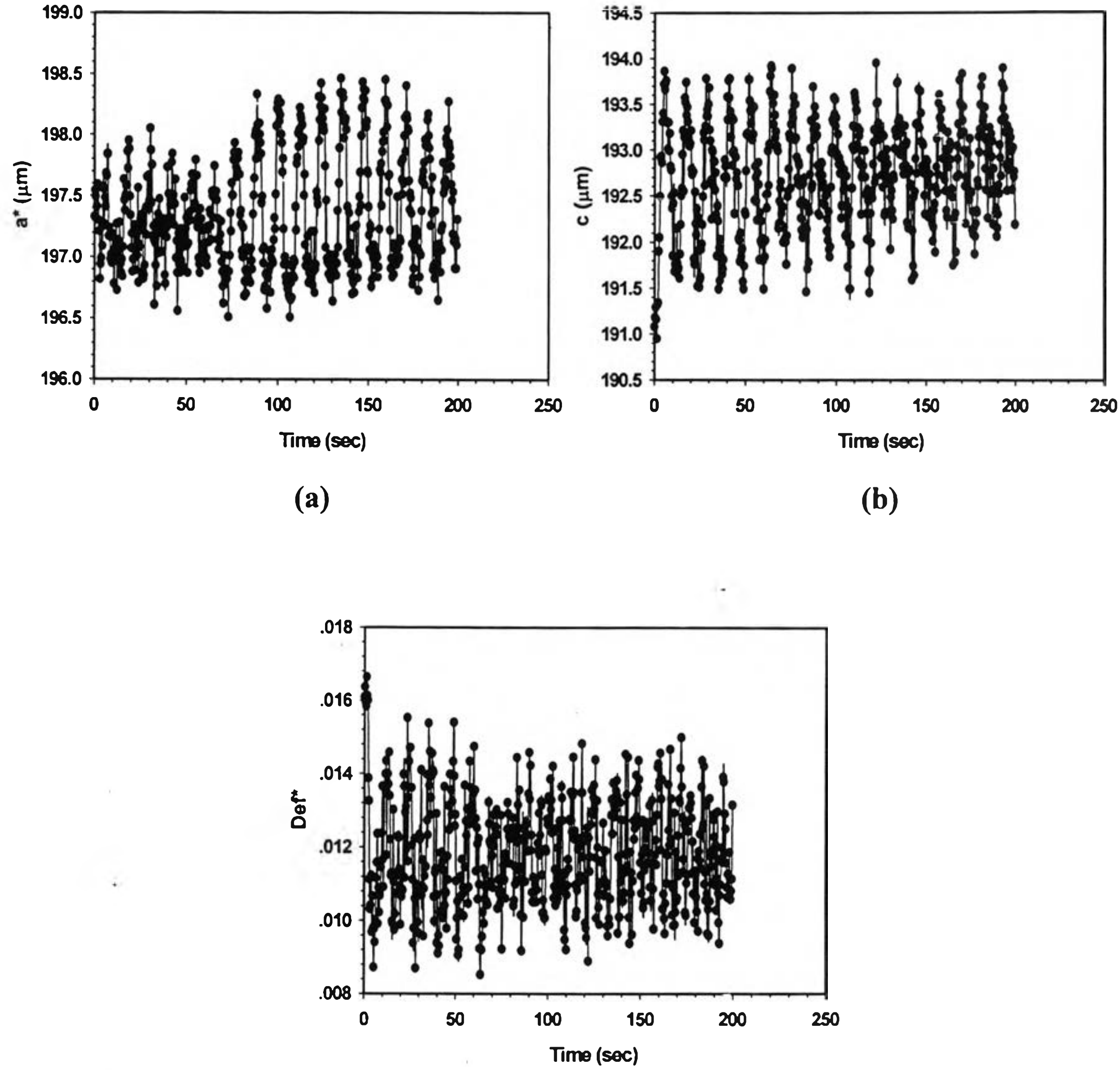

(a) (b)

(c)

Figure E40 Deformation parameters vs. time of 0.02% high Mw PBd sol$^{\underline{n}}$/PDMS at strain 10%, frequency 0.099 Hz, $\tau_r = 0.2$, $G''_r = 1$, $d_o \sim 200$ μm, gap = 2,200 μm: a) a* vs. time; b) c vs. time; c) Def* vs. time.

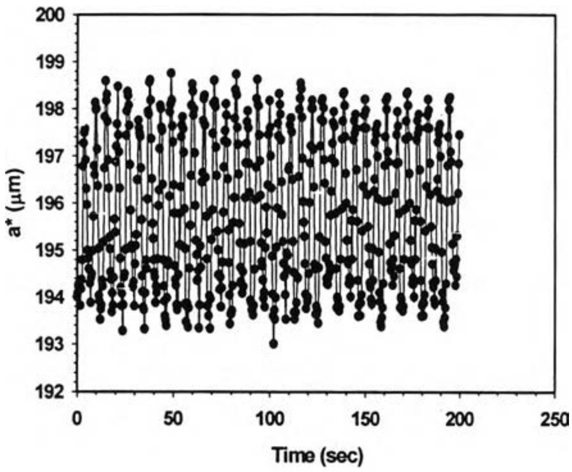

(a)

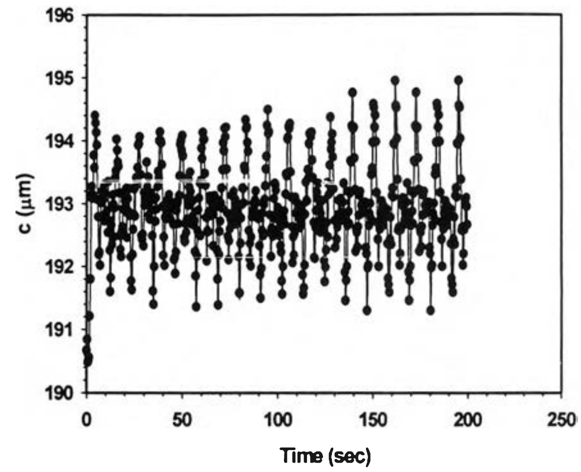

(b)

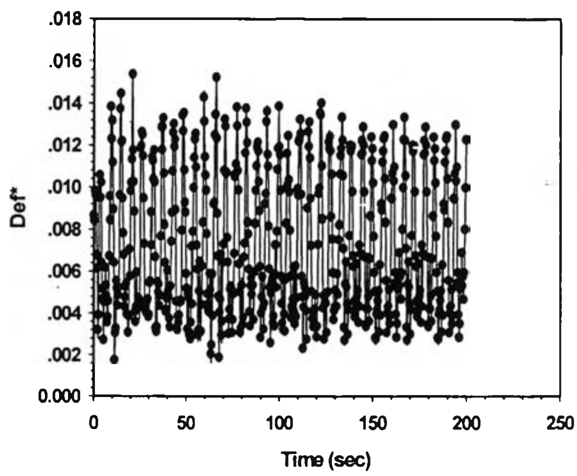

(c)

Figure E41 Deformation parameters vs. time of 0.02% high Mw PBd sol^{n}/PDMS at strain 30%, frequency 0.099 Hz, τ_r = 0.2, G"$_r$ =1, d_o ~ 200 μm, gap = 2,200 μm: a) a* vs. time; b) c vs. time; c) Def* vs. time.

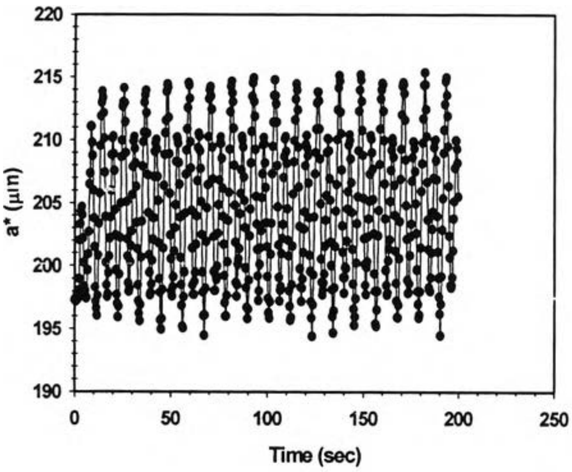

(a)

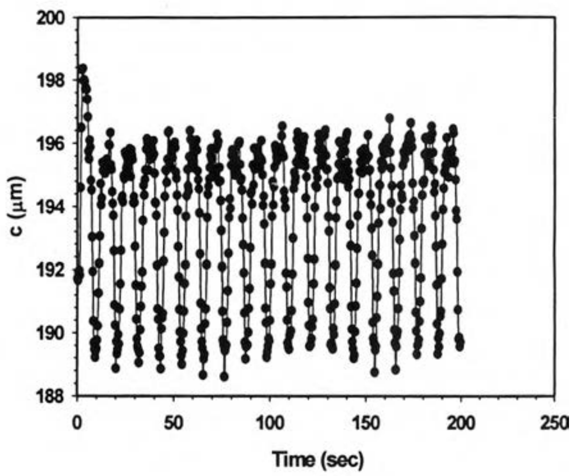

(b)

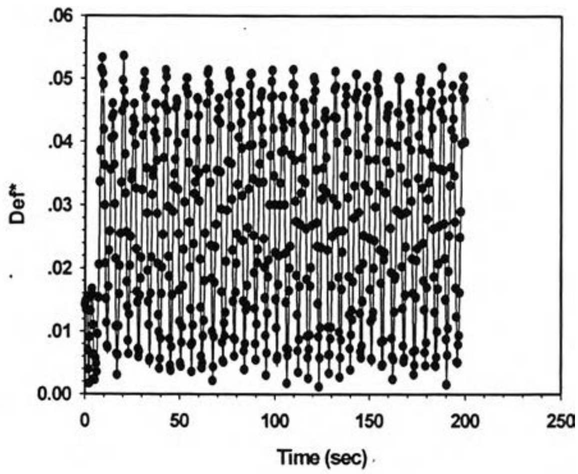

(c)

Figure E42 Deformation parameters vs. time of 0.02% high Mw PBd sol^{n}/PDMS at strain 50%, frequency 0.099 Hz, $\tau_r = 0.2$, $G''_r = 1$, $d_o \sim 200$ μm, gap = 2,200 μm: a) a* vs. time; b) c vs. time; c) Def* vs. time.

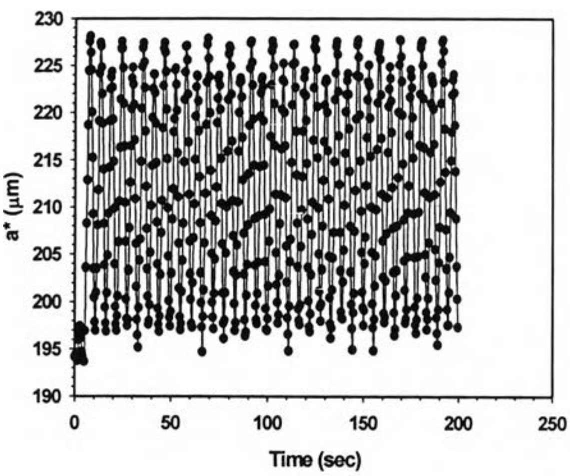

(a)

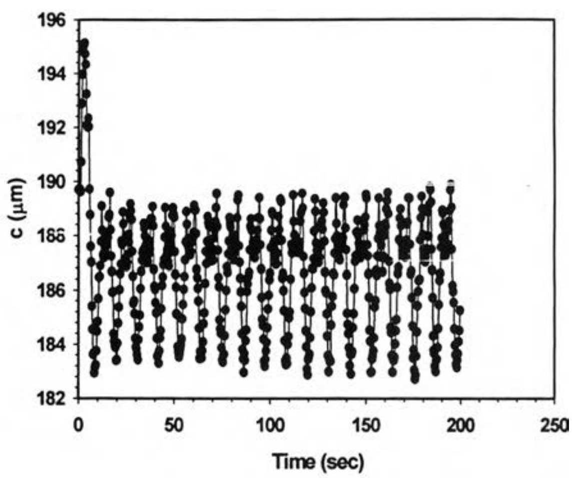

(b)

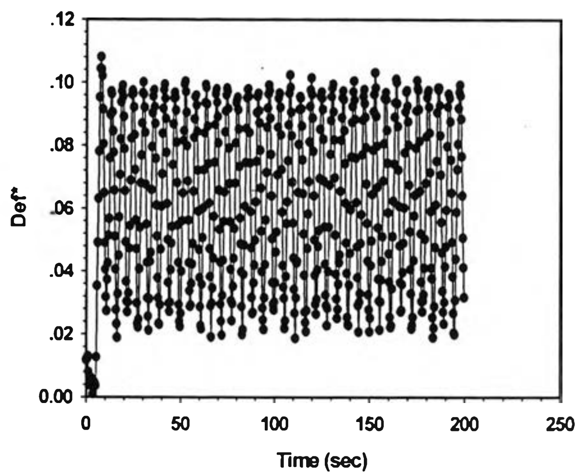

(c)

Figure E43 Deformation parameters vs. time of 0.02% high Mw PBd sol$^{\underline{n}}$/PDMS at strain 70%, frequency 0.099 Hz, $\tau_r = 0.2$, $G''_r = 1$, $d_o \sim 200$ µm, gap = 2,200 µm: a) a* vs. time; b) c vs. time; c) Def* vs. time.

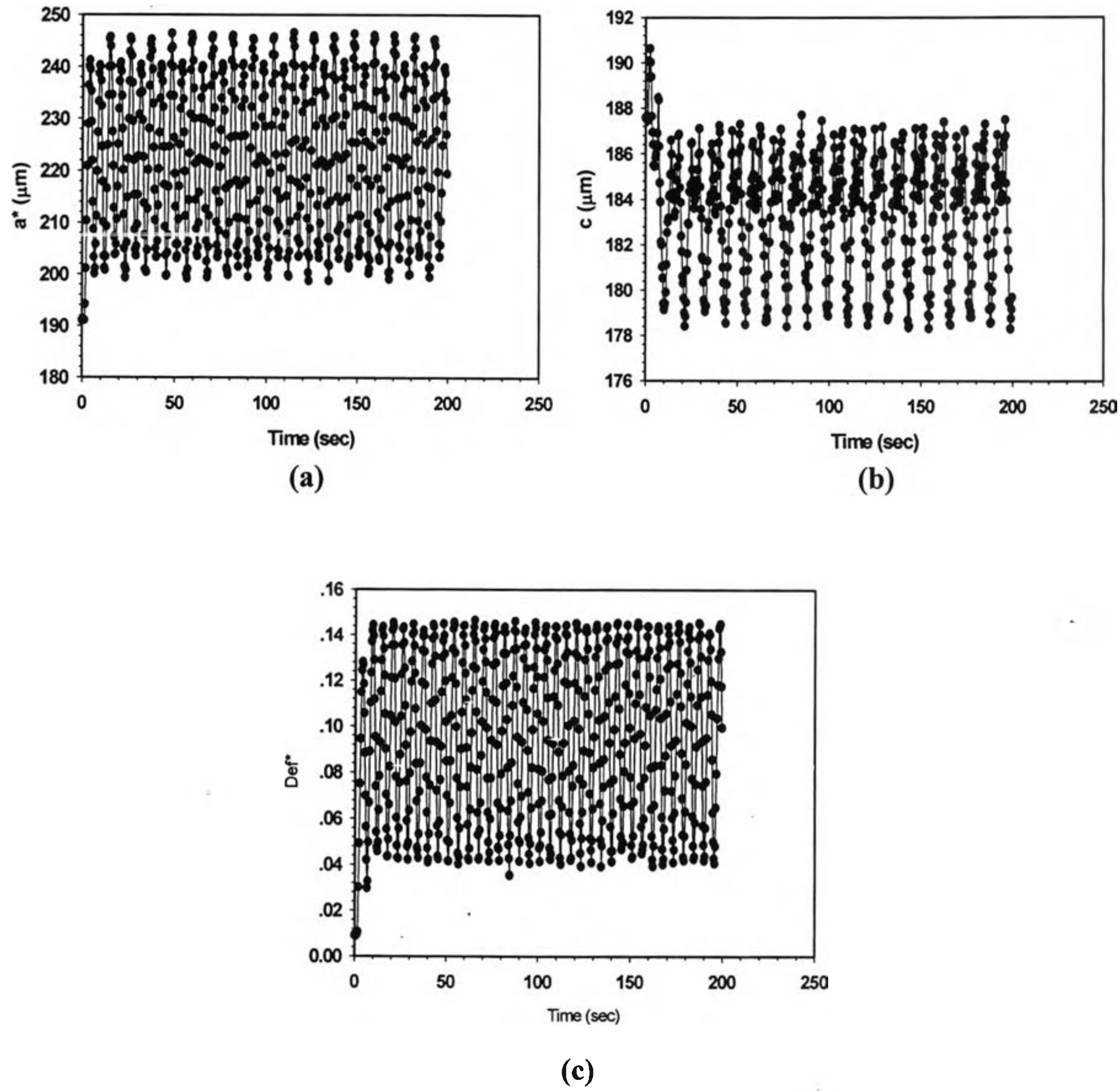

Figure E44 Deformation parameters vs. time of 0.02% high Mw PBd sol$^{\underline{n}}$/PDMS at strain 90%, frequency 0.099 Hz, $\tau_r = 0.2$, $G''_r = 1$, $d_o \sim 200$ μm, gap = 2,200 μm: a) a* vs. time; b) c vs. time; c) Def* vs. time.

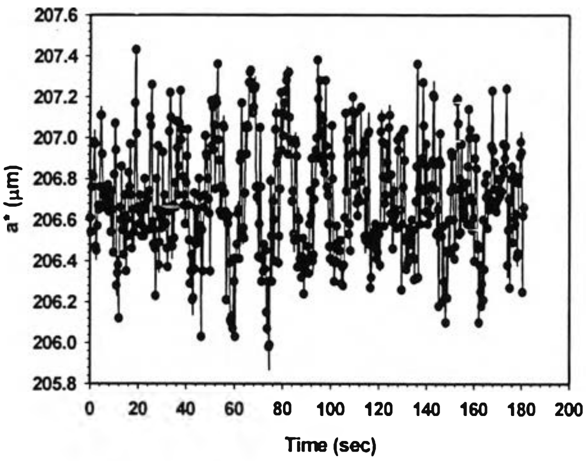

(a)

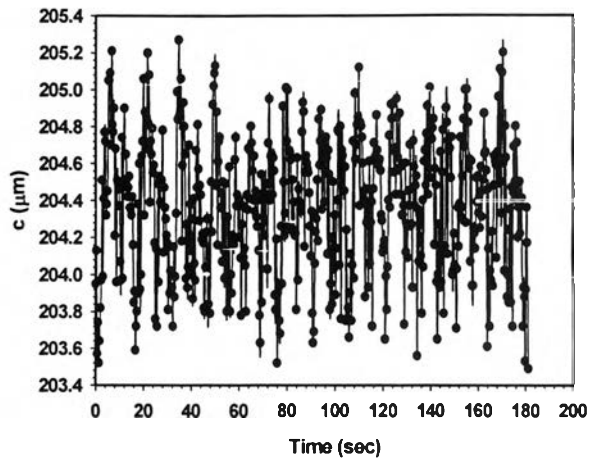

(b)

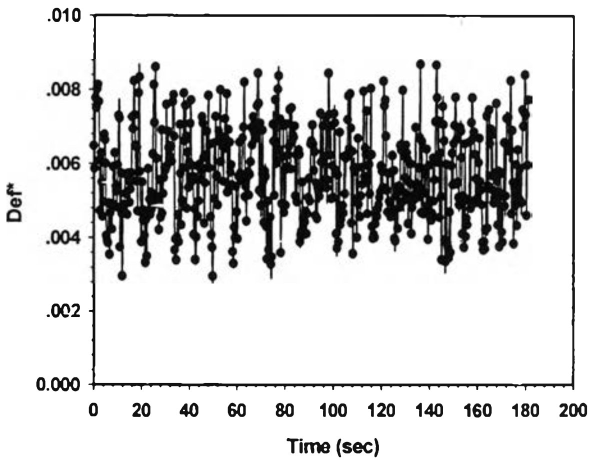

(c)

Figure E45 Deformation parametcrs vs. time of 0.05% high Mw PBd sol$^{\underline{n}}$/PDMS at strain 10%, frequency 0.087 Hz, $\tau_r = 0.2$, $G''_r = 1$, $d_o \sim 200$ µm, gap = 2,200 µm: a) a* vs. time; b) c vs. time; c) Def* vs. time.

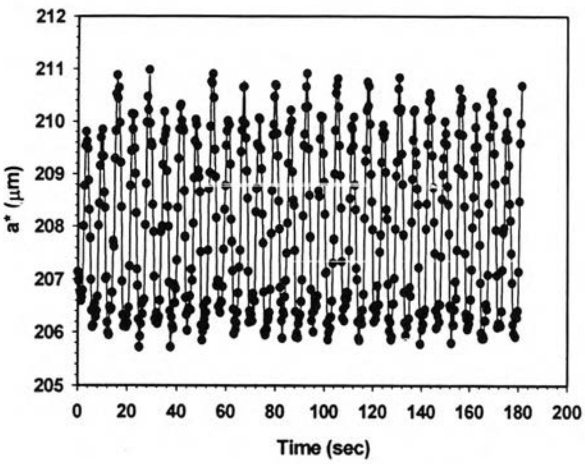

(a)

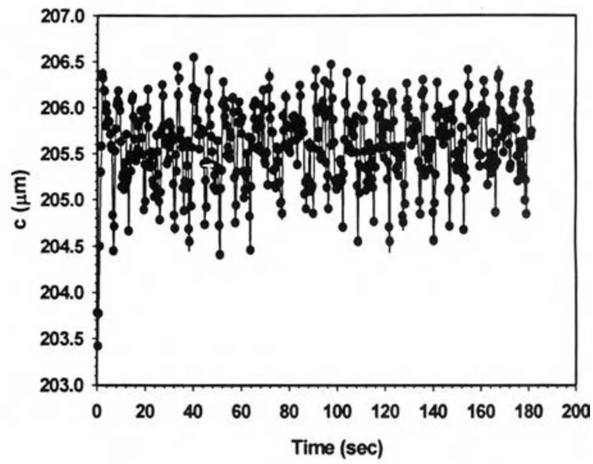

(b)

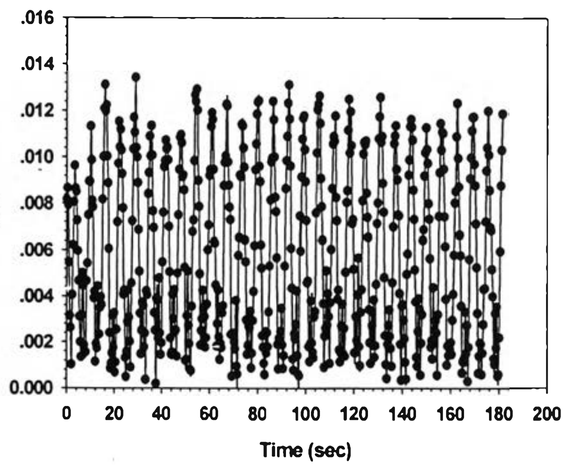

(c)

Figure E46 Deformation parameters vs. time of 0.05% high Mw PBd sol^{n}/PDMS at strain 30%, frequency 0.087 Hz, τ_r = 0.2, G"$_r$ =1, d_o ~ 200 μm, gap = 2,200 μm: a) a* vs. time; b) c vs. time; c) Def* vs. time.

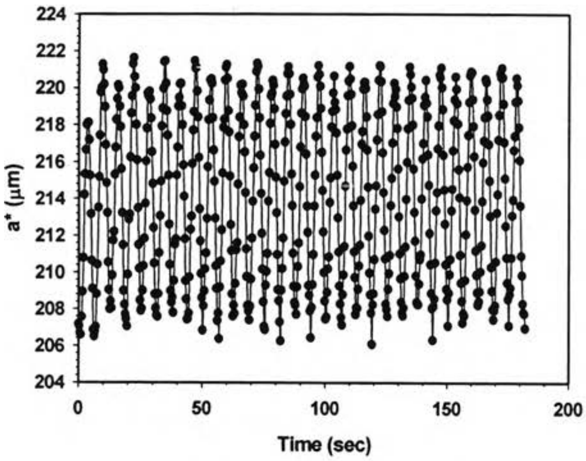

(a)

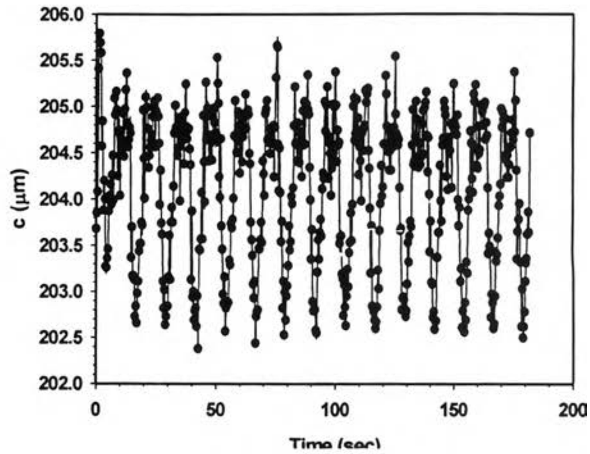

(b)

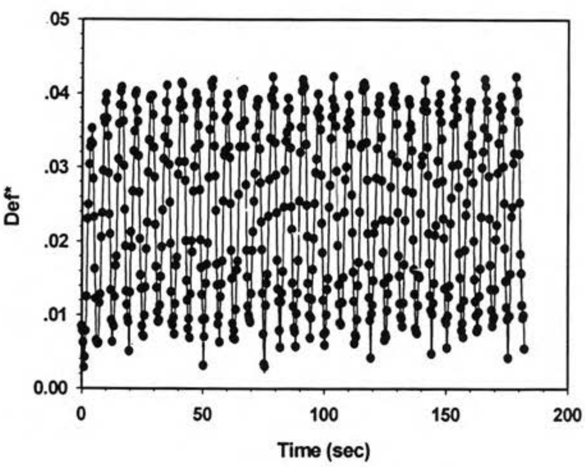

(c)

Figure E47 Deformation parameters vs. time of 0.05% high Mw PBd sol$^{\underline{n}}$/PDMS at strain 50%, frequency 0.087 Hz, τ_r = 0.2, G"$_r$ =1, d_o ~ 200 μm, gap = 2,200 μm: a) a* vs. time; b) c vs. time; c) Def* vs. time.

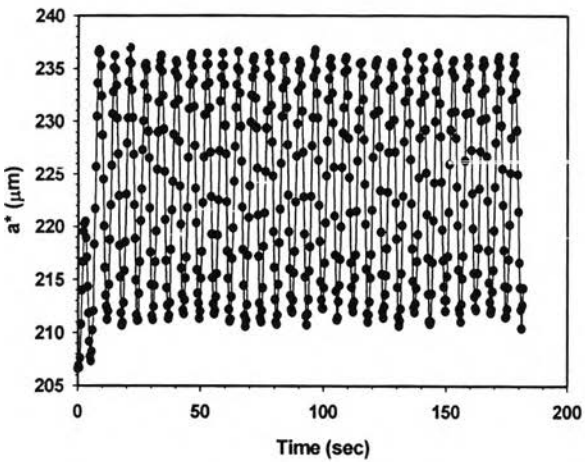

(a)

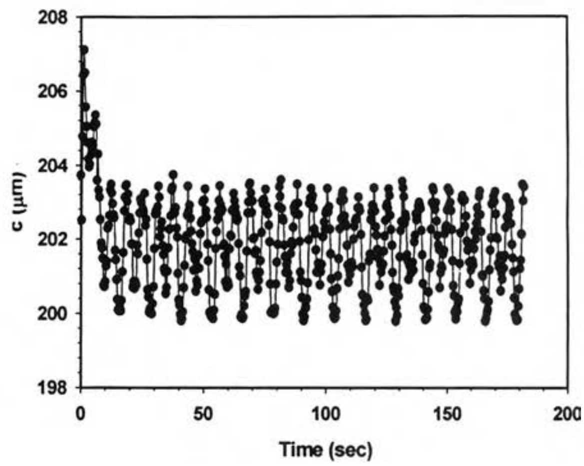

(b)

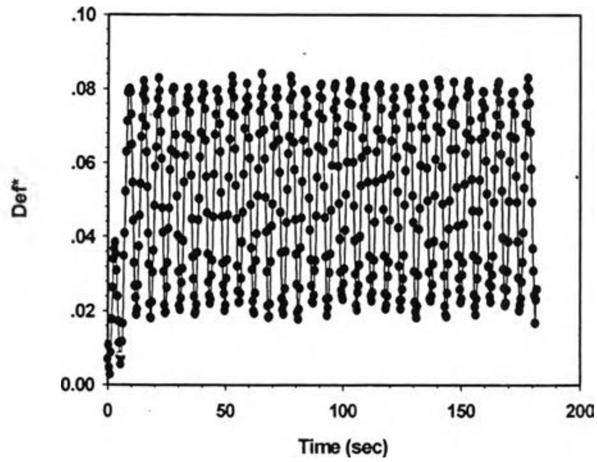

(c)

Figure E48 Deformation parameters vs. time of 0.05% high Mw PBd sol^{n}/PDMS at strain 70%, frequency 0.087 Hz, $\tau_r = 0.2$, $G''_r = 1$, $d_o \sim 200$ μm, gap = 2,200 μm: a) a* vs. time; b) c vs. time; c) Def* vs. time.

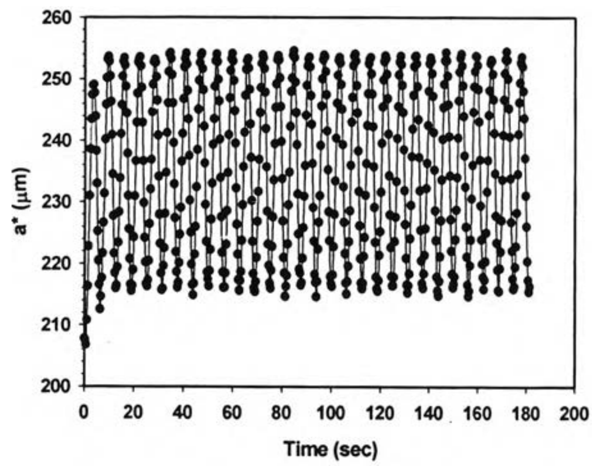

(a)

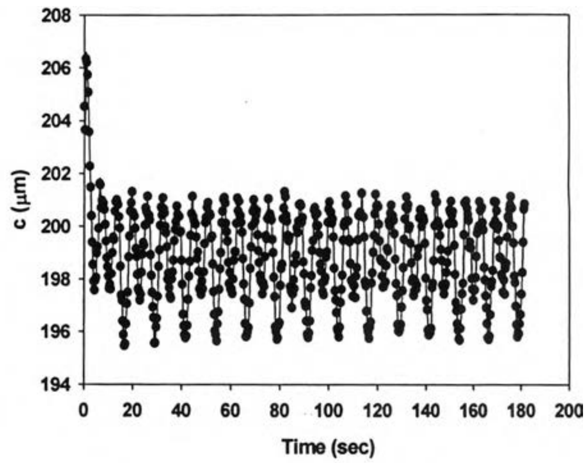

(b)

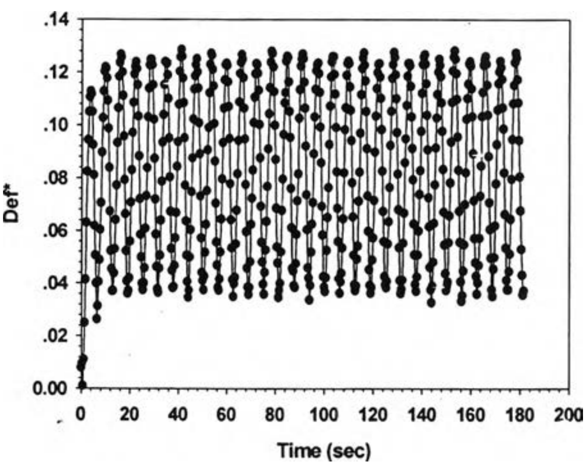

(c)

Figure E49 Deformation parameters vs. time of 0.05% high Mw PBd sol$^{\underline{n}}$/PDMS at strain 90%, frequency 0.087 Hz, $\tau_r = 0.2$, $G''_r = 1$, $d_o \sim 200$ μm, gap = 2,200 μm: a) a* vs. time; b) c vs. time; c) Def* vs. time.

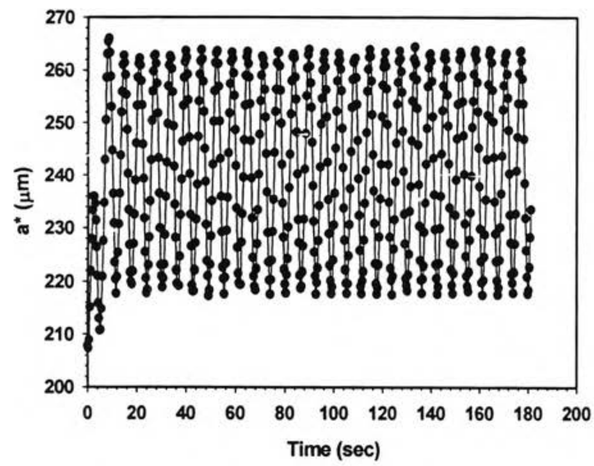

(a)

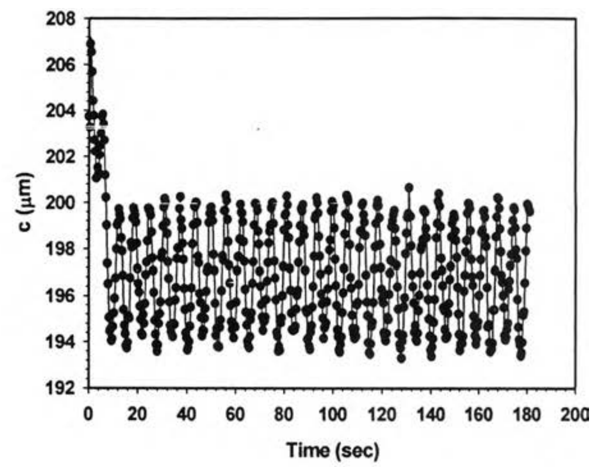

(b)

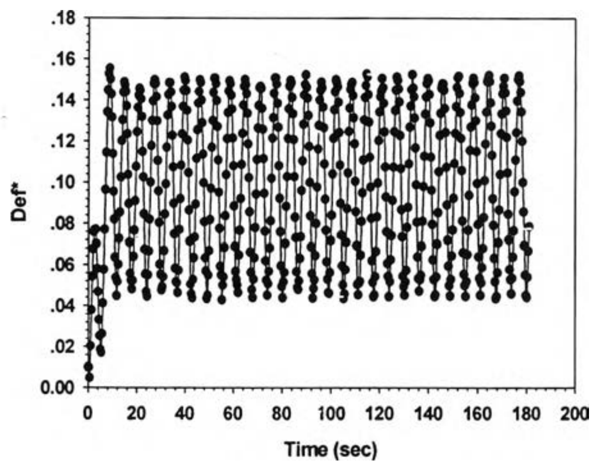

(c)

Figure E50 Deformation parameters vs. time of 0.05% high Mw PBd sol$^{\underline{n}}$/PDMS at strain 100%, frequency 0.087 Hz, τ_r = 0.2, G"$_r$ =1, d_o ~ 200 μm, gap = 2,200 μm: a) a* vs. time; b) c vs. time; c) Def* vs. time.

Appendix F Amplitude of deformation parameters of deformed droplet

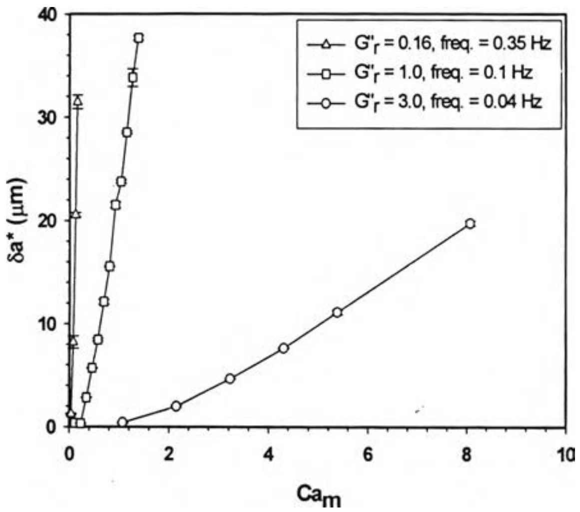

(a)

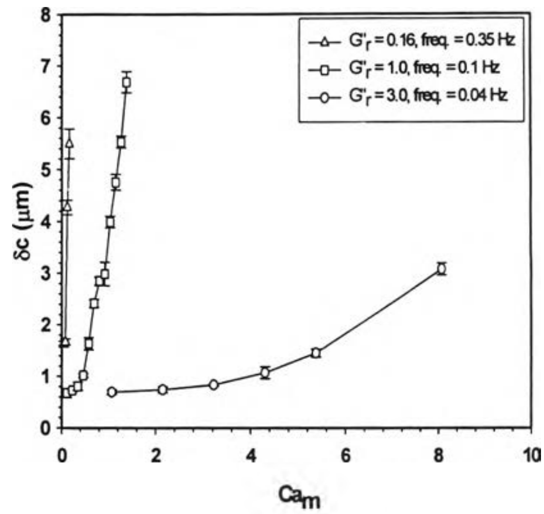

(b)

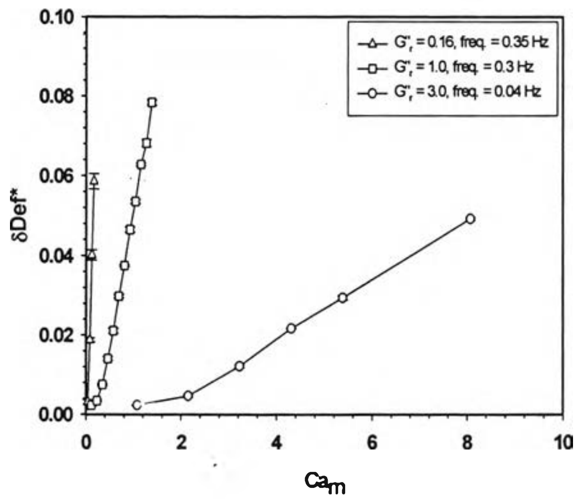

(c)

Figure F1 Amplitude of deformation parameters vs. Ca_m of pure PBd/PDMS at τ_r = 1, $d_o \sim 200$ μm ,gap = 2200 μm: a) δa* vs. Ca_m; b) δc vs. Ca_m; c) δDef* vs. Ca_m.

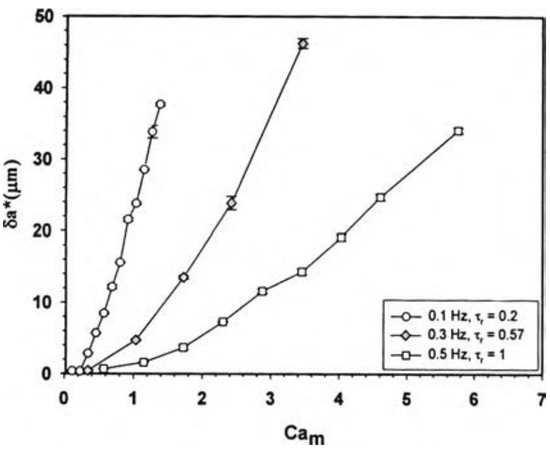

(a)

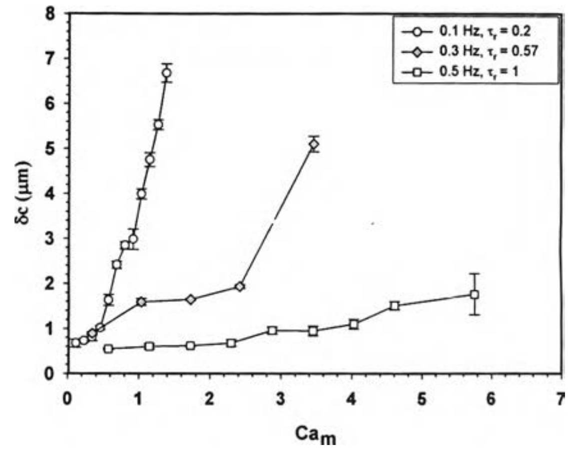

(b)

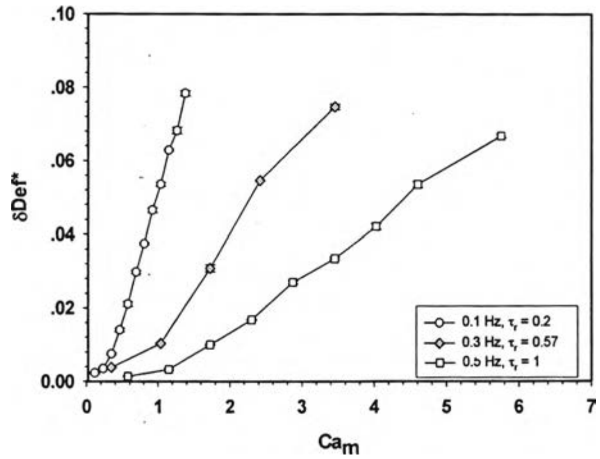

(c)

Figure F2 Amplitude of deformation parameters vs. Ca_m, of pure PBd/PDMS at G''_r = 1, d_o ~ 200 μm ,gap = 2200 μm: a) δa* vs. Ca_m; b) δc vs. Ca_m; c) δDef* vs. Ca_m.

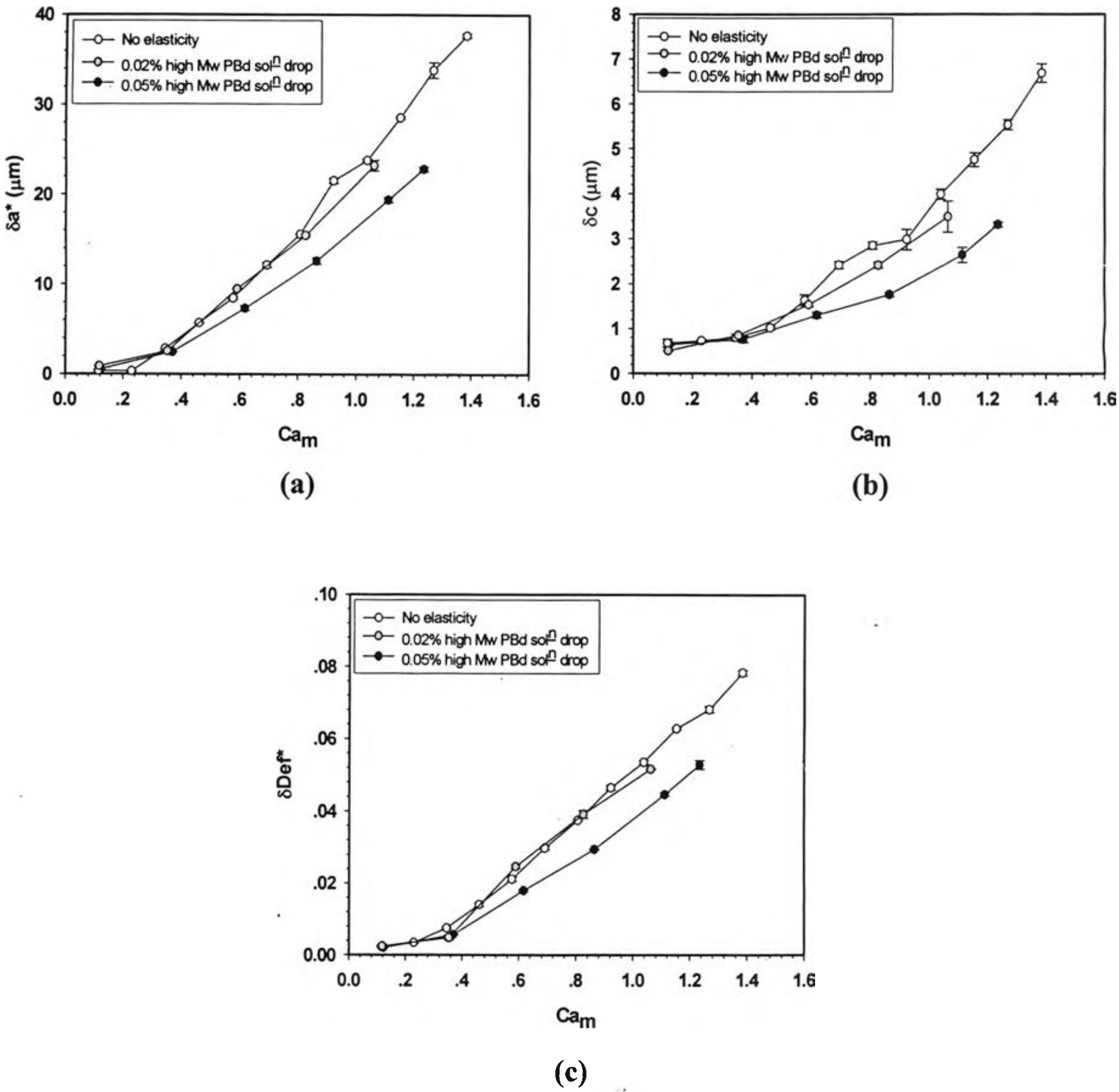

Figure F3 Amplitude of deformation parameters vs. Ca_m of pure PBd/PDMS; 0.02 % high Mw PBd sol^{n}/PDMS and 0.05% high Mw PBd sol^{n}/PDMS at $G''_r = 1$, $\tau_r = 0.2$, $d_o \sim 200$ μm ,gap = 2200 μm: a) δa* vs. Ca_m; b) δc vs. Ca_m; c) δDef* vs. Ca_m.

CURRICULUM VITAE

Name: Mr. Vitsarut Janpaen

Date of Birth: September 27, 1980

Nationality: Thai

University Education:

1998-2001 Bachelor Degree of Engineering in Chemical Engineering, Faculty of Engineering, Thammasat University, Pathumtani, Thailand.

Working Experience:

2000 Position: Process Control

Company name: Gas Separation Plant PTT Company Limited